

Republic of Iraq  
Ministry of Higher Education  
And Scientific Research  
University of Baghdad  
College of Education for Pure  
Science (Ibn-AL-Haitham)



# **Study of Electronic Charge Transmission in Liquid/Semiconductor System**

**A Thesis**

**Submitted to Council of College of Education for  
Pure Science (Ibn-AL-Haitham)/University of  
Baghdad in Partial Fulfillment of Requirements for  
the Degree of Master of Science in Physics**

*By*

**Hazim Hadi Dhayef Al Hasan**

**B.Sc. in physics 2003**

*Supervisor by*

**Prof. Dr. Hadi Jabbar Mujbil Al Agealy**

**2019 A.D.**

**1441 A.H.**

بِسْمِ اللَّهِ الرَّحْمَنِ الرَّحِيمِ

« قَالَ لَهُ مُوسَىٰ هَلْ أَتَّبِعُكَ  
عَلَىٰ أَنْ تُعَلِّمَنِي مِمَّا عَلَّمْتَ رُشْدًا »

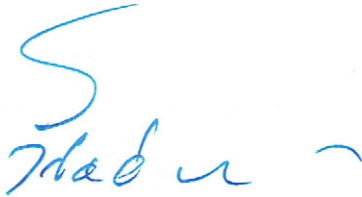
صدق الله العلي العظيم

[ الكهف 66 ]

## Supervisore Certification

I certify that this thesis titled “**Study of Electronic Charge Transmission in Liquid/Semiconductor System**” was prepared by (**Hazim Hadi Dhayef**), under my supervision at the University of Baghdad/Education College for Pure Science (Ibn-AL-Haitham)/Department of Physics in partial fulfillment of the requirements for the degree of Master of Science in Physics.

Signature:



Name: Dr. Hadi Jabbar Mujbil Al-Agealy

Title: Professor.

University of Baghdad/College of Education for Pure  
Science (Ibn-AL-Haitham)/Department of Physics

Date: 27/6/2019

The Council of the Department of Physics has approved the examining committee:

Signature:



Name: Dr. Samir Ata Maki

Title: Professor.

University of Baghdad/College of Education for Pure  
Science (Ibn-AL-Haitham)/Department of Physics.

Date: 27/6/2019

## Certification of the discussion committee

We are members of the discussion committee, the undersigned, we witness we have looked in the thesis which it titled "**Study of Electronic Charge Transmission in Liquid/Semiconductor System**" by (Hazim Hadi Dhayef) and we have discussed the student in the thesis contents then we found it worth to accept and get the degree of Master of Science in Physics), for that we signed.

Signature: 

Name: Dr. Ali Husein Abd Al Razak

Title: Assistant Professor

Adress: University of Baghdad

Date: 9/12/2019

Chairman

Signature: 

Name: Dr. Muslim Azzalden Abid

Title: Assistant Professor

Adress: Al-Mustansyriah University

Date: 9/12/2019

Member

Signature: 

Name: Dr. Mudhafar Jasim Sahib

Title: Instructor

Adress: University of Baghdad

Date: 9/12/2019

Member

Signature: 

Name: Dr. Hadi Jabbar Mujbil

Title: Professor

Adress: University of Baghdad

Date: 9/12/2019

Member-Supervisor

**Deanship Authentication of the Education College for Pure Science Ibn-Al-Haitham/University of Baghdad:**

Signature: 

Name: Assist. Prof. Dr. Firas Abdulhameed Abdullatif

Adress : Behalf / the Dean of College of Education for Pure Science Ibn-Al-Haitham/University of Baghdad

Date: 17/12/2019

## **Dedication**

To the spring of pure love and high compassion to those who were the most courageous and wise people I knew,

My deceased father .....

To the source of comfort and tranquility and warmth and affection and the tree of tender renewed,

My loving mother.

To whom I grew up my longing and nostalgia after he left me early, support and my friend

My brother martyr.

To those who have committed and believed in the seat of truth have fallen, the martyrs of Iraq.

**HAZIM**

## **Acknowledgments**

For those whose beauty and generosity I cannot find in my words, the description may not be able to capture all that I have been given to my brother (as he calls me), my professor and mentor Dr. Hadi Jabbar Mujbil Al Agealy

To my legal and support in my preparatory and research career my colleagues in the study

To all who stood beside me and supported my friends, relatives and family members

Thank you very much.

## Abstract

In this study, a simple theoretical model of Marcus theory has been used to study the flow charge rate across semiconductor-liquid system. A quantum mechanics theory has employed to investigate and obtain the flow charge rate at donor acceptor system. we investigate the mechanism of the flow charge transfer at semiconductor-liquid interfaces system based on the donor acceptor model by considering continuum energy levels of semiconductors and molecules dye. The calculations of the flow charge transfer rate were carried out for InAs/D149, ZnO/D149, MgO/D149, InAs/N749, ZnO/N749 and MgO/N749 through reorientation transition energy  $\mathcal{T}_S^L(eV)$ , potential barrier  $\Delta\mathcal{U}^{LS}(eV)$  and the strength coupling of energy levels for interface system  $\mathcal{C}_{S/L}(\epsilon)$ . We further study the reorientation transition energy that help the six systems to reorganize their energy levels to start the transition of the charges from the dye to the conduction bands of the semiconductor. We found that the reorientation transition energy increased along with decreasing the refractive index of the solvents and increasing the dielectric constant in all the six systems. The potential barrier was determined based on the difference between the absorption energy of the sensitized dye and the reorientation energy of a continuum model in a polarity medium. The calculation of the potential at the interface of both surfaces using theoretical results of the reorientation transition energy explained the transition process across the interface of semiconductor-dye system in the polarity medium. It also shows enhancement of the potential barrier  $\Delta\mathcal{U}^{LS}(eV)$  with absorption energy and reorientation transition energy. The flow charge rate reaches its maximum value when using the Propanol as a solvent, while it gradually decreased when using butanol, octanol, dichloroethane and acetonitrile solvents, the MgO/D149 has the largest flow charge rate compared to InAs/D149 and ZnO/D149 system for the same overlapping coupling, Calculated flow charge rate was decreased with increasing the potential barrier and increased with decreasing the reorientation transition energy for all system.

# List of Contents

List of Contents .....	I
List of Figures .....	IV
List of Tables .....	V
List of Abbreviations and Symbols .....	VIII

## Chapter One

### (Introduction and Literature Survey)

(1-1) Introduction .....	2
(1-2) Literature Survey .....	3
(1-3) Aim of the Present Work .....	11

## Chapter Two

### Background and Concept of Charge Transfer Reaction

(2-1) Introduction .....	13
(2-2) Microscopic Concept of Charge Transfer Reaction .....	14
(2-3) Analysis of Charge Transfer at Molecule-Semiconductor System .....	16
(2-4) Classical Rate of Charge Transfer Reactions .....	17
(2-5) Inner and Outer Reorganization Energies for Electron Transfer .....	18
(2-6) The Electronic Strength Coupling .....	19
(2-7) The Mechanism of Charge Transfer In Semiconductor-Molecule System .....	21
(2-8) Dye Sensitized .....	23
(2-9) Semiconductors .....	26
(2-10) Organic Material / Semiconductor Interfaces .....	27
(2-11) Solvents .....	27



## Chapter Three

### ( Theoretical Model )

(3-1) Theoretical Model .....	29
-------------------------------	----

## Chapter Four

### ( The Result and Discussion )

(4-1) Introduction .....	40
(4-2) Evaluation of the Reorientation Transition Energy $\mathcal{J}_S^L(eV)$ ..	40
(4-3) Evaluation of the Potential Barrier $\Delta\mathcal{U}^{LS}$ (eV) at Interface...	43
(4-4) Estimation of the Electronic Coupling Strength	
Coefficient $\mathbb{C}_{S/L}(\epsilon)$ .....	48
(4-5) Evaluation of Flow Charge Transfer Rate Constant .....	48
(4-6) Discussion .....	64
(4-6-1) Theoretical Model of Charge Transfer at Semiconductor/ Molecule Interface .....	64
(4-6-2) Modeling of Charge Transfer Mechanism .....	64
(4-6-3) Influence of Reorientation Transition Energy $\mathcal{J}_S^L$ (eV) on the Flow Charge Transition Rate .....	67
(4-6-4) Influence of Polarity Solvents on the Flow Charge Rate .....	68
(4-6-5) Effect of Polarity Function on the Flow Charge Transfer....	69
(4-6-6) Influence of the Experimental Potential Force on Flow Charge Rate $\Delta\mathcal{U}^{LS} = E_{cb} - qE^0$ .....	70
(4-6-7) Influence of Theoretical Potential Barrier Hight $\Delta\mathcal{U}^{LS}$ (eV) on the Flow Charge Transfer.....	71
(4-6-8) Influence of the Strength Coupling Coefficient $\mathbb{C}_{S/L}(\epsilon)$ (eV) on Flow Charge Transition Rate .....	72

## **Chapter Five**

### **( Conclusion and Suggested Future work )**

<b>(5-1) Conclusion .....</b>	<b>75</b>
<b>(5-2) Suggested Future Work .....</b>	<b>76</b>
<b>References .....</b>	<b>77</b>

# *List of Figure*

## *Chapter Two*

<i>Figure</i>	<i>Title</i>	<i>page</i>
<b>(2-1)</b>	Solid/ molecules interface	<b>14</b>
<b>(2-2)</b>	Potential energy surface for an electron transfer reaction $ \varphi_D\rangle +  \varphi_A\rangle \rightarrow  \varphi_D^+\rangle +  \varphi_A^-\rangle$ reactants and the products .	<b>15</b>
<b>(2-3)</b>	(a)-Charge transfer potential surface between reactant state (S*-CB) and product states (S+-CB-). (b) Schematic illustration of variation of the density of semiconductor states with energy E.	<b>16</b>
<b>(2-4)</b>	Illustration of semiconductor –molecule cells .	<b>22</b>
<b>(2-5)</b>	Chemical structure of the molecules N719, Black Dye.	<b>24</b>
<b>(2-6)</b>	Chemical structure of D149 sensitized dye .	<b>25</b>
<b>(2-7)</b>	Schematic of charge transfer principle of Dye-Semiconductor system .	<b>25</b>

## *Chapter Three*

<i>Figure</i>	<i>Title</i>	<i>page</i>
<b>(3-1)</b>	Schematic of the basic charge transition at molecules dye on semiconductor surfaces contact .	<b>30</b>

## *Chapter Four*

<i>Figure</i>	<i>Title</i>	<i>page</i>
<b>(4-1)</b>	Absorption spectrum UV/V of N749 of sensitized dye .	<b>44</b>
<b>(4-2)</b>	Absorption spectrum UV/V of D149 of sensitized dye .	<b>44</b>

# *List of Table*

## *Chapter Four*

<i>NO.</i>	<i>Title</i>	<i>page</i>
<b>(4-1)</b>	Properties of molecules.	<b>41</b>
<b>(4-2)</b>	General properties of InAs and ZnO semiconductor.	<b>41</b>
<b>(4-3)</b>	Results of radii calculation	<b>42</b>
<b>(4-4)</b>	General properties of solvents .	<b>42</b>
<b>(4-5)</b>	Results data of reorientation transition energy for six systems	<b>43</b>
<b>(4-6)</b>	Calculated potential barrier for InAs/ N749 system under different reorientation energies and absorption energy (eV)	<b>45</b>
<b>(4-7)</b>	Calculated potential barrier for MgO/ N749 system under different reorientation energies and absorption energy (eV)	<b>45</b>
<b>(4-8)</b>	Calculated potential barrier for ZnO/ N749 system under different reorientation energies and absorption energy (eV)	<b>46</b>
<b>(4-9)</b>	Calculated potential barrier for InAs/ D149 system under different reorientation energies and absorption energy (eV)	<b>46</b>
<b>(4-10)</b>	Calculated potential barrier for MgO/ D149 system under different reorientation energies and absorption energy (eV)	<b>47</b>
<b>(4-11)</b>	Calculated potential barrier for ZnO/ D149 system under different reorientation energies and absorption energy (eV) .	<b>47</b>
<b>(4-12)</b>	Calculated flow charge transition rate at InAs/N749 as a function of potential barrier $\Delta\mathcal{U}^{LS}$ at coupling strength $2 \times 10^{-2}$ eV	<b>49</b>
<b>(4-13)</b>	Calculated flow charge transition rate at InAs/N749 as a function of potential barrier $\Delta\mathcal{U}^{LS}$ at coupling strength $7 \times 10^{-2}$ eV	<b>49</b>
<b>(4-14)</b>	Calculated flow charge transition rate at InAs/N749 as a function of potential barrier $\Delta\mathcal{U}^{LS}$ at coupling strength $1.2 \times 10^{-3}$ eV	<b>50</b>
<b>(4-15)</b>	Calculated flow charge transition rate at InAs/N749 as a function of potential barrier $\Delta\mathcal{U}^{LS}$ at coupling strength $1.7 \times 10^{-4}$ eV	<b>50</b>
<b>(4-16)</b>	Calculated flow charge transition rate at InAs/N749 as a function of potential barrier $\Delta\mathcal{U}^{LS}$ at coupling strength $2.2 \times 10^{-4}$ eV	<b>51</b>
<b>(4-17)</b>	Calculated flow charge transition rate at InAs / D149 as function of potential barrier $\Delta\mathcal{U}^{LS}$ at coupling strength $2 \times 10^{-2}$ eV	<b>51</b>

(4-18)	Calculated flow charge transition rate at InAs/D149 as a function of potential barrier $\Delta\mathcal{U}^{LS}$ at coupling strength $7 \times 10^{-2}$ eV	52
(4-19)	Calculated flow charge transition rate at InAs/D149 as a function of potential barrier $\Delta\mathcal{U}^{LS}$ at coupling strength $1.2 \times 10^{-3}$ eV	52
(4-20)	Calculated flow charge transition rate at InAs/D149 as a function of potential barrier $\Delta\mathcal{U}^{LS}$ at coupling strength $1.7 \times 10^{-4}$ eV	53
(4-21)	Calculated flow charge transition rate at InAs/D149 as a function of potential barrier $\Delta\mathcal{U}^{LS}$ at coupling strength $2.2 \times 10^{-4}$ eV	53
(4-22)	Calculated flow charge transition rate at MgO / N749 as a function of potential barrier $\Delta\mathcal{U}^{LS}$ at coupling strength $2 \times 10^{-2}$ eV	54
(4-23)	Calculated flow charge transition rate at MgO / N749 as a function of potential barrier $\Delta\mathcal{U}^{LS}$ at coupling strength $7 \times 10^{-2}$ eV	54
(4-24)	Calculated flow charge transition rate at MgO / N749 as a function of potential barrier $\Delta\mathcal{U}^{LS}$ at coupling strength $1.2 \times 10^{-3}$ eV	55
(4-25)	Calculated flow charge transition rate at MgO / N749 as a function of potential barrier $\Delta\mathcal{U}^{LS}$ at coupling strength $1.7 \times 10^{-4}$ eV	55
(4-26)	Calculated flow charge transition rate at MgO / N749 as a function of potential barrier $\Delta\mathcal{U}^{LS}$ at coupling strength $2.2 \times 10^{-4}$ eV	56
(4-27)	Calculated flow charge transition rate at MgO / D149 as a function of potential barrier $\Delta\mathcal{U}^{LS}$ at coupling strength $2 \times 10^{-2}$ eV	56
(4-28)	Calculated flow charge transition rate at MgO / D149 as a function of potential barrier $\Delta\mathcal{U}^{LS}$ at coupling strength $7 \times 10^{-2}$ eV	57
(4-29)	Calculated flow charge transition rate at MgO / D149 as a function of potential barrier $\Delta\mathcal{U}^{LS}$ at coupling strength $1.2 \times 10^{-3}$ eV	57
(4-30)	Calculated flow charge transition rate at MgO / D149 as a function of potential barrier $\Delta\mathcal{U}^{LS}$ at coupling strength $1.7 \times 10^{-4}$ eV	58
(4-31)	Calculated flow charge transition rate at MgO / D149 as a function of potential barrier $\Delta\mathcal{U}^{LS}$ at coupling strength $2.2 \times 10^{-4}$ eV	58
(4-32)	Calculated flow charge transition rate at ZnO / N749 as a function of potential barrier $\Delta\mathcal{U}^{LS}$ at coupling strength $2 \times 10^{-2}$ eV	59
(4-33)	Calculated flow charge transition rate at ZnO / N749 as a function of potential barrier $\Delta\mathcal{U}^{LS}$ at coupling strength $7 \times 10^{-2}$ eV	59

<b>(4-34)</b>	Calculated flow charge transition rate at ZnO / N749 as a function of potential barrier $\Delta\mathcal{U}^{LS}$ at coupling strength $1.2 \times 10^{-3}$ eV	<b>60</b>
<b>(4-35)</b>	Calculated flow charge transition rate at ZnO / N749 as a function of potential barrier $\Delta\mathcal{U}^{LS}$ at coupling strength $1.7 \times 10^{-4}$ eV	<b>60</b>
<b>(4-36)</b>	Calculated flow charge transition rate at ZnO / N749 as a function of potential barrier $\Delta\mathcal{U}^{LS}$ at coupling strength $2.2 \times 10^{-4}$ eV	<b>61</b>
<b>(4-37)</b>	Calculated flow charge transition rate at ZnO / D149 as a function of potential barrier $\Delta\mathcal{U}^{LS}$ at coupling strength $2 \times 10^{-2}$ eV	<b>61</b>
<b>(4-38)</b>	Calculated flow charge transition rate at ZnO / D149 as a function of potential barrier $\Delta\mathcal{U}^{LS}$ at coupling strength $7 \times 10^{-2}$ eV	<b>62</b>
<b>(4-39)</b>	Calculated flow charge transition rate at ZnO / D149 as a function of potential barrier $\Delta\mathcal{U}^{LS}$ at coupling strength $1.2 \times 10^{-3}$ eV	<b>62</b>
<b>(4-40)</b>	Calculated flow charge transition rate at ZnO / D149 as a function of potential barrier $\Delta\mathcal{U}^{LS}$ at coupling strength $1.7 \times 10^{-4}$ eV	<b>63</b>
<b>(4-41)</b>	Calculated flow charge transition rate at ZnO / D149 as a function of potential barrier $\Delta\mathcal{U}^{LS}$ at coupling strength $2.2 \times 10^{-4}$ eV	<b>63</b>

## List of Abbreviations and Symbols

D149	Sensitized dye under name( 5-[[4-[4-(2,2-Diphenylethenyl)phenyl]-1,2,3-3a,4,8b-hexahydrocyclopent[ <i>b</i> ]indol-7-yl]methylene]-2-(3-ethyl-4-oxo-2-thioxo-5-thiazolidinylidene)-4-oxo-3-thiazolidineacetic acid, Indoline)
N749	Tris(tetrabutylammonium) Tris(isothiocyanato)(2,2':6',6''-terpyridyl-4,4',4''-tricarboxylato)ruthenium(II)
DNA	Deoxyribo Nucleic Acid
InAs	Indium Arsenide
ZnO	Zinc Oxide
MgO	Magnesium Oxide
GaAs	Gallium Arsenide
SECM	Scanning Electron Chemical Microscopy
PM567	viz., 4,4-difluoro-1,3,5,7,8-pentamethyl-2,6-diethyl-4-bora-3a,4a-diaza-s-indecene (PM567) dye
UV	Ultra Violet
PTCDA	( <i>N, N'</i> -di(2,6-diisopropylphenyl)-1,6,7,12-tetra(4-tert-butylphenoxy)-perylene-3,4,9,10- tetracarboxylic diimide Dye.
TD-DFT	Time Dependent - Density Functional Theory
DSSCs	Dye Sensitized Solar Cell
OLEDs	Organic Light Emitting Diodes
OSCs	Organic Solar Cells
OFETs	Organic Field Effect Transistors
HOMO	The Highest Occupied Molecular Orbit
LUMO	The Lowest Unoccupied Molecular Orbit
$ \varphi_A\rangle$	Ket Donor Wave Function
$ \varphi_D\rangle$	Bra Acceptor Wave Function

$\Delta G$ (eV)	Free Energy (eV)
(S*-CB)	Reactant State
(S <sup>+</sup> -CB <sup>-</sup> )	Product States.
k	Wave number.
G(E)	Driving Force (eV).
$\lambda$	Reorganization Energy (eV).
$\Delta G^0$	Gibbs Energy of Reaction (eV).
B	Arrhenius Factor Constant.
$E_b$	The Activation Energy
$\nu_N$	Nuclear Frequency Parameter.
$K_{eL}$	Transmission Electronic Coefficient.
$\lambda_{in}$	Inner Transition Energy
$\lambda_{out}$	The Outer Transition Energy
$\bar{k}$	Force Constant
$r_r^q$	Equilibrium Bonding Length for Reactant States
$r_p^q$	Equilibrium Bonding Length for Product States
e	Electric Charge
$a_D$	Initially Radii of the Donor
$a_A$	Radius of the Acceptor is central
$d$	Distance Between Donor and Acceptor
$C_{el}$	Coupling Strength
$\langle \varphi_r(r, t)  $	The Wave Function of Reactant
$ \varphi_p(r, t)\rangle$	The Wave Function of Product
$ \varphi_L^S(\vec{r})\rangle$	The wave function of position
$\alpha_L^{S*}(t)$	conjugate of amplitude



$\alpha_L^S(t)$	the amplitude of wave function
$\hat{H}_{el}$	Overlapping Hamiltonian Operator
$H_{el}$	The Coupling of Charge Transfer
$\hat{H}_{S-L}$	Real Hamilton Operator
$\Psi$	Wave function of semiconductor-liquid state
$\hat{H}_S$	Semiconductor Hamiltonian State
$\hat{H}_L$	Molecules Liquid Hamiltonian State
$\hat{H}_{S/L}$	interaction Hamiltonian between semiconductor and liquid states
$n$	Refractive index
T	Absolute temperature (K)
$\mathcal{F}_{SL}$	Flow charge rate ( $\frac{1}{\text{Sec}}$ )
$\hbar$	Dirac constant
$\mathbb{C}_{S/L}(\epsilon)$	coupling strength coefficient
$\rho_{L-S}$	density of state of system
$\delta(\epsilon_S - \epsilon_L)$	Dirac function
$\epsilon_S$	semiconductor energy levels
$\epsilon_L$	liquid energy levels
$k_B$	Boltzmann constant $1.38 * 10^{-23} \text{ J.K}^{-1}$
$\mathcal{T}_S^L(\text{eV})$	reorientation transition energy
$\Delta\mathcal{U}^{LS}(\text{eV})$	effective activation energy for system
$F(\epsilon)$	Fermi function
$l_{ecl}$	effective coupling length
$\rho_a$	atomic density of semiconductor
$D_S(\epsilon)$	density of semiconductor states
$D_{eff(S)}(\epsilon)$	effective density of states for the charge-transfer process

$n_s$	concentration of electron at the Fermi level
$\epsilon_f$	Fermi energy
$E_{cb}$	conduction band of semiconductor
$qE^0$	electrochemical potential of dye
$c$	velocity of light $3 * 10^8 \left(\frac{m}{sec}\right)$
$\beta_d$	distance decay constant relatively
$\delta(n, \epsilon)$	polarity function
$\sigma(n_s, n)$	optical dielectric function
$\sigma(\epsilon_s, \epsilon)$	static dielectric function
$\epsilon_0$	vacuum permittivity
$\epsilon$	static dielectric constant of solvent
$\epsilon_{(\infty)}$	The Optical Dielectric Constants
$\epsilon_{sc}$	dielectric constant of the semiconductor
$n_{s0}$	refractive index of the solvent
$n_{sc}$	refractive index of the semiconductor
$D$	Radius of molecule dye
$R$	distance between the dye and the semiconductor(nm)
$q$	charge of electron.
$M$	molecular weight (g/mol)
$N$	Avogadro number( $6.02 * 10^{23} molecule/mole$ )
$\rho$	Mass density

**Chapter One**

**Introduction**

**and**

**Literature survey**

# Chapter One

## 1.1 Introduction

In the modern daily life, advanced technology which basically depends on power, high technology and modern electrical devices has resulted as a product of electronic transfer components. Therefore, demands for energy become very essential to fulfill the living standard for energy consumption by the population around the world [1].

The electron transition process reactions are very important in nearly most of physical, chemical, biophysical and nanotechnological devices. The simple scenario of single electron transfer has been widely used in organic and inorganic molecules [2], applied physics devices [3], solar energy, renewable energy nanotechnology and nanoscience. The electronic transfer reaction is of great importance in many applications which involve transition of charge from donor to acceptor states. In the fact, charge transfer process is easy in oxidized and reduced precursor systems [4], and it has exploited in difference research areas, including chemical sensors [5], optical memory and display devices [6], photoelectrochromic materials [7], molecular shift registers [8], industrial waste treatment [9], DNA recognition sensors, [10], solar energy [11] and a consequence development of artificial photosynthesis to achieve higher efficiency [12]. The solar energy is clean and environmentally friendly sources which provided a satisfying available energy [13]. Marcus R. introduced the classical charge transfer theory in 1964 and he has award Nobel prize at 1999. Electrons are the main elementary particles have mobile in electronic device and in different condensed materials [14-15]. The charge transfer is the basic processes in molecular electronics, i.e., the charge can transfers cross the potential building at molecule contacts with semiconductor. The charge transfer between molecule and a substrate solid interfaces involves rearrangement of atoms to change

in the electronic distribution, its spatially localized event occurs in system [16]. The transfer occurs when assume continue interaction between the conduction bands and molecular levels [17]. The molecules have been bounded to the semiconductor same as to affect the energy and density of states [18]. In the past decade, the development in the organic opto-electronic field became rapidly, the charge transfer theory in organic-semiconductors has been important subject of extensive investigations [19]. The rate of heterogeneous charge transfer at semiconducting and metallic electrodes have received attention in years ago [20]. The dynamic of electron transfer between molecule photosensitizes and semiconductor systems have been widely investigated in the context of Dye Sensitized Solar Cell (DSSC) systems according to the injection of electron from the photosensitizer to semiconductor in this devices [21]. The main focus of this thesis is the discussion and investigation of the flow charge transition rate factors and the transition energy of controlling the flow charge transfer in semiconductor/molecular of dye interface systems using donor acceptor mechanism, in particular those studies applicable on ZnO/D149, InAs/D149, MgO/D149, ZnO/N749, InAs/N749 and MgO/N749.

## **1.2 Literature survey**

The charge transition at molecular level is a basic role in many research of physics and materials science. Since the first seminar work of Marcus in more than 60 years ago, the electronic transition becomes the fundamental of a mechanism interaction in technical devices [22]. There are many research in the field of charge transfer at molecule-semiconductor system. Here, we will address some of these studies.

**In (2000) Yi Qin Gao et al**, calculated the constants rate of electron transfer reaction at interfaces of semiconductor/liquid system using the tight-binding model and Fermi Golden rule. The surfaces and electronic structures of semiconductors are studied

and compared using z-transform method and slab method. The tight-binding calculations used to calculate the maximum electron transfer constants rate at a semiconductor liquid interface, and the extended-Huckel method also used to calculate the coupling at the interface. Theoretical results are in a good agreement with the experimental measurements [23].

**In (2001) John B. et al**, had been measured the kinetic and dynamics of interfacial electron transfer at semiconductor/molecular interface system using the femtosecond mid-infrared spectroscopic technique. The electron transfer was designed studied to understand the interfacial transition dynamics according to the properties of molecule and semiconductors. They recognized that the transfer of charge was happened from sensitized molecule to semiconductor when the excited molecules promote an electron to the donor state. The transition process has been characterized by the transition time for both fast and slow electrons. The electron transition in molecule/semiconductor systems was affective by the vibrational energy process at the excited state of the molecules. To understand the transfer of electrons observations, they are examined different factors that control the transition, such as driving force, density of states and electronic coupling [24].

**In (2002) Ayelet Vilan and David Cahen**, studied the transition of electron in molecular electronic devices. Molecule of gallium arsenide (GaAs) sensor, gold-silicon and Au-GaAs diodes systems were used in this study. The effect of surfaces of semiconductors and metals with molecules on the electronic energy levels were studied for all systems. The electronic properties were effected rather than electrodynamic properties at interfaces and control on resulting devices based on both dipole and electrical monopole effects of the molecules. The actual electron transport through molecules via chemical bonding to semiconductor surfaces was depend on molecules and electron transport properties of semiconductors. Molecular

thin layers and surface dipole were controlled to the electronic properties of a semiconductor surface and the performance of the sensors and Schottky diode devices [25].

**In (2003) Yuri A. Berlin et al**, were theoretically investigated the electron transport in molecular using a simple hopping model. This model assumes that the elementary charge was hopping a step by step due to electron transfer reaction between donor and acceptor states. The mechanism scenario of charge transfer by hopping were crucially depended on the internal reorientation energy. The density function and Hartree-Fock theories were used to evaluate all the structural parameters that used for chemical attachment in real molecular system. The calculations showed that the charge transfer depends on the configuration and electronic coupling [26].

**In (2004) Francois O. Laforge et al**, reported on the kinetic of electron transfer at water/organic and liquid/water interface. The scanning electrochemical microscopy (SECM) used to measure the electron transfer rate constant the interface of water/organic and ferrocene dissolved in liquid and aqueous ferricyanide. The studies of charge-transfer processes at liquid interfaces and the water/organic solvent were different. The rate constant magnitude of liquid/water was found to be higher than the rate constant of water/organic solvent interface. The factor of electron transfer rate such as driving force and potential are measured over a range of potential at the interface [27].

**In (2005) Neil A. Anderson and Tianquan Lian**, used the analytical study the electron transfer at the contact of molecule-semiconductor interface. They are introduced a fundamental progress to understand the dynamics of electron transfer from molecule to semiconductor nanoparticles. They used the photoexcitation method for the excited states of adsorbed molecule followed by the injection of

electron into semiconductor nanoparticles. This electronic injection method was investigated by electronic and vibrational spectra to measure the injection rate. It has noticed that the injection rate depends on the molecular adsorption, anchoring group, intervening bridging, interfacial environment and the properties of semiconductor nanoparticle. The results were compared with Marcus theory of electron transfer [28].

**In (2006) Sumanta Bhattacharya et al**, had been investigated electron transfer in simple donor-acceptor model of fullerene with vis. 4,4-difluoro-1,3,5,7,8-pentamethyl-2, 6-diethyl-4-bora-3a, 4a-diaza-s-indecene (PM567) dye complexes in toluene solution using the UV-Vis spectroscopy. The charge transitions have been studied in the visible region. The potential of PM567 has been estimated using Mulliken's equation. The interactions between electronic subsystems in PM567 were discussed using a possible mechanism. The electronic coupling, strong and the resonance energies of the electron transfer were estimated using ab initio calculations [29].

**In (2007) Veaceslav Coropceanu et al**, had been discussed the major parameters achieved in the description of charge transport in organic and inorganic semiconductors. The electronic structure of these materials shows that the charge transfer in organic semiconductors is more complex than in inorganic semiconductors. The inorganic semiconductors were described by one-electron (band structure), while the organic semiconductors were described using electron-electron and electron-phonon interactions [30].

**In (2008) Krause S. et al**, had been discussed and determined the transport cross the energy levels for *N,N'*-di(2,6-diisopropylphenyl)-1, 6, 7, 12-tetra(4-tert-butylphenoxy)-perylene-3, 4, 9, 10-tetracarboxylic diimide Dye (PTCDA) organic and semiconductors material using photoemission spectroscopies. The polarization



effects transition charge, vibrations resolution and inhomogeneous broadening contribute were experimentally studied. The results suggested that this model gives a good explains about the dynamic the charge delocalization. The effect of the energy levels of the highest occupied molecular orbit (HOMO) and the lowest unoccupied molecular orbit (LUMO) states were studied and it used to evaluated the exciton binding energies in PTCDA organic materials and finding their effects on the surface polarization of the system [31].

**In (2009) Jaehyung Hwang and et al**, have been focused on understanding and study the mechanisms of charge transfer in organic semiconductor system devices. The electronic properties at the interfaces were determined as a function of molecular levels position and charge transport states. They found that the interface of the system and the dielectric are controlling the charge injection and the transport through the device. This study provided the mechanism of the transport based on the differences between material interfaces, electronic structure and molecular level alignment at the difference between organic-on-metal and metal-on-organic interfaces energetics [32].

**In (2010) Andrew S. Leathers and et al**, has been studied the pathways of electronic transition induced by direct excitation and indirect excitation in metal/semiconductor surface. The direct excitation leads to excite the system resulting in electron transfer state. The indirect excitation leads to photoexcited the system firstly and it transfers to intermediate state undergoes to transitions to the final state nonadiabatically transitions. A theoretical calculation of electronic transition rates has been made based on Liouville-Von Neumann equation and reduced density matrix. The nonadiabatic electronic couplings and Franck-Condon overlap factors are used to describe the populations and quantum coherences throw photoinduced

excitations. They found that the indirect electron transfer is predominant for the transitions in the system compared to the direct electron transfer [16].

**In (2011) Aguiar J. et al**, studied the charge transfer in heterostructures and thin-film devices. The magnetic, magnetoresistive, magnetoelectric and magnetoelastic transport properties are studied in magnetic multilayered thin-film devices. The potential function in manganite-based of magneto transport in molecule /semiconductor constricts by the magnetic coupled with magnetoelectric effects at interfaces. On the other hand, the electron energy loss was studied using the spectroscopy to describe the chemical interplay and the charge transfer at interfaces. The transport properties, electrical and magnetic properties in multilayer devices were determined as a function of the interface structure and associated local chemical environment [33].

**In (2012) Carina Faber et al**, studied and analyzed the excitonic and electronic properties of an organic–semiconductor system in organic photovoltaic solar cells based on developed theory of many-body perturbation and ab initio calculation. The Bethe-Salpeter formalisms technique was used to mark the molecules of the solar cell. They described the charge-transfer excitations in acceptor-donor complexes electronic properties and the electron-phonon coupling. The energy of the charge transfer excitations and the effective potential of electron-phonon coupling was calculated for organic systems. The calculations are based on developed Gaussian auxiliary basis and Bethe-Salpeter formalism with deformation techniques. The results show that the charge-transfer excitations rate and electron-phonon coupling were excellent for quasiparticle properties [34].

**In (2013) Linjun Wanga and David Beljonne**, used the mean field theory to estimate the charge transfer rate between molecules and organic semiconductors

system. The mean field theory with semi-classical Marcus formula and quantum-mechanical Fermi Golden Rule are used to investigate the charge transfer with/without system-bath interaction. The kinetic Monte-Carlo simulation and Pauli master equation have considered to calculate charge transfer rates under different initial conditions. The intermolecular electronic coupling and electron-phonon coupling are carefully investigated for charge transport mobility in molecular dimers. It is found that the field theory with system-bath interaction approaches under Marcus formula as a reference was yielding fully consistent charge transfer rates in molecules system. It was noticed that the mean field simulation indicate that charged molecule and neglected system-bath interaction could be reproduce thermally activated transport [19].

**In (2014) Benlin He, et al**, have demonstrated accelerating the charge transfer in N719 dye complex with  $\text{TiO}_2$  and  $\text{SiO}_2$  by a reflux technique. New absorption bands and light-absorbing species are detected due to UV-Vis is absorption spectra and the fluorescence excitation of complexes. The charge transfer measurements has been carried out to determine the kinetics of charge-transfer. However, the resultant complexes are expected as good electrical-conduction and electrocatalytic behaviors of dye in electrochemical activity and electron transfer [35].

**In (2015) Dorine Ameline et al**, Studied and investigated the electronic properties of semiconductor-dye molecule system using the indigo derivatives. Charge transfer band and Gibbs free energies are used to study the characteristic of injection and dye regeneration with iodide and cobalt electrolytes. They used the time dependent density functional theory (TD-DFT), cyclic voltammetry and UV/visible spectroscopy to investigate the characteristics of the system. The study depends on the use of N, N-di(4-benzoic acid) phenyl amine dye as a donor group, and the indigo as an acceptor group. The quantum chemistry calculations modeled according to TD-

DFT theory to study the electronic and charge transfer band between the donor and acceptor groups at a wavelength of (700 nm) [36].

**In (2016) Hyunwoong Park et al**, studied the kinetics and mechanisms of charge transfers at molecule dye and semiconductor in a solar cell system. The influence of charge transfers by surface and bulk properties of the semiconductor are studied. They found that the efficiency of the solar cell depends on the effective separation of photogenerated charge carriers and the transport to the semiconductor. The surface properties are the main important control factor due to its effect on the interfacial charge transfer. Also, the surface of semiconductor has influenced by photo induced charge transfer behaviors at the interface region. The photo induced charge carriers follow different pathways included trapping and transfer to electron acceptors-donors in the system region [37].

**In (2017) Hadi J.M Al-agealy et al**. Theoretically investigated the electronic transfer rate in dye-semiconductor system devices. Quantum theory has used to evaluate the electronic constant rate depending on the calculation of the effective free energy and reorientation energy of dye-semiconductor system. The electric properties was studied due to results of electronic constant rate. The constant rate investigated according to the estimation of the effective free energy, the reorientation energy, penetration coefficient, square overlapping, unit cell volume and temperature [38].

**In (2018) Hadi J.M Al-agealy et al**, studied the electronic transfer kinetics in N719 with  $\text{TiO}_2$  and ZnO semiconductors using a simple donor acceptor model. The evaluation of current rate for electronic transition in N719 with  $\text{TiO}_2$  and ZnO systems were studied as a function of coupling parameter, transition energies and potential parameters, The analysis of the results shows that the current constant rate

increases with increasing the coupling parameter and decreasing the potential at the interface. The electronic transfer depends on the absorption spectrum and the polarity of the solvents. This different in the rate of electron transfer were related to a difference in semiconductor types in both systems [39].

### **1.3 Aim of the present work**

The main aim of this study is to investigate theoretically the mechanism of flow charge transfer by calculating the flow transition rate of electronic. This study also focuses in the selection of a suitable dye coupled with semiconductor in the system devices that expected to be used in Dye Sensitized Solar Cells.

**Chapter Two**

**Background**

**and**

**Concept of Charge**

**Transfer Reaction**

## Chapter Two

### 2.1 Introduction

The charge transfer reactions in a donor acceptor system confirms no changes in the systems bond through the simplest transformation. It may be also occurs within a large molecule system, from one molecule to another as a results of photo induced, lasers and thermal excitation [40]. The theoretical treatment has showed that moving of charge cross individual molecular, can easily investigated experimentally. However, the charge transfer through solid/molecular interfaces was rarely studied so far. The charge transfer due interfaces of different materials play a key role in variety emerging fields. The transfer cross the solid molecules contact showing in figure (2-1) [41], stays the most important fundamental study in different research field such as photo induced charge transfer at molecular/solid devices, molecular electronics, photo electrolysis, color photography and photo catalysis [42].

In contract, there are many parameters limits the charge transfer including, the configuration of energy levels for molecules relative to solid energy and the electronic binding energies. These parameters create the scenario of charge transfer through organic-solid interface [43]. The structure of energy levels of a molecule with a solid material (semiconductor) refers to the high potential barrier at surfaces of the two materials .

On the other hand, all the studies of charge transfer processes are seeking to investigate the role in which their transition rate depends on material properties, polarity of the solvent media and strength coupling for energy states. In the recent years, theoretical and experimentally studies have been carried out on charge transfer mechanism and the ways that affected the qualitative and quantitative of the electronic transfer process.

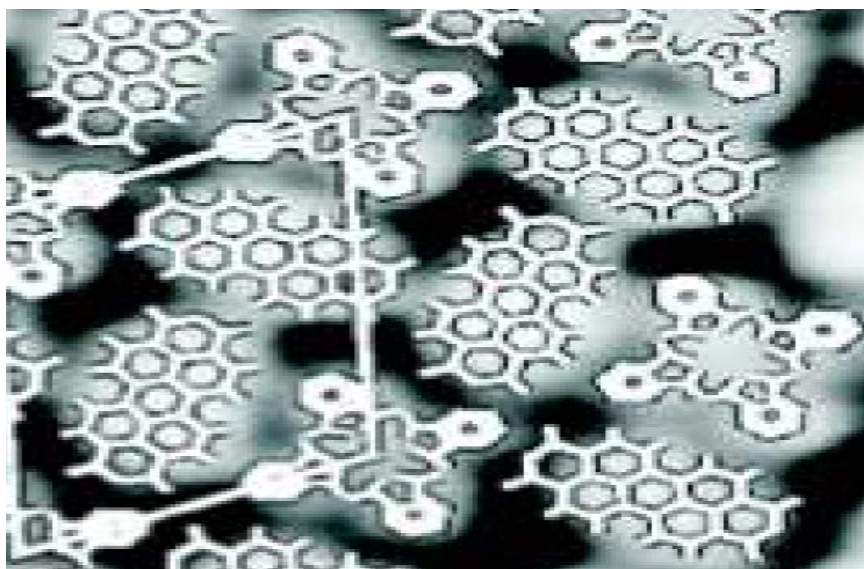


Figure (2-1): Solid/molecules interface [41].

The transfer a cross donor/acceptor system depends on the electrochemical phenomena [44]. The charge transfer field has been introduced by many analytical theories according to standards Marcus theory [45].

## 2.2 Microscopic Concept of Charge Transfer Reaction

The simple concept of charge transfer reactions refers to a simple process which happened in donor-acceptor Marcus model system of molecules. It means that single electron will be transfer from molecule to another in chemical or/and biological system.

In general, the charge transfer reactions that include an electron transfer is named a redox reaction. It could be noted that electron is actually transferring in redox reactions [46].

By considering charge transfer theory, the charge transfer reaction from a donor state  $|\varphi_D\rangle$  to an acceptor state  $|\varphi_A\rangle$  in Eq.(2-1)





where it denoted that initial state as ( $|\varphi_D\rangle + |\varphi_A\rangle$ ) and the final state as ( $|\varphi_D^+\rangle + |\varphi_A^-\rangle$ ).

The resultant charge separation state was created and consisted of the radical cation and anion of the donor  $|\varphi_D^+\rangle$  and acceptor  $|\varphi_A^-\rangle$  electronic states [47]. Different methods of excitation (i.e. thermal, lasers, photo) are well defined the redox potential at the interface and facilitated the charge transfer to generate radical ions. These methods of excitation for acceptor state or donor state show good changes in redox properties due to Marcus parabolas as shown in figure (2-2).

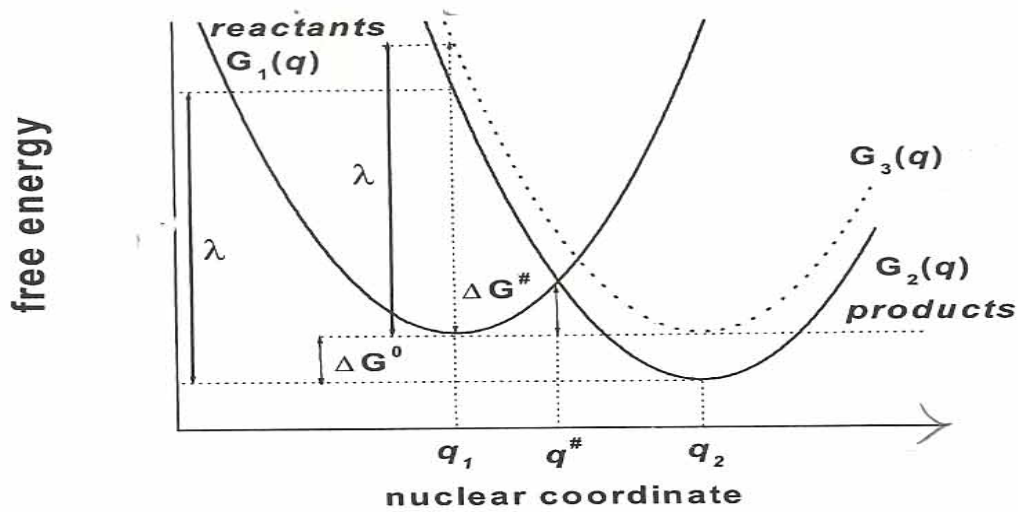


Figure (2-2): Potential energy surface for an electron transfer reaction [48].

The Marcus parabola is a free energy curve which describe the reactant and the product state in Eq.(2-1) . Both excited states  $|\varphi_D\rangle$  and  $|\varphi_A\rangle$ , and charge separated states  $|\varphi_D^+\rangle$  and  $|\varphi_A^-\rangle$  for nuclei that rearrange the configuration at a crossing point in figure (2-2) become energetically degenerate and the electrons will be transfer. classical Marcus theory shows that the energy barrier  $\Delta G^\#$  is the difference between the crossing point ( $q^\#$ ) and the bottom of the reactant free energy  $G$ (eV) of the parabola if the entropy changes are ignored [49]. The quantum statistical analysis introduced the best theory for potential surfaces energy based on multidimensional

coordinates. This statistical calculation investigate and discuss the charge transfer reaction due to Franck-Condon principle and donor-acceptor system with solvent polarity under the stationary and the tunneling phenomena [50].

### **2.3 Analysis of Charge Transfer at Molecule-Semiconductor System**

Fundamentally, the electronic transition is the basic of elementary reactions processes that involved the transfer of an electron from donor state to acceptor state. Electron transfer process is a key aspect in different applications such as light harvesting solar panels and diodes [51]. Since, the flux of electrons can injected from the excited molecular state to the conduction band of a semiconductor when activated by photoinduced, this may described as electron transfer between localized and discrete energy levels of molecules and a continuum energy levels in the semiconductor [28]. In 1960s, the field of charge transfer in solid/liquid interfaces has been developed and advanced by the detailed analytic theory introduced by Marcus [52], Gerischer [53], and Levich [54]. The electron transfer from molecule excited state to conduction band of a semiconductor as shown in figure (2-3) indicates that the electron transfers from reactant state (donor state ) in the molecule excited state to product states (acceptor state) in the conduction band of a semiconductor [28].

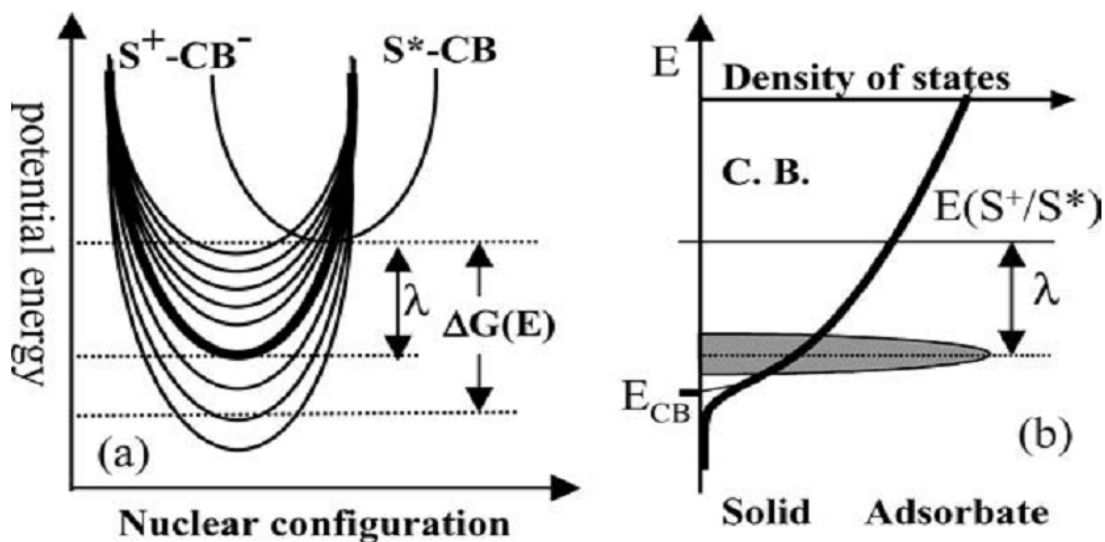


Figure (2-3): a- Charge transfer potential surface between reactant state ( $S^*-CB$ ) and product states ( $S^+-CB^-$ ). b- Schematic illustration of variation of the density of semiconductor states with energy  $E$ . [28].

According to figure (2-3), we can show that the reactant state is connected with a continuous product states, and each state corresponds to the electronic state of electrons in multi variant  $k$  states in semiconductor material. It can be shown from figure (2-3) that the driving force  $G(E)$  and the potential energy of charge transfer vary with the energy of the  $k$  states, and barrier less charge transfer to states at the reorganization energy  $\lambda$  below adsorbed potential. The electronic acceptor states were determined by the adsorbed excited state, oxidation potential [ $E(S^+/S^*)$ ] and the reorganization energy  $\lambda$  [28]. It should be noted that the charge transfer rate could be expressed to all possible acceptor states in the semiconductor [55].

Unfortunately, the theory of potential barrier and activation energy are not easily accessible. Marcus had established activation energy as a function of the Gibbs energy of reaction  $\Delta G(E)$  and the classical reorganization energy  $\lambda$  according to free enthalpy of the reactants and products state as parabolas and using harmonic approximation [56].

## 2.4 Classical Rate of Charge transfer reactions

The Marcus theory introduces a good and simple model for electron transfer depends on the well-known Arrhenius reaction rate as giving by [57].

$$R_{ct} = B e^{\left(\frac{-E_b}{k_B T}\right)} \dots\dots\dots(2-2)$$

where B is Arrhenius factor constant depends on the frequency,  $E_b$  is the activation energy corresponds to the difference between the energy at the crossing point and the energy of the reactants in their equilibrium,  $k_B$  is the Boltzman constant and T is the temperature. The activation energy  $E_b(eV)$ , and the constant B are determined experimentally from the reaction rate and temperature and computationally using transition theory [57,58].

The activation free energy has needed to be supplied the electron transfer reaction to occur is determined to intersection energy relative to the initial state. Additionally, the photo induced charge transfer rate depends on the reorganization energy ( $\lambda$ ) of molecules media which supplied new equilibrium system, which indicates the effect of electrostatic force from nuclei and changed polarity organic media. The photoinduced charge reaction rate is given by [59,60]

$$k_{cT} = v_N K_{eL} e^{-\left(\frac{\Delta G_o + \lambda}{4\lambda RT}\right)} \dots\dots\dots(2-3)$$

where  $v_N$  is nuclear frequency parameter,  $K_{eL}$  the transmission electronic coefficient,  $\Delta G_o$  the activation potential energy and  $\lambda$  is reorganization energy.

## 2.5 Inner and Outer Reorganization Energies for Electron Transfer

The transition energy is a reorientation energy of any system and called the reorganization energy in classical transition theory. The reorganization energy  $\lambda$  for

any system is presented in two contributions; the inner reorganization energy  $\lambda_{in}$  and the outer reorganization energy  $\lambda_{out}$  which written as [61]:

$$\lambda = \lambda_{in} + \lambda_{out} \dots\dots\dots (2-4)$$

The inner reorganization energy is the differences in the reactant state and product state of the molecules. This refers to all the molecular vibrational and rotational movements. The inner reorganization energy is obtained simply by [62];

$$\lambda_{in} = \frac{1}{2} \Sigma \bar{k} (r_r^q - r_p^q)^2 \dots\dots\dots (2-5)$$

where  $\bar{k}$  is a force constant,  $r_r^q$  and  $r_p^q$  are the equilibrium bonding length for reactant states and product states respectively. The outer reorganization energy is the contribution of the transition energy arises from the differences between the polarization properties of the molecules around reactant and product states. The outer reorganization energy can be investigated simply by Marcus model [63].

$$\lambda_{out} = \frac{1}{2} e^2 \left( \frac{1}{4\pi\epsilon_{\square}} \right) \left[ \frac{1}{\epsilon_{(\infty)}} - \frac{1}{\epsilon_{(0)}} \right] \left[ \frac{1}{a_D} + \frac{1}{a_A} - \frac{2}{d} \right] \dots\dots\dots (2-6)$$

where  $e$  is the electron charge,  $\epsilon_{\square}$  is the permittivity of free space,  $\epsilon_{(\infty)}$  and  $\epsilon_{(0)}$  are the optical and static dielectric constants respectively,  $a_D$  and  $a_A$  are initially radii of the donor and acceptor of super molecules and  $d$  is a central distance between donor and acceptor. The outer transition energy is found to be higher than the inner transition energy in any system .

## 2.6 The Electronic Strength Coupling

The electronic strength coupling parameter is applied on the charge transfer reaction between the reactants and products [56]. In Marcus theory, the charge transfer

reactant overlapping with the product state exactly at the crossing point in energy curves. Due to Marcus theory [64]. The coupling strength cross system can discussion the transfer mechanism across interfaces involve weak or force interactions between redox sites and may be defined as [46].

$$C_{el} = \sum \langle \varphi_r(r, t) | \hat{H}_{el} | \varphi_p(r, t) \rangle \dots\dots\dots (2-7)$$

where  $\langle \varphi_r(r, t) |$  and  $|\varphi_p(r, t) \rangle$  are the wave function of the reactant and the product electronic states respectively and  $\hat{H}_{el}$  is the overlapping Hamiltonian operator of the electronic system [65]. The nonadiabatic transition reaction indicates that the transition state was formed before the reactant states are successfully convert to product states. The overlapping of the transition state with product state is due to the transition probability from the donor electronic state to the acceptor electronic state [66]. The coupling of charge transfer  $H_{el}$  indicates that the electronic strength interaction between the donor state of a solid substrate to the acceptor state of a molecule is continuum and vice versa. The electronic strength coupling over molecule and solid occurs when the wave function of the two states is overlapping to each other and the transition rate can estimated based on the matching in oscillations of the wave functions [67]. At the interface photochemistry of the solid, the transition of photo excited substate levels of electrons to molecules resonances are the a dominant mechanism [68]. The interaction between a molecule and a solid is strong at the solid surface. Then the wave function of molecule is overlapping with the wave function of solid as imagine by a molecule wave function mixed with the solid state band energy. This mixing is illustrated schematically as an oscillating of the wave function tail in a periodic lattice [67]. On the other hand, the tunneling occurs at the interface was determined the flow rate of electrons from donor to acceptor states. The electrons were moved between donor and acceptor states for a strong coupling, while the transfer moving between potential energy curves of the reactant

and product states and the electronic states are delocalized. Further, the electronic wave functions are localized on the donor or acceptor state for a small coupling strength. According to the electronic strength coupling for the donor-acceptor system, the charge transition reaction can be classified as non-adiabatic and adiabatic reactions [69].

i- Non-adiabatic charge transition for a weak electronic strength coupling over the donor-acceptor system.

ii- Adiabatic charge transition for a strong electronic strength coupling  $H_{el}$  is larger than adiabatic transition at room temperature T.

## **2.7 The Mechanism of Charge Transfer in Semiconductor-Molecule System**

The semiconductor-molecule system has considered a promising technology owing to its low cost and widely used in different applications. The charge transfer process is the basic of the work of many technology devices such as solar cells, sensors, organic light emitting diodes (OLEDs), organic solar cells (OSCs), organic field effect transistors (OFETs) and nanoelectronic devices. It is describing the conversion of light into electrons in a semiconductor-molecule system as seen in Figure (2-4) [70]. In the heterojunction semiconductor-molecule system, the electrons transfer from molecule to the conducting states in semiconductor a cross the potential that forming at the interfaces between the two materials. The basic of kinetic semiconductor-molecule devices are majority carrier of electrons. In these devices, the dye is photo excited by absorbing the incident light on the surface. However, the semiconductor-molecule devices are classified under the excitonic cells, indicate that the molecule was absorbed light to reach the excited state electrons transfer in these devices [71,72].

In the semiconductor-molecule heterojunction devices shown in figure (2-4) the molecule excites at the interface resulting in more electrons were injected to the conduction band of the semiconductor [72]. The types of semiconductors (P or N) are very important parameters along with the sensitized molecule systems because they control the efficiency of the solar cell. The sensitized molecule photocathodes based on semiconductor, promotes the electron injection into the energy level of the semiconductor under the light excitation of the sensitizer [36]. However, the kinetics of the charge transfer do not significantly change when the electrolyte mediator charged by a solid-state material. This indicates that the injection of the charges by the sensitizer molecules in bath electrolyte and solid-state solar cells are same [73]. The charges transfer in semiconductor-molecule devices depends on different parameters such as the potential at interface between donor and acceptor [74], the electronic coupling between molecule and the semiconductor [75] and the election density of states [76] .

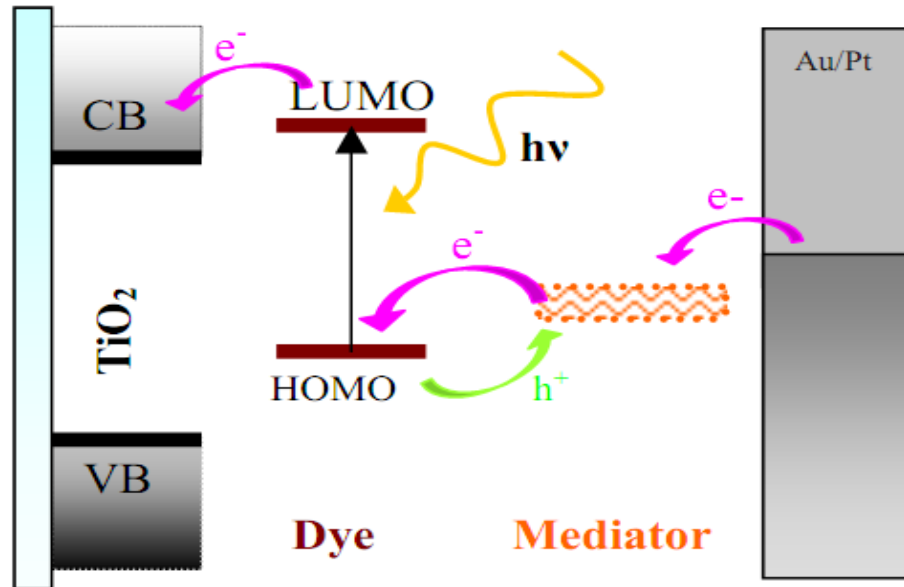


Figure (2-4). Schematic diagram of semiconductor-molecule cells [70].



Further, the classical Marcus theory indicates that the charge transfer rate depends on the overlapping energetic of donor (molecule) and acceptor (semiconductor) states that correspond to the density of states at energy related to the conduction band edge, reorientation energy, and temperature (T). At a specific temperature, the overlapping energetic increases with increasing the density of state and the smaller reorientation energy reaches its maximum value when the donor state energy level lies above the conduction band of the semiconductor [77]. However, the electronic properties of sensitized molecule supplied the better characterized as a mobile excited state and make the charge transfer was very matching to semiconductor. Also, the charge transfer to the electrode is happened either by hopping or diffusing mechanism depends on the nature of the mediator [69].

## **2.8 Dye Sensitized**

In early time of the 19th century, the dye sensitized molecules were used in photography field after Moser and Rigollot showed that the photoelectric effect in silver plates were enhanced in sensitized dye. In the late 1960's, the sensitized mechanism in dye-sensitization process was studied by Gerischer [78]. Gerischer studied the photosensitized stability in the visible region by dye adsorption with semiconductors surface. Recently, Moser and Gerischer introduce the fundamental basic to understand and investigate the charge transition processes in the conduction band of a semiconductor that immersed in a redox electrolyte. However, the electrolyte redox chemistry leads to increase and improve the selection of photoelectrode materials and sensitizers [79,80]. With increasing demand for technology devices, researches were to focused on fabricating pointed and high efficient sensitizers dyes that used in these devices [81]. The sensitizer molecules have been reached efficiencies in the range of 3-8% [82]. Different sensitizers such as N749 and N3 were synthesized and the obtained efficiencies for them were around

11% [83,84]. Furthermore, the “black dye” and D149 have developed to match the energy levels of the sensitizer groups with the energy state of semiconductor which lead to charges transfer across the interface [78]. The most common sensitized dyes that used in charge transfer studies is the N749, which is green in color and composed of terpyridyl ligand around ruthenium metal [85]. Although the N749 has a wide range of studies and also named black dye with a chemical structure as shown in figure (2-5) [86].

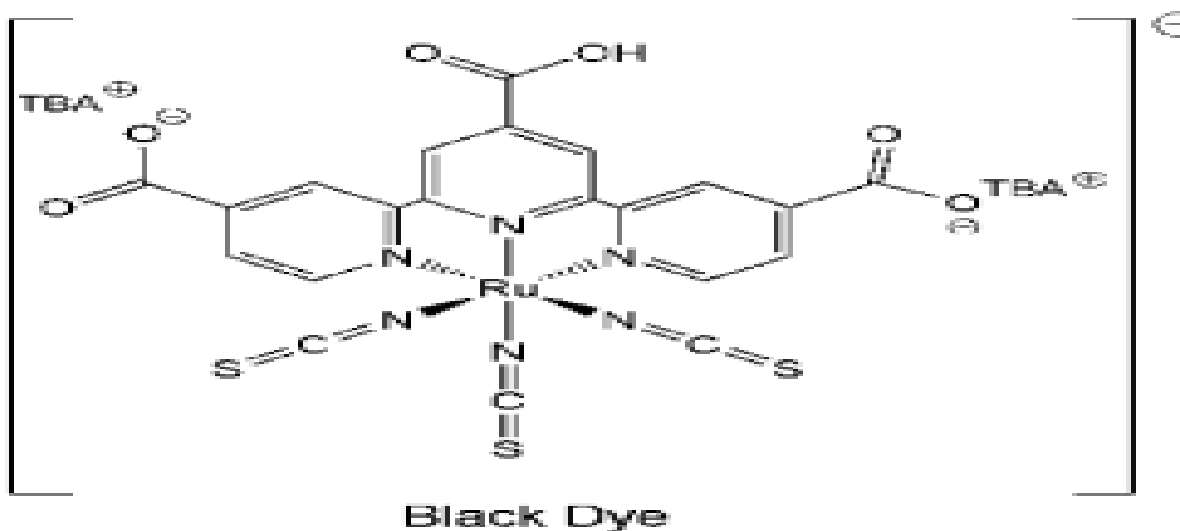


Figure (2-5): Chemical structure of the Black Dye molecules N749 [86]

However, the N749 is showing the highest efficiency comparing with organic dyes [87]. The N749 dye has over efficient around 9.9% for a small area and 11% for a large area [88]. Further, the D149 molecule dye is the most attracted organic dye using in dye sensitized solar cells. The excited state lifetimes depend strongly on the solvent concentration. The D149 is the most important efficient pure organic dyes and have given efficiency around 9% [89]. The indoline-based dye D149 is a new organic sensitizer and its chemical structure is shown in figure (2-6) [90]. The fundamental mechanism of the charge transfer process shown in figure (2-7) that

takes place in dye-semiconductor interface devices after the absorption of light (photon) by sensitized dye, is an interfacial electron transition from the electronically dye's excited state to the conduction band of the semiconductor (CB) within a few hundred femtoseconds.

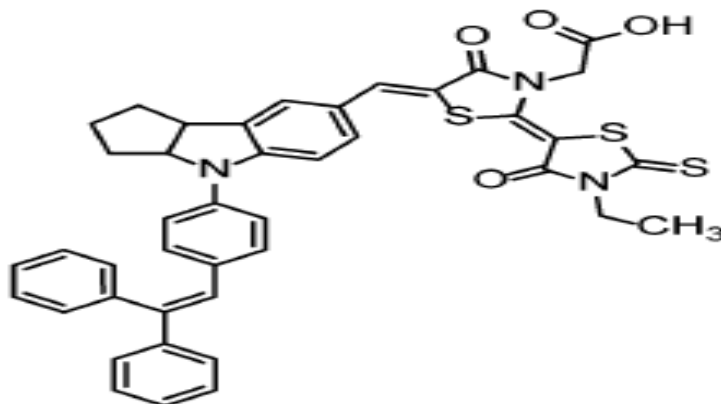
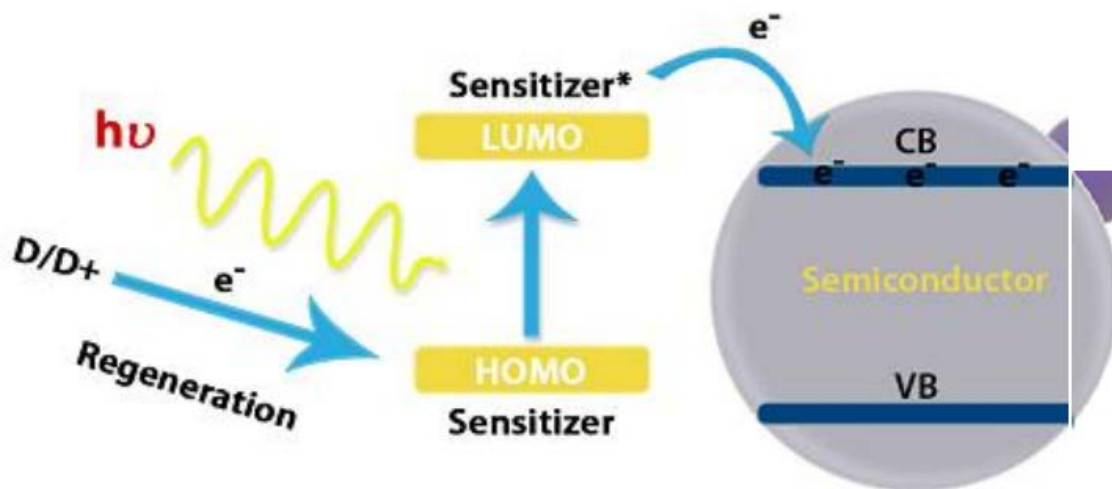


Figure (2-6): Chemical structure of D149 sensitized dye [90].



Figure(2-7):Schematic diagram of the charge transfer of Dye-Semiconductor system [91].

## 2.9 Semiconductors

The semiconductor materials have electrical conductivity lies between metals and insulators. Unlike the insulator, The semiconductor conducts electricity under certain conditions. However, the discussion of this behavior depends on understanding the conduction and the valence bands structure. Due to continuum model, it can be considered that the discrete energy levels in the molecule are occupied by electrons in molecules. In order to the molecule contained more atoms, the orbital of atoms will be transformation to a molecular orbital. In contract the charge transfer happened where the discrete energy levels reform to continuous bands of energy states for macroscopic crystalline structures. The semiconductor has the upper energy band which called the conduction band (CB) separated by the energy gap from the lower energy band which called the valence band (VB). Energy gap play an important role for the electrical properties of metals. The metals show zero energy gap resulting in more electrons distributed in the energy states of the conduction band, whereas the energy gaps is very big in insulators force. Metals also appear high electrical conductivity due to free electrons that filled their states, While insulators have very few filled states to restricted valence band alone and cannot easily to accepted electrons [92-93]. On the other hand, the semiconductor materials behave as insulators in their ground state with a large energy gap. But, when they excited by heat or light, their energy gaps become relatively small and the electron can easily cross the energy gap toward the conduction band [93]. Indium arsenide (InAs) is one of the III/V compound semiconductors, and it widely used in different application such as heterostructures and nanostructures due to its small energy gap and high electron mobility. The N-type InAs has a minimum conduction band situated in the center of the Brillouin zone [94]. On the other hand, the ZnO and MgO semiconductors are the most common binary II-VI semiconductor materials.

The ZnO and MgO have been widely used in modern electronic applications, While the ZnO shows a wurtzite structure with energy-band gap around 3.4 eV, MgO shows a rock salt structure with energy band-gap around 7.7 eV. [95-96].

## **2.10 Organic Material/Semiconductor Interfaces**

Recently, many optoelectronic devices were developed and investigated based on molecular-semiconductor interfaces. Different types of organic sensitized molecules can modify the interface potential of new molecular/semiconductor devices [97]. In interface contact, the interactions between semiconductor bands and energy levels of molecules will be leading to interesting effects differential resistance [98]. Due to the electronic applications, the molecules are covalently attached to semiconductor [99]. Studies of molecule-semiconductor contact devices are employed degenerated doping and treating the substrate of devices [100] and used moderator to treated on a Schottky diode [101]. These indicate that the systems have large energy differences between the semiconductor Fermi level and molecular energy levels. The chemical bounded of molecules to the semiconductor was likely to the energy density and density of surface state effect and the semiconductor will be band bending [18]. Furthermore, the charge at the semiconductor/molecule interface can be affected by the barrier at interfaces [102]. Some researchers suggested that the electron transport mechanisms are operating in device limited by transition over Schottky barrier or by tunneling through the system [103].

## **2.11 Solvents**

As part of the charge transfer reaction study of semiconductor-molecule systems, the solvents play an important role as media to par electrons transferring. The solvents that widely investigated are Propanol, Butanol, Octanol, Dichloroethane and Acetonitrile. The general properties of these solvents are listed in table (2-1) [104].

# **Chapter Three**

## **Theoretical Part**

## Chapter Three

### 3.1 Theoretical Model

The evolution of flux current for semiconductor-liquid system has been determined due to real Hamilton operator  $\hat{H}_{S-L}$ . On the other hand, the equation of motion based on the Liouville equation and using the density of state  $\hat{\rho}_{L-S}$  is given by [105].

$$\frac{d\hat{\rho}_{L-S}}{dt} = -\frac{i}{\hbar} [\hat{H}_{S-L}, \hat{\rho}_{L-S}] \dots \dots \dots (3-1)$$

This equation is equivalent to Schrödinger equation of motion for pure states [106].

$$\frac{d}{dt} |\Psi_{S-L}(r, t)\rangle = -\frac{i}{\hbar} \hat{H}_{S-L} |\Psi_{S-L}(r, t)\rangle \dots \dots \dots (3-2)$$

Where  $|\Psi_{S-L}(r, t)\rangle$  is the wave function of semiconductor-liquid state and  $\hbar$  is Dirac constant. The wave function of semiconductor-liquid state is given by [107].

$$|\Psi_{S-L}(r, t)\rangle = \sum_{n=0}^{\infty} \alpha_L^S(t) |\varphi_L^S(\vec{r})\rangle e^{-i\frac{\epsilon_n t}{\hbar}} \dots \dots \dots (3-3)$$

where  $\alpha_L^S(t)$  is the amplitude of wave function,  $t$  is the time,  $|\varphi_L^S(\vec{r})\rangle$  is the wave function of position,  $\epsilon_n$  is the energy of electron at conduction band of semiconductor or molecule energy level and the  $\hat{H}_{S-L}$  is given by [108].

$$\hat{H}_{S-L} = \hat{H}_S + \hat{H}_L + \hat{H}_{S/L} \dots \dots \dots (3-4)$$

where  $\hat{H}_S$  is the semiconductor state Hamiltonian,  $\hat{H}_L$  is the molecules liquid state Hamiltonian and  $\hat{H}_{S/L}$  is the interaction Hamiltonian between semiconductor and liquid states. The flow charge through liquid and semiconductor system is illustrated in Figure (3-1) [25] it has been treated using a quantum postulate theory. This theory is a time dependent theory, not because it uses some special time solution of Schrödinger equation, but because it refers to the time scale of perturbation itself. On the other hand the Hamiltonian of metal/molecule system must satisfied the Eigen values equation.

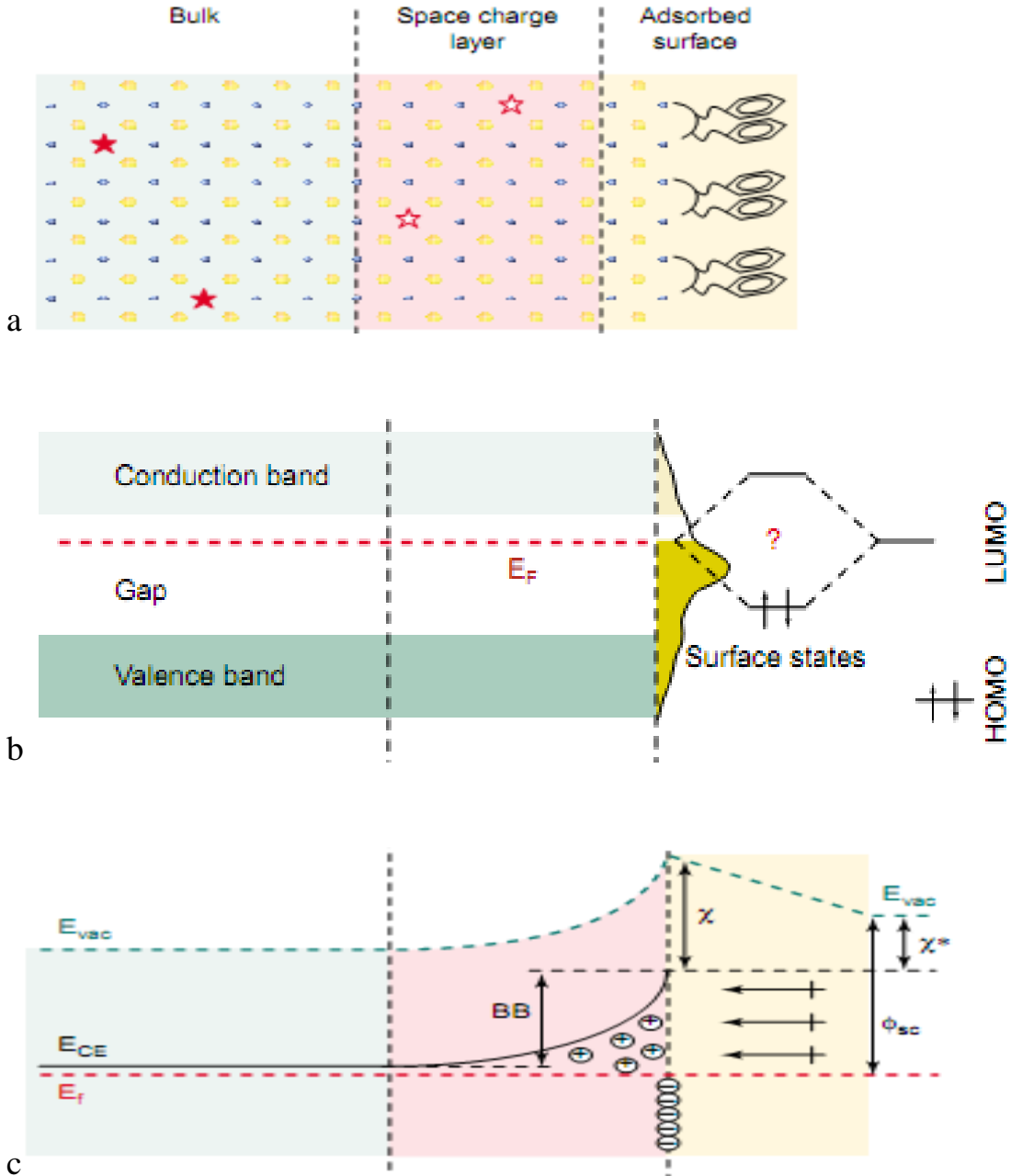


Figure (3-1): A schematic diagram of the basic of charge transition at molecules dye and semiconductor surfaces contact [25]

One can substitute Eq.(3-4) in Eq.(3-2),

$$\begin{aligned} \frac{d}{dt} |\Psi_{S-L}(r, t)\rangle &= -\frac{i}{\hbar} (\hat{H}_S + \hat{H}_L + \hat{H}_{S/L}) |\Psi_{S-L}(r, t)\rangle \\ &= -\frac{i}{\hbar} [\hat{H}_S |\Psi_{S-L}(r, t)\rangle + \hat{H}_L |\Psi_{S-L}(r, t)\rangle + \hat{H}_{S/L} |\Psi_{S-L}(r, t)\rangle] \dots\dots (3-5) \end{aligned}$$



By derivation Eq.(3-3) for wave function at liquid state with respect to time we get:

$$\frac{d}{dt} |\Psi_{S-L}(r, t)\rangle = \sum_{n=0}^{\infty} \left[ \frac{d\alpha_L^S(t)}{dt} (|\varphi_L^S(\vec{r})\rangle e^{-i\frac{\epsilon_L t}{\hbar}}) + \alpha_L^S(t) \frac{d(|\varphi_L^S(\vec{r})\rangle e^{-i\frac{\epsilon_L t}{\hbar}})}{dt} \right] \dots (3-6)$$

By substituting Eq.(3-3) and Eq.(3-6) in Eq.(3-5) we get.

$$\sum_{n=0}^{\infty} \left[ \frac{d\alpha_L^S(t)}{dt} (|\varphi_L^S(\vec{r})\rangle e^{-i\frac{\epsilon_L t}{\hbar}}) + \alpha_L^S(t) \frac{d(|\varphi_L^S(\vec{r})\rangle e^{-i\frac{\epsilon_L t}{\hbar}})}{dt} \right] = -\frac{i}{\hbar} \sum_{n=0}^{\infty} (\hat{H}_S + \hat{H}_L) \alpha_L^S(t) (|\varphi_L^S(\vec{r})\rangle e^{-i\frac{\epsilon_L t}{\hbar}}) - \frac{i}{\hbar} \sum_{n=0}^{\infty} \hat{H}_{S/L} \alpha_L^S(t) (|\varphi_L^S(\vec{r})\rangle e^{-i\frac{\epsilon_L t}{\hbar}}) \dots (3-7)$$

The second term in both sides of Eq.(3-7) is neglected according to the time independent Schrödinger equation  $(\hat{H}_S + \hat{H}_L) |\Psi_{S-L}(r, t)\rangle = \hat{E} |\Psi_{S-L}(r, t)\rangle$  then

$$\alpha_L^S(t) \frac{d(|\varphi_L^S(\vec{r})\rangle e^{-i\frac{\epsilon_L t}{\hbar}})}{dt} = -\frac{i}{\hbar} \sum_{n=0}^{\infty} (\hat{H}_S + \hat{H}_L) \alpha_L^S(t) (|\varphi_L^S(\vec{r})\rangle e^{-i\frac{\epsilon_L t}{\hbar}}) \dots (3-8)$$

While the Eq.(3-7) become

$$\sum_{n=0}^{\infty} \left[ \frac{d\alpha_L^S(t)}{dt} (|\varphi_L^S(\vec{r})\rangle e^{-i\frac{\epsilon_L t}{\hbar}}) \right] = -\frac{i}{\hbar} \sum_{n=0}^{\infty} \hat{H}_{S/L} \alpha_L^S(t) (|\varphi_L^S(\vec{r})\rangle e^{-i\frac{\epsilon_L t}{\hbar}}) \dots (3-9)$$

The electrons at conduction energy level describe by Bra wave function for semiconductor is given by.

$$\langle \Psi_{S-L}(r, t) | = \sum_{n=0}^{\infty} \alpha_L^{*S}(t) \langle \varphi_L^S(\vec{r}) | e^{+i\frac{\epsilon_S t}{\hbar}} \dots (3-10)$$

Multiply both sides of Eq.(3-9) by Bra wave function for semiconductor to give us a coupling coefficient function that leads to.

$$\sum_{n=0}^{\infty} \frac{d\tilde{\alpha}_L^S(t)}{dt} \langle \varphi_L^S(\vec{r}) e^{+i\frac{\epsilon_S t}{\hbar}} | \varphi_L^S(\vec{r}) e^{-i\frac{\epsilon_L t}{\hbar}} \rangle = -\frac{i}{\hbar} \sum_{n=0}^{\infty} \alpha_L^{*S}(t) \langle \varphi_L^S(\vec{r}) | e^{+i\frac{\epsilon_S t}{\hbar}} \hat{H}_{S/L} \alpha_L^S(t) | \varphi_L^S(\vec{r}) \rangle e^{-i\frac{\epsilon_L t}{\hbar}} \dots (3-11)$$

where  $\alpha_L^{*S}(t)$  is the conjugate of amplitude, assumption  $\tilde{\alpha}_L^S(t) = \alpha_L^S(t) \alpha_L^{*S}(t)$ .

The summation of complete set wave function is satisfied

$$\langle \varphi_L^S(\vec{r}) e^{+i\frac{\epsilon_S t}{\hbar}} | \varphi_L^S(\vec{r}) e^{-i\frac{\epsilon_L t}{\hbar}} \rangle = \begin{cases} 1 & \text{for normalized} \\ 0 & \text{for orthogonal} \end{cases} \dots (3-12)$$

The Eq.(3-11) can be written as

$$\frac{d\tilde{\alpha}_L^S(t)}{dt} = -\frac{i}{\hbar} \sum_{n=0}^{\infty} e^{+i\frac{\epsilon_S t}{\hbar}} \alpha_{L}^{*S}(t) \langle \varphi_L^S(\vec{r}) | \hat{H}_{S/L} \alpha_L^S(t) | \varphi_L^S(\vec{r}) \rangle e^{-i\frac{\epsilon_L t}{\hbar}} \dots\dots\dots (3-13)$$

We simplified Eq.(3-13) to

$$\frac{d\tilde{\alpha}_L^S(t)}{dt} = -\frac{i}{\hbar} \sum_{n=0}^{\infty} e^{+i\frac{\epsilon_S t}{\hbar}} \langle \alpha_{L}^{*S}(t) \varphi_L^S(\vec{r}) | \hat{H}_{S/L} | \alpha_L^S(t) \varphi_L^S(\vec{r}) \rangle e^{-i\frac{\epsilon_L t}{\hbar}} \dots\dots\dots (3-14)$$

The expectation values of the strength coupling is given by [109].

$$\mathbb{C}_{S/L}(\epsilon) = \langle \alpha_L^S(t) \varphi_L^S(\vec{r}) | \hat{H}_{S/L} | \alpha_L^S(t) \varphi_L^S(\vec{r}) \rangle \dots\dots\dots (3-15)$$

However, we can find how  $\alpha_L^S(t)$  evolves in time from t=0, then Eq.(3-14)

was rewritten as an integral .

$$\tilde{\alpha}_L^S(t) = -\frac{i}{\hbar} \int_0^t \mathbb{C}_{S/L}(\epsilon) e^{-i\frac{(\epsilon_L - \epsilon_S)t}{\hbar}} dt \dots\dots\dots (3-16)$$

We solved the integral in Eq.(3-16) to results .

$$\int_0^t \mathbb{C}_{S/L}(\epsilon) e^{-i\frac{(\epsilon_L - \epsilon_S)t}{\hbar}} dt = \mathbb{C}_{\frac{S}{L}}(\epsilon) \frac{[e^{-i\frac{(\epsilon_L - \epsilon_S)t}{\hbar}} - 1]}{-i\frac{(\epsilon_L - \epsilon_S)}{\hbar}} \dots\dots\dots (3-17)$$

Inserting Eq.(3-17) in Eq.(3-16) to results .

$$\tilde{\alpha}_L^S(t) = \frac{1}{\hbar} \mathbb{C}_{\frac{S}{L}}(\epsilon) \frac{[e^{-i\frac{(\epsilon_L - \epsilon_S)t}{\hbar}} - 1]}{\frac{(\epsilon_L - \epsilon_S)}{\hbar}} \dots\dots\dots (3-18)$$

Then the probability of current flow charge transfer is given by [110].

$$PFC = |\tilde{\alpha}_L^S(t)|^2 = \left| \frac{1}{\hbar} \mathbb{C}_{\frac{S}{L}}(\epsilon) \frac{[e^{-i\frac{(\epsilon_L - \epsilon_S)t}{\hbar}} - 1]}{\frac{(\epsilon_L - \epsilon_S)}{\hbar}} \right|^2 \dots\dots\dots (3-19)$$

Simply to

$$PFC = |\tilde{\alpha}_L^S(t)|^2 = \frac{|\mathbb{C}_{\frac{S}{L}}(\epsilon)|^2}{\hbar^2} \left| \frac{[e^{-i\frac{(\epsilon_L - \epsilon_S)t}{\hbar}} - 1]}{\frac{(\epsilon_L - \epsilon_S)}{\hbar}} \right|^2 \dots\dots\dots (3-20)$$

Assuming that  $z = \frac{(\epsilon_L - \epsilon_S)t}{\hbar}$  then [129].

$$|e^{iz} - 1|^2 = 4(\text{Sin} \frac{z}{2})^2 \dots \dots \dots (3-21)$$

Then Eq. (3-20) may be written as.

$$PFC = \frac{|\mathbb{C}_S(\epsilon)|^2}{\hbar^2} \frac{4(\text{Sin} \frac{(\epsilon_L - \epsilon_S)t}{2\hbar})^2}{[\frac{(\epsilon_L - \epsilon_S)}{\hbar}]^2} \dots \dots \dots (3-22)$$

Simply to

$$PFC = \frac{|\mathbb{C}_S(\epsilon)|^2}{\hbar^2} \frac{(\text{Sin} \frac{(\epsilon_L - \epsilon_S)t}{2\hbar})^2}{[\frac{(\epsilon_L - \epsilon_S)}{2\hbar}]^2} \dots \dots \dots (3-23)$$

For the long time  $t = \infty$  with assuming  $x = \frac{(\epsilon_L - \epsilon_S)}{2\hbar}$  and depending on relationship [130].

$$\frac{(\text{Sin}xt)^2}{x^2} \Big|_{t=\infty} = \pi t \delta(x) \dots \dots \dots (3-24)$$

So that, making the probability is.

$$PFC = \frac{|\mathbb{C}_S(\epsilon)|^2}{\hbar^2} \pi t \delta\left(\frac{(\epsilon_L - \epsilon_S)}{2\hbar}\right) \dots \dots \dots (3-25)$$

Where  $\delta$  is the Dirac delta function [131].

$$\frac{1}{|a|} \delta(y) = \delta(ay) \dots \dots \dots (3-26)$$

Then  $\delta\left(\frac{(\epsilon_L - \epsilon_S)}{2\hbar}\right)$  according to Eq.(3-26) for  $y = (\epsilon_L - \epsilon_S)$  , and  $a=1/2\hbar$

$$\delta\left(\frac{(\epsilon_L - \epsilon_S)}{2\hbar}\right) = 2\hbar \delta(\epsilon_L - \epsilon_S) \dots \dots \dots (3-27)$$

For substituting Eq.(3-27) in Eq.(3-25) ,we gate[110].

$$PFC = \frac{2\pi}{\hbar} |\mathbb{C}_{S/L}(\epsilon)|^2 \delta(\epsilon_S - \epsilon_L)t \dots\dots\dots(3-28)$$

The total probability of current flow charge transfer due to density of state  $\rho_{L-S}$  is given by:

$$\overline{PFC} = \frac{2\pi}{\hbar} |\mathbb{C}_{S/L}(\epsilon)|^2 \rho_{L-S} \delta(\epsilon_S - \epsilon_L)t \dots\dots\dots (3-29)$$

The flow current rate of transition is [111].

$$\mathcal{F}_{ET} = \frac{\overline{PFC}}{t} \dots\dots\dots(3-30)$$

We inserting Eq.(3-29) in Eq.(3-30) and integrating to give us a flow current rate of transition.

$$\mathcal{F}_{SL} = \frac{2\pi}{\hbar} \int |\mathbb{C}_{S/L}(\epsilon)|^2 \rho_{L-S} \delta(\epsilon_S - \epsilon_L) d\epsilon \dots\dots\dots (3-31)$$

The density of state depends on the perturbation methods and given by [112,55].

$$\rho_{S-L}(\epsilon) = (4\pi k_B T \mathcal{J}_S^L)^{-\frac{1}{2}} \exp - \left[ \frac{(\Delta\mathcal{U}^{LS} + \mathcal{J}_S^L)^2}{4k_B T \mathcal{J}_S^L} \right] \dots\dots\dots (3-32)$$

For charge transfer in semiconductor/liquid system, the difference in energy  $\epsilon_L - \epsilon_S$  is the potential barrier height  $\Delta\mathcal{U}^{LS}$  and is given as [104].

$$\Delta\mathcal{U}^{LS} = \epsilon_L - \epsilon_S \dots\dots\dots (3-33)$$

By substituting Eq.(3-32) in Eq.(3-31), we get.

$$\mathcal{F}_{SL} = \frac{2\pi}{\hbar} \int (4\pi k_B T \mathcal{J}_S^L)^{-\frac{1}{2}} |\mathbb{C}_{S/L}(\epsilon)|^2 \exp - \frac{(\Delta\mathcal{U}^{LS} + \mathcal{J}_S^L)^2}{4k_B T \mathcal{J}_S^L} \delta(\epsilon_S - \epsilon_L) d\epsilon \dots\dots\dots(3-34)$$

where  $k_B$  is Boltzman constant,  $T$  is a temperature ( $T=25^\circ\text{c}$ ),  $\mathcal{J}_S^L$  is the reorientation transition energy,  $\Delta\mathcal{U}^{LS}$  is the effective activation energy (potential) of the system. The flow charge transfer rate in Eq.(3-34) will

reformed with Fermi occupancy function due to the continuum level energies for the system material of the charge density of state  $F_{(\epsilon)}$  results in.

$$\mathcal{F}_{S-L} = \frac{2\pi}{\hbar} \int (4\pi k_B T \mathcal{J}_S^L)^{-\frac{1}{2}} |\mathbb{C}_{S/L}(\epsilon)|^2 \exp - \frac{(\Delta u^{LS} + \mathcal{J}_S^L)^2}{4k_B T \mathcal{J}_S^L} F_{(\epsilon)} \delta(\epsilon_S - \epsilon_L) d\epsilon \dots (3-35)$$

For flow charge transfer of electrons, the effective density of state for semiconductor-liquid system  $D_S(\epsilon)$  can be given by [113].

$$D_{eff(S)}(\epsilon) = \sum_{S,L} \delta(\epsilon_S - \epsilon_L) \dots \dots \dots (3-36)$$

Thus, the effective density of states for the charge-transfer process is [114].

$$D_{eff(S)}(\epsilon) = D_S \frac{l_{ecl}}{\rho_a^{2/3} (\frac{6}{\pi})^{1/3}} \dots \dots \dots (3-37)$$

Where  $D_S$  is the density of electronic states in the semiconductor material at room temperature,  $l_{ecl}$  is the effective coupling length and  $\rho_a$  is the atomic density of semiconductor.

The density of states for semiconductor material  $D_S$ , results by applying the Drude model for free-electrons [115].

$$D_S = \frac{3}{2} \left( \frac{n_S(\epsilon_f)}{\epsilon_f} \right) \dots \dots \dots (3-38)$$

Where  $n_S$  is the concentration of electron at Fermi level and  $\epsilon_f$  is the Fermi energy. By inserting Eq.(3-36) and Eq.(3-37) in Eq.(3-35) we get.

$$\mathcal{F}_{S-L} = \frac{2\pi}{\hbar} \int (4\pi k_B T \mathcal{J}_S^L)^{-\frac{1}{2}} |\mathbb{C}_{S/L}(\epsilon)|^2 \exp - \frac{(\Delta u^{LS} + \mathcal{J}_S^L)^2}{4k_B T \mathcal{J}_S^L} D_S \frac{l_{ecl}}{\rho_a^{2/3} (\frac{6}{\pi})^{1/3}} F_{(\epsilon)} d\epsilon \dots \dots (3-39)$$

However, the nuclear terms over the interface region are out of integral and one obtains.

$$\mathcal{F}_{S-L} = \frac{2\pi}{\hbar} (4\pi k_B T \mathcal{T}_S^L)^{\frac{-1}{2}} \frac{l_{ecl}}{\rho_a^{2/3} (\frac{6}{\pi})^{1/3}} \int |\mathbb{C}_{S/L}(\epsilon)|^2 \exp - \frac{(\Delta\mathcal{U}^{LS} + \mathcal{T}_S^L)^2}{4k_B T \mathcal{T}_S^L} D_S F(\epsilon) d\epsilon \dots (3-40)$$

The potential at interface of semiconductor-liquid contact is given by [116]

$$\mathcal{U}^{LS} = E_{cb} - qE^0 \dots \dots \dots (3-41)$$

Where  $E_{cb}$  is the energy of conduction band of the semiconductor and  $qE^0$  is the electrochemical potential of the dye. The flow charge rate as a function of distance decay constant  $\beta_d$  is given by [55] .

$$\mathcal{F}_{S/L} \left( \mathcal{T}_S^L, \Delta\mathcal{U}^{LS}, \mathbb{C}_S(\epsilon), E_{cb}, qE^0 \right) = \frac{\mathcal{F}_{S-L}(\mathcal{T}_S^L, \Delta\mathcal{U}^{LS}, \mathbb{C}_{S/L}(\epsilon),)}{\beta_S} \dots \dots \dots (3-42)$$

By substituting Eq.(3-40) in Eq.(3-42) the following expression is obtained:

$$\mathcal{F}_{S/L} \left( \mathcal{T}_S^L, \Delta\mathcal{U}^{LS}, \mathbb{C}_{S/L}, E_{cb}, qE^0 \right) = \frac{2\pi}{\hbar} \frac{((4\pi k_B T \mathcal{T}_S^L)^{\frac{-1}{2}})}{\beta_S} \frac{l_{ecl}}{\rho_a^{2/3} (\frac{6}{\pi})^{1/3}} \int_{-\infty}^{+\infty} |\mathbb{C}_{S/L}(\epsilon)|^2 \exp - \frac{(\Delta\mathcal{U}^{LS} + \mathcal{T}_S^L)^2}{4k_B T \mathcal{T}_S^L} D_S F(\epsilon) d\epsilon \dots \dots \dots (3-43)$$

On the other hand, the flow charge rate can be reformed by inserting Eq.(3-41) in Eq.(3-43).

$$\mathcal{F}_{S/L} \left( \mathcal{T}_S^L, \Delta\mathcal{U}^{LS}, \mathbb{C}_S, E_{cb}, qE^0 \right) = \frac{2\pi}{\hbar} \frac{((4\pi k_B T \mathcal{T}_S^L)^{\frac{-1}{2}})}{\beta_S} \frac{l_{ecl}}{\rho_a^{2/3} (\frac{6}{\pi})^{1/3}} \int_{-\infty}^{+\infty} |\mathbb{C}_{S/L}(\epsilon)|^2 \exp - \frac{(E_{cb} - qE^0 + \mathcal{T}_S^L)^2}{4k_B T \mathcal{T}_S^L} D_S F(\epsilon) d\epsilon \dots \dots \dots (3-44)$$

Thus, the nuclear terms are essentially constant over the region where the integrand in eq.(3-44) was non negligible, and one obtains

$$\mathcal{F}_{S/L}(\mathcal{J}_S^L, \Delta\mathcal{U}^{LS}, \mathbb{C}_{S/L}, E_{cb}, qE^0) = \frac{2\pi}{\hbar} \frac{((4\pi k_B T \mathcal{J}_S^L)^{\frac{-1}{2}})}{\beta_S} \frac{l_{ecl}}{\rho_a^{2/3} (\frac{6}{\pi})^{1/3}} |\mathbb{C}_{S/L}(\epsilon)|^2 \exp - \frac{(E_{cb} - qE^0 + \mathcal{J}_S^L)^2}{4k_B T \mathcal{J}_S^L} \int_{-\infty}^{E_{cb}} D_S F(\epsilon) d\epsilon \dots \dots \dots (3-45)$$

The integral in Eq.(3-45) is a well-known the effective density of states in the conduction band of the semiconductor  $N_c(\text{cm}^{-3})$  [117]. On the other hand, the statistics of Boltzmann could be described the Fermi function at an electrode for semiconductor accurately under depletion conditions for nondegenerately doped, and the integral in Eq.(3-45) reduces to electrons concentration at the surface of semiconductor  $n_s(\epsilon)$  [117-119].

$$\int_{-\infty}^{E_{cb}} D_S F(\epsilon) d\epsilon = n_s(\epsilon) \dots \dots \dots (3-46)$$

The flow charge transition in Eq.(3-45) with Eq.(3-46) reduce to form.

$$\mathcal{F}_{S/L}(\mathcal{J}_S^L, \Delta\mathcal{U}^{LS}, \mathbb{C}_{S/L}, E_{cb}, qE^0) = \frac{2\pi}{\hbar} \frac{((4\pi k_B T \mathcal{J}_S^L)^{\frac{-1}{2}})}{\beta_S} \frac{l_{ecl}}{\rho_a^{2/3} (\frac{6}{\pi})^{1/3}} |\mathbb{C}_{S/L}(\epsilon)|^2 \exp - \frac{(E_{cb} - qE^0 + \mathcal{J}_S^L)^2}{4k_B T \mathcal{J}_S^L} n_s(\epsilon) \dots \dots \dots (3-47)$$

Then, the flow electrons rate per concentration  $n_s(\epsilon)$  for transition processes is reduced to

$$\mathcal{F}_S(\text{cm}^4 \text{S}^{-1}) = \frac{\mathcal{F}_{S-L}}{n_s(\epsilon)} = \frac{2\pi}{\hbar} \frac{((4\pi k_B T \mathcal{J}_S^L)^{\frac{-1}{2}})}{\beta_S} \frac{l_{ecl}}{\rho_a^{2/3} (\frac{6}{\pi})^{1/3}} |\mathbb{C}_{S/L}(\epsilon)|^2 \exp - \frac{(E_{cb} - qE^0 + \mathcal{J}_S^L)^2}{4k_B T \mathcal{J}_S^L} \dots \dots \dots (3-48)$$

The potential at the interface of semiconductor-liquid contact is given by [120].

$$\Delta\mathcal{U}^{LS} = \frac{hc}{\lambda} - \mathcal{J}_S^L \dots \dots \dots (3-49)$$

Where  $c$  is the velocity of light and  $\lambda$  is the wave length of spectrum for dyes.

The orientation energy of the solvent molecules around the new equilibrium of system is given by [121].

$$\mathcal{J}_S^L(eV) = \frac{e^2}{8\pi\epsilon_0} \left[ \frac{1}{D} \delta(n, \epsilon) - \frac{1}{2R} (\sigma(n_S, n) - \sigma(\epsilon_S, \epsilon)) \right] \dots\dots\dots (3-50)$$

Where  $\delta(n, \epsilon) = \frac{1}{n^2} - \frac{1}{\epsilon_{s0}}$  is the polarity function,  $\sigma(n_S, n) = \frac{n_S^2 - n^2}{n_S^2 + n^2} \frac{1}{n^2}$  is the optical dielectric function and  $\sigma(\epsilon_S, \epsilon) = \frac{\epsilon_S^2 - \epsilon^2}{\epsilon_S^2 + \epsilon^2} \frac{1}{\epsilon^2}$  is static dielectric function.

$$\delta(n, \epsilon) = \frac{1}{n^2} - \frac{1}{\epsilon_{s0}} \dots\dots\dots (3-51)$$

$$\sigma(n_S, n) = \frac{n_S^2 - n^2}{n_S^2 + n^2} \frac{1}{n^2} \dots\dots\dots (3-52)$$

$$\sigma(\epsilon_S, \epsilon) = \frac{\epsilon_S^2 - \epsilon^2}{\epsilon_S^2 + \epsilon^2} \frac{1}{\epsilon^2} \dots\dots\dots (3-53)$$

here  $\epsilon_0$  is the vacuum permittivity,  $\epsilon$  is the static dielectric constant of solvent,  $n_{s0}$  is the refractive index of the solvent,  $n_s$  is the refractive index of the semiconductor,  $\epsilon_{sc}$  dielectric constant of the semiconductor,  $D$  is the radius of the molecular dye, and  $R$  is the distance between the dye and the semiconductor, and  $e$  is the charge of electron. The radius of the dye molecule can be evaluated from the apparent molar volumes using spherical approach [121].

$$D(m) = \left( \frac{3}{4\pi} \frac{M}{N\rho} \right)^{\frac{1}{3}} \dots\dots\dots (3-54)$$

Where  $M$  is the molecular weight,  $N$  is Avogadro number, and  $\rho$  is the mass density .



# **Chapter Four**

## **Results**

### **And**

## **Discussions**

## Chapter Four

### 4.1 Introduction

In this study, simple theoretical model of quantum postulate theory was used to study and evaluate the behaviour of charge transfer processes and analyse the flow charge rate of electrons in semiconductor-molecule devices. A donor and acceptor wave function states in the charge transfer process assume to be localized in quantum space. The flow charge rate results of InAs/D149, ZnO/D149, MgO/D149, InAs/N749, ZnO/N749 and MgO/N749 systems have been evaluated and discussed as a function of the orientation transition energy  $\mathcal{J}_S^L$  (eV), potential barrier  $\Delta\mathcal{U}^{LS}$  (eV), the electronic coupling strength coefficient  $\mathbb{C}_{S/L}(\epsilon)$ , and the flow charge rate  $\mathcal{F}_{S/L}(\frac{1}{\text{Sec}})$  and all other parameters were calculated using a MATLAB program.

### 4.2 Evaluation of The Orientation Transition Energy $\mathcal{J}_S^L$ (eV)

The flow charge rate contribution of the electrons in semiconductor-molecule system has been theoretically calculated as a function of the reorientation transition energy  $\mathcal{J}_S^L$  (eV) and it depends on the polarities of the system and the solvents. We found that orientation transition energy of the system is very important parameters to satisfy the electronic transition. In general, the orientation transition energy of the system can be theoretically estimated using the Marcus classical equation Eq.(3-50). The first fundamental steps to estimate the orientation transition energy, is to evaluate the radii of the donor molecule states of N749 and D149 dyes and the radii of acceptor states of InAs, ZnO and MgO semiconductors using the approach radii formula from Eq.(3-54). By inserting the values of Avogadro's constant  $N = 6.02 \times 10^{23} \frac{\text{Molecule}}{\text{mol}}$ , molecular weight M, and densities of masses  $\rho$  for both N749 and D149 dyes from tables (4-1) and (4-2) in Eq.(3-54). The volume of InAs, ZnO and MgO semiconductors are calculated using the volume of unit cell (  $V = a \cdot b \times c$  ).

where a,b and c are lattice constant. the values of the radii for all dyes and semiconductors were estimated, and the results, are shown in table (4-3).

Table (4-1): The properties of molecules.

Molecule type	Chemical formula	Molecule weight ( $g \cdot mol^{-1}$ )	Density $g/cm^3$	Radii ( $\text{\AA}$ )
N749 dye	$C_{69}H_{117}N_9O_6RuS_3$	781.73	0.749	7.45
D149 dye	$C_{42}H_{35}N_3O_4S_3$	741.94	2.141	5.16

Table (4-2): The properties of InAs, MgO and ZnO semiconductor.

Properties	InAs [122]	MgO [123]	ZnO [112]
Molecular weight g/mol	189.74	40.3	81.38
Crystal structure	Zinc blende	Rock salt	Wurzite
Mass Density ( $g/cm^3$ )	5.68	3.58	5.66
Refractive index	4.10	1.735	2.0033
Dielectric Constant	15.15	9.7	8.5
Density of state $N_s /cm^3$ )	$8.3 \times 10^{16}$	$4.3 \times 10^{18}$	$2.22 \times 10^{24}$
Lattice constant( $\text{\AA}$ )	a= 0.605, c= 2.9885	4.130	a=0.3.249, c=0.5206
Radius( $\text{\AA}$ )	1.7547	1.646	3.8025
Electron affinity (eV)	4.9	4.25	4.3

Table (4-3): Calculated results of radii for all dyes and semiconductors .

Molecule type	Molecule weight (g. mol <sup>-1</sup> )	Density (g/cm <sup>3</sup> )	Radii (Å)
N749 dye	781.73	0.749	7.45
D149 dye	741.94	2.141	5.16
InAs	189.74	5.68	1.7547
MgO	40.3	3.58	1.6463
ZnO	81.38	5.66	3.8025

Table (4-4): General properties of solvents [124].

Solvent	Molecular weight	Empirical formula	Specific gravity	Refractive index	Dielectric constant
Propanol	60	C <sub>3</sub> H <sub>8</sub> O1	0.804	1.383	20.1
Butanol	74	C <sub>4</sub> H <sub>10</sub> O1	0.807	1.395	16.56
Octanol	130	C <sub>8</sub> H <sub>18</sub> O1	0.827	1.427	10.3
Dichloroethae	99	C <sub>2</sub> H <sub>4</sub> Cl <sub>2</sub>	1.253	1.444	10.45
Acetonitrile	41	C <sub>2</sub> H <sub>3</sub> N1	0.782	1.342	37.5

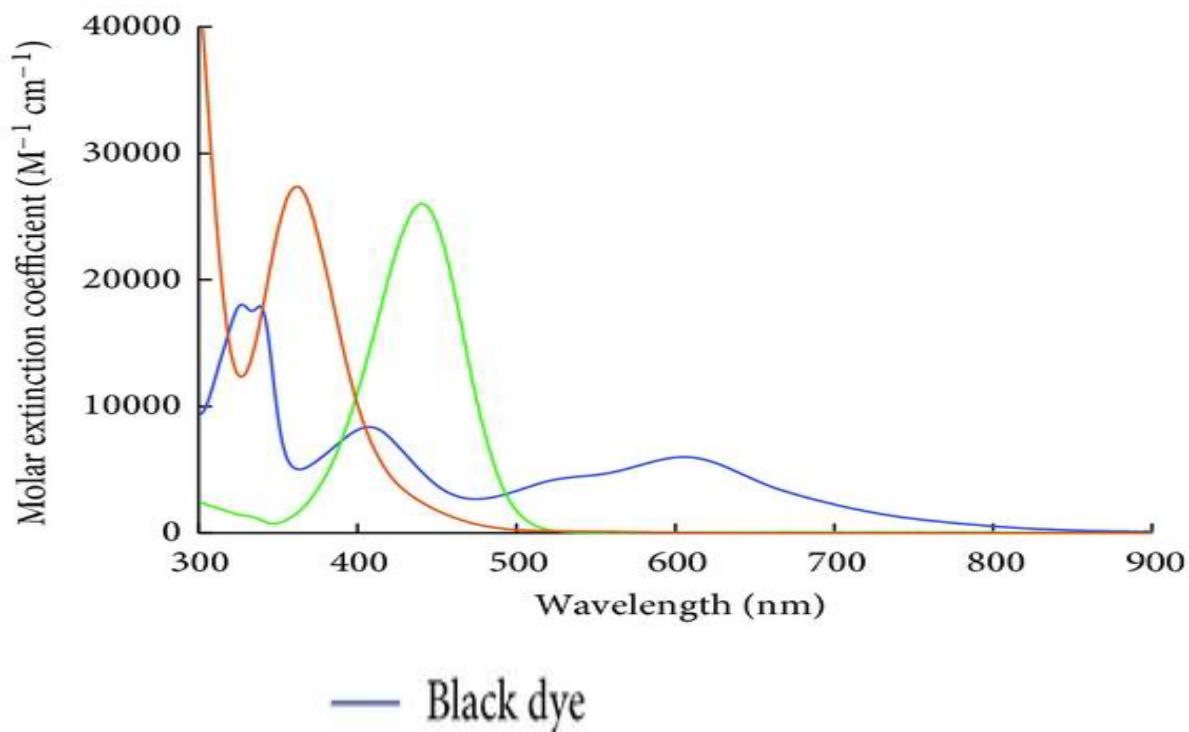
For the charge transition processes, the reorientation transition energy  $T_S^L$ (eV) for InAs/D149, ZnO/D149, MgO/D149, InAs/N749, ZnO/N749 and MgO/N749 systems was calculated using Eq.(3-50) and Matlab program after inserting the radii values  $D$ (m) from table (4-3) and the refractive indices  $n$  and static dielectric constants  $\epsilon$  for the solvents and semiconductors from tables (4-4) and (4-2) respectively. The distance between the center of dye and the center of semiconductor was ( $R = D + r$ ), The results of orientation transition energy  $T_S^L$ (eV) for InAs/N749, InAs/D149, ZnO/N749, ZnO/D149, MgO/N749 and MgO/D149 are shown in table (4-5).

Table (4-5): Results of the reorientation transition energy for six systems

Solvent	Reorientation transition energy $\mathcal{J}_S^L$ (eV) for all systems					
	InAs/N749	ZnO/N749	MgO/N749	InAs/D149	ZnO/D149	MgO/D149
Propanol	0.2942	0.3973	0.4104	0.4427	0.5849	0.5976
Butanol	0.2788	0.3805	0.3938	0.4201	0.5603	0.5734
Octanol	0.2315	0.3288	0.3430	0.3507	0.4845	0.4993
Dichloroethane	0.2261	0.3219	0.3362	0.3424	0.4740	0.4892
Acetonitrile	0.3355	0.4430	0.4553	0.5036	0.6524	0.6634

### 4.3 Evaluation of The Potential Barrier $\Delta\mathcal{U}^{LS}$ (eV) at Interface.

An important parameter that limits the quantity and mechanism of charge transfer in a semiconductor dye system is the potential barrier. The potential barrier at interface of InAs, MgO and ZnO semiconductors and N749 and D149 dyes is an important factor that limited the probability of charge transition from a donor state to an acceptor state at semiconductor/molecule devices. For transferring electron from a donor state to an acceptor state, the energy should be greater than potential barrier height that forms due to the interface of semiconductor/molecules. The potential barrier can be theoretically calculated from the absorption spectrum of N749 and D149 dyes as shown in figures (4-1) and (4-2) respectively .



**Figure (4-1):** UV-Vis absorption spectrum of N749 sensitized dye. [125]

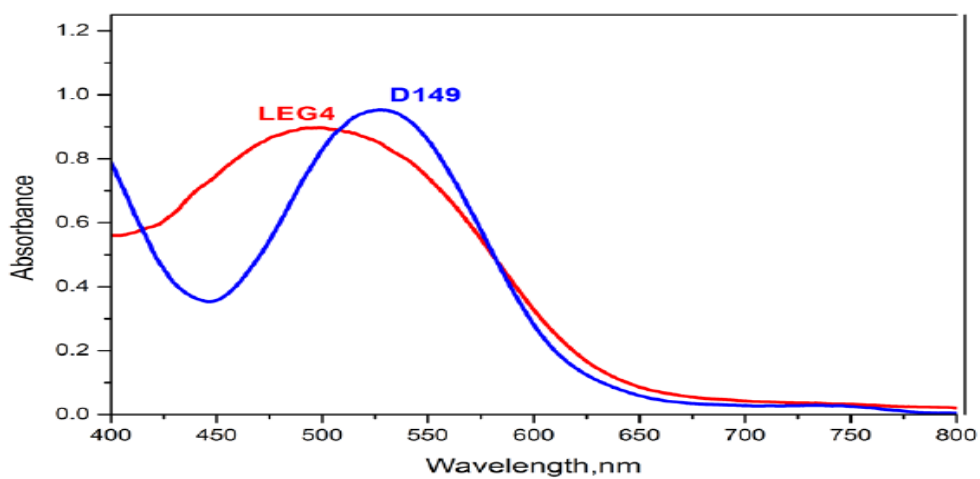


**Figure ( 4-2).** UV-Vis absorption spectrum of D149 sensitized dye. [126]

The potential barrier height values for the semiconductors, molecule liquid and solvents systems were theoretically evaluated using Eq.(3-49) as a function of the

absorption energy from figures (4-1) and (4-2) by the substituting the results of the reorientation energy from table (4-5). The results of the potential barrier height for InAs/N749, MgO/N749, ZnO/N749, InAs/D149, MgO/D149 and ZnO/D149 systems are listed in tables (4-6) to (4-11) respectively.

Table(4-6): The potential barrier result of InAs/N749 system as a function of the reorientation energy and absorption energy (eV).

Wavelength (nm)	Absorption energy (eV)	The potential barrier $\Delta U^{LS}$ (eV)				
		Propanol	Butanol	Octanol	Dichloroethe	Acetonitrile
450	2.750	2.456	2.472	2.519	2.524	2.415
500	2.475	2.181	2.197	2.244	2.249	2.140
550	2.250	1.956	1.972	2.019	2.024	1.915
600	2.062	1.768	1.784	1.831	1.836	1.727
650	1.907	1.610	1.626	1.673	1.678	1.569
700	1.767	1.473	1.489	1.536	1.541	1.432
750	1.650	1.356	1.372	1.419	1.424	1.315
800	1.550	1.252	1.268	1.315	1.320	1.211

Table(4-7): The potential barrier result of MgO/N749 system as a function of the reorientation energy and absorption energy (eV).

Wavelength (nm)	Absorption energy (eV)	The potential barrier $\Delta U^{LS}$ (eV)				
		Propanol	Butanol	Octanol	Dichloroethane	Acetonitrile
450	2.750	2.340	2.357	2.407	2.414	2.295
500	2.475	2.065	2.082	2.132	2.139	2.020
550	2.250	1.840	1.857	1.907	1.914	1.795
600	2.062	1.652	1.669	1.719	1.726	1.607
650	1.904	1.494	1.511	1.561	1.568	1.449
700	1.767	1.357	1.374	1.424	1.431	1.312
750	1.650	1.240	1.257	1.307	1.314	1.195
800	1.546	1.136	1.153	1.203	1.210	1.091

Table(4-8): The potential barrier result of ZnO/N749 system as a function of the reorientation energy and absorption energy (eV).

Wavelength (nm)	Absorption energy (eV)	The potential barrier $\Delta U^{LS}$ (eV)				
		Propanol	Butanol	Octanol	Dichloroete	Acetonitrile
450	2.750	2.353	2.370	2.422	2.429	2.307
500	2.475	2.078	2.095	2.147	2.154	2.032
550	2.250	1.853	1.870	1.922	1.929	1.807
600	2.062	1.665	1.682	1.734	1.741	1.619
650	1.904	1.507	1.524	1.576	1.583	1.461
700	1.767	1.370	1.387	1.439	1.446	1.324
750	1.650	1.253	1.270	1.322	1.329	1.207
800	1.546	1.149	1.166	1.218	1.225	1.103

Table(4-9): The potential barrier result of InAs/D149 system as a function of the reorientation energy and absorption energy (eV).

Wavelength (nm)	Absorption Energy(eV)	The potential barrier $\Delta U^{LS}$ (eV)				
		Propanol	Butanol	Octanol	Dichloroethane	Acetonitrile
400	3.093	2.651	2.673	2.743	2.751	2.590
450	2.750	2.308	2.330	2.400	2.408	2.247
500	2.475	2.033	2.055	2.125	2.133	1.972
550	2.250	1.808	1.830	1.900	1.908	1.747
600	2.062	1.620	1.642	1.712	1.720	1.559
650	1.904	1.462	1.484	1.554	1.562	1.401
700	1.767	1.325	1.347	1.417	1.425	1.264
750	1.650	1.208	1.230	1.300	1.308	1.147
800	1.546	1.104	1.126	1.196	1.204	1.043



Table(4-10): The potential barrier result of MgO/D149 system as a function of the reorientation energy and absorption energy (eV).

Wavelength (nm)	Absorption energy(eV)	The potential barrier $\Delta U^{LS}$ (eV)				
		Propanol	Butanol	Octanol	Dichloroethane	Acetonitrile
400	3.093	2.496	2.520	2.594	2.604	2.430
450	2.750	2.153	2.177	2.251	2.261	2.087
500	2.475	1.878	1.902	1.976	1.986	1.812
550	2.250	1.653	1.677	1.751	1.761	1.587
600	2.062	1.465	1.489	1.563	1.573	1.399
650	1.904	1.307	1.331	1.405	1.415	1.241
700	1.767	1.170	1.194	1.268	1.278	1.104
750	1.650	1.053	1.077	1.151	1.161	0.987
800	1.546	0.949	0.973	1.047	1.057	0.883

Table(4-11): The potential barrier result of ZnO/D149 system as a function of the reorientation energy and absorption energy (eV).

Wavelength (nm)	Absorption energy(eV)	The potential barrier $\Delta U^{LS}$ (eV)				
		Propanol	Butanol	Octanol	Dichloroethane	Acetonitrile
400	3.093	2.509	2.533	2.609	2.619	2.441
450	2.750	2.166	2.190	2.266	2.276	2.098
500	2.475	1.891	1.915	1.991	2.001	1.823
550	2.250	1.666	1.690	1.766	1.776	1.598
600	2.062	1.478	1.502	1.578	1.588	1.410
650	1.904	1.320	1.344	1.420	1.430	1.252
700	1.767	1.183	1.207	1.283	1.293	1.115
750	1.650	1.066	1.090	1.166	1.176	0.998
800	1.546	0.962	0.986	1.062	1.072	0.894

#### 4.4 Estimation of the Electronic Coupling Strength Coefficient $\mathbb{C}_{S/L}(\epsilon)$

The electronic strength coupling coefficient  $\mathbb{C}_{S/L}(\epsilon)$  for the overlapping wave function for semiconductor state and molecule state along a real space coordinate is a very important parameters to evaluate the flow charge rate. The electronic strength coupling is a key aspect in controlling the charge transfer types either it is adiabatic or non-adiabatic transition. systems are nearly at interface then effective coupling strength of two electrons state, The strength coupling  $\mathbb{C}_{S/L}(\epsilon)$  for InAs/N749, MgO/N749 and ZnO/N749, InAs/D149, MgO/D149 and ZnO/D149 systems was estimated by typical values from the experimental results in ref. [127] and approximated to be  $|\mathbb{C}_{S/L}(\epsilon)|^2 \approx 2 \times 10^{-2}$  eV,  $7 \times 10^{-2}$  eV,  $1.2 \times 10^{-3}$  eV,  $1.7 \times 10^{-4}$  eV and  $2.2 \times 10^{-4}$  eV [127].

#### 4.5 Evaluation of the Flow Charge Transfer Rate Constant

Due to quantum theory, the charge transfer reaction mechanism has been discussed for a donor acceptor system. The flow charge rate of electron transfer and the electronic transitions probability at the semiconductor/molecule interface system has been investigated. As discussed previously, the properties of electronic transition reaction depend on the flow charge rate. However, the probability of the flow charge rate were evaluated at room temperature based on the calculation of the reorientation transition energy, electronic strength coupling coefficient and the potential energy. To evaluate the flow charge rate at semiconductor/molecule system, it is necessary to use out Eq.(3-48) to get all the information about the electrical properties of InAs/N749, MgO/N749, ZnO/N749, InAs/D149, MgO/D149 and ZnO/D149 systems at different solvents.

A MATLAB program is used to evaluate the orientation transition energy, the potential barrier, the strength coupling and the flow charge rate of electrons for these

systems using Eq.(3-48). The results of these calculation for InAs/N749, InAs/D149, MgO/N749, MgO/D149, ZnO/N749 and ZnO /D149 are listed in Tables [ (4-12) - (4-41) ] respectively [20].

Table (4-12): The flow charge transition rate of InAs/N749 as a function of a potential barrier  $\Delta U^{LS}$  and a coupling strength of  $2 \times 10^{-2}$  eV

$\Delta U^{LS} = E_{cb} - qE^0$ (eV)	The current of electron transfer ( $\text{cm}^4\text{sec}^{-1}$ )				
	Solvent Types				
	Propanol	Butanol	Octanol	Dichloroethane	Acetonitrile
0.2	$1.184 \times 10^{-11}$	$1.316 \times 10^{-11}$	$1.729 \times 10^{-11}$	$1.772 \times 10^{-11}$	$8.673 \times 10^{-12}$
0.3	$2.929 \times 10^{-13}$	$2.964 \times 10^{-13}$	$2.699 \times 10^{-13}$	$2.627 \times 10^{-13}$	$2.644 \times 10^{-13}$
0.4	$3.671 \times 10^{-15}$	$3.257 \times 10^{-15}$	$1.776 \times 10^{-15}$	$1.608 \times 10^{-15}$	$4.442 \times 10^{-15}$
0.5	$2.331 \times 10^{-17}$	$1.747 \times 10^{-17}$	$4.925 \times 10^{-18}$	$4.064 \times 10^{-18}$	$4.112 \times 10^{-17}$
0.6	$7.503 \times 10^{-20}$	$4.573 \times 10^{-20}$	$5.757 \times 10^{-21}$	$4.241 \times 10^{-21}$	$2.096 \times 10^{-19}$
0.7	$1.223 \times 10^{-22}$	$5.842 \times 10^{-23}$	$2.837 \times 10^{-24}$	$1.827 \times 10^{-24}$	$5.890 \times 10^{-22}$
0.8	$1.010 \times 10^{-25}$	$3.642 \times 10^{-26}$	$5.892 \times 10^{-28}$	$3.251 \times 10^{-28}$	$9.117 \times 10^{-25}$

Table (4-13): The flow charge transition rate of InAs/N749 as a function of a potential barrier  $\Delta U^{LS}$  and a coupling strength of  $7 \times 10^{-2}$  eV

$\Delta U^{LS} = E_{cb} - qE^0$ (eV)	The current of electron transfer ( $\text{cm}^4\text{sec}^{-1}$ )				
	Solvent Types				
	Propanol	Butanol	Octanol	Dichloroethane	Acetonitrile
0.2	$4.144 \times 10^{-11}$	$4.607 \times 10^{-11}$	$6.052 \times 10^{-11}$	$6.202 \times 10^{-11}$	$3.035 \times 10^{-11}$
0.3	$1.025 \times 10^{-12}$	$1.037 \times 10^{-12}$	$9.447 \times 10^{-13}$	$9.195 \times 10^{-13}$	$9.256 \times 10^{-13}$
0.4	$1.284 \times 10^{-14}$	$1.140 \times 10^{-14}$	$6.216 \times 10^{-15}$	$5.628 \times 10^{-15}$	$1.555 \times 10^{-14}$
0.5	$8.160 \times 10^{-17}$	$6.113 \times 10^{-17}$	$1.723 \times 10^{-17}$	$1.422 \times 10^{-17}$	$1.439 \times 10^{-16}$
0.6	$2.626 \times 10^{-19}$	$1.600 \times 10^{-19}$	$2.015 \times 10^{-20}$	$1.484 \times 10^{-20}$	$7.338 \times 10^{-19}$
0.7	$4.282 \times 10^{-22}$	$2.045 \times 10^{-22}$	$9.929 \times 10^{-24}$	$6.397 \times 10^{-24}$	$2.061 \times 10^{-21}$
0.8	$3.538 \times 10^{-25}$	$1.275 \times 10^{-25}$	$2.062 \times 10^{-27}$	$1.138 \times 10^{-27}$	$3.191 \times 10^{-24}$

Table (4-14): The flow charge transition rate of InAs/N749 as a function of a potential barrier  $\Delta U^{LS}$  and a coupling strength of  $1.2 \times 10^{-3}$  eV

$\Delta U^{LS} = E_{cb} - qE^0$ (eV)	The current of electron transfer ( $\text{cm}^4\text{sec}^{-1}$ )				
	Solvent Types				
	Propanol	Butanol	Octanol	Dichloroethane	Acetonitrile
0.2	$7.104 \times 10^{-13}$	$7.897 \times 10^{-13}$	$1.037 \times 10^{-12}$	$1.063 \times 10^{-12}$	$5.204 \times 10^{-13}$
0.3	$1.757 \times 10^{-14}$	$1.778 \times 10^{-14}$	$1.619 \times 10^{-14}$	$1.576 \times 10^{-14}$	$1.586 \times 10^{-14}$
0.4	$2.202 \times 10^{-16}$	$1.954 \times 10^{-16}$	$1.065 \times 10^{-16}$	$9.649 \times 10^{-17}$	$2.665 \times 10^{-16}$
0.5	$1.398 \times 10^{-18}$	$1.048 \times 10^{-18}$	$2.955 \times 10^{-19}$	$2.438 \times 10^{-19}$	$2.467 \times 10^{-18}$
0.6	$4.501 \times 10^{-21}$	$2.744 \times 10^{-21}$	$3.454 \times 10^{-22}$	$2.545 \times 10^{-22}$	$1.258 \times 10^{-20}$
0.7	$7.341 \times 10^{-24}$	$3.505 \times 10^{-24}$	$1.702 \times 10^{-25}$	$1.096 \times 10^{-25}$	$3.534 \times 10^{-23}$
0.8	$6.065 \times 10^{-27}$	$2.185 \times 10^{-27}$	$3.535 \times 10^{-29}$	$1.951 \times 10^{-29}$	$5.470 \times 10^{-26}$

Table (4-15): The flow charge transition rate of InAs/N749 as a function of a potential barrier  $\Delta U^{LS}$  and a coupling strength of  $1.7 \times 10^{-4}$  eV

$\Delta U^{LS} = E_{cb} - qE^0$ (eV)	The current of electron transfer ( $\text{cm}^4\text{sec}^{-1}$ )				
	Solvent Types				
	Propanol	Butanol	Octanol	Dichloroethane	Acetonitrile
0.2	$1.006 \times 10^{-13}$	$1.118 \times 10^{-13}$	$1.469 \times 10^{-13}$	$1.506 \times 10^{-13}$	$7.372 \times 10^{-14}$
0.3	$2.489 \times 10^{-15}$	$2.519 \times 10^{-15}$	$2.294 \times 10^{-15}$	$2.233 \times 10^{-15}$	$2.248 \times 10^{-15}$
0.4	$3.120 \times 10^{-17}$	$2.768 \times 10^{-17}$	$1.509 \times 10^{-17}$	$1.366 \times 10^{-17}$	$3.776 \times 10^{-17}$
0.5	$1.981 \times 10^{-19}$	$1.485 \times 10^{-19}$	$4.186 \times 10^{-20}$	$3.454 \times 10^{-20}$	$3.495 \times 10^{-19}$
0.6	$6.377 \times 10^{-22}$	$3.887 \times 10^{-22}$	$4.894 \times 10^{-23}$	$3.605 \times 10^{-23}$	$1.782 \times 10^{-21}$
0.7	$1.040 \times 10^{-24}$	$3.887 \times 10^{-25}$	$2.411 \times 10^{-26}$	$1.553 \times 10^{-26}$	$5.006 \times 10^{-24}$
0.8	$8.593 \times 10^{-28}$	$3.096 \times 10^{-28}$	$5.008 \times 10^{-30}$	$2.763 \times 10^{-30}$	$7.749 \times 10^{-27}$

Table (4-16): The flow charge transition rate of InAs/N749 as a function of a potential barrier  $\Delta U^{LS}$  and a coupling strength of  $2.2 \times 10^{-4}$  eV

$\Delta U^{LS} = E_{cb} - qE^0$ (eV)	The current of electron transfer ( $\text{cm}^4\text{sec}^{-1}$ )				
	Solvent Types				
	Propanol	Butanol	Octanol	Dichloroethane	Acetonitrile
0.2	$1.299 \times 10^{-13}$	$1.444 \times 10^{-13}$	$1.897 \times 10^{-13}$	$1.944 \times 10^{-13}$	$9.518 \times 10^{-14}$
0.3	$3.214 \times 10^{-15}$	$3.252 \times 10^{-15}$	$2.962 \times 10^{-15}$	$2.883 \times 10^{-15}$	$2.902 \times 10^{-15}$
0.4	$4.028 \times 10^{-17}$	$3.574 \times 10^{-17}$	$1.949 \times 10^{-17}$	$1.764 \times 10^{-17}$	$4.875 \times 10^{-17}$
0.5	$2.558 \times 10^{-19}$	$1.917 \times 10^{-19}$	$5.405 \times 10^{-20}$	$4.460 \times 10^{-20}$	$4.512 \times 10^{-19}$
0.6	$8.234 \times 10^{-22}$	$5.019 \times 10^{-22}$	$6.318 \times 10^{-23}$	$4.655 \times 10^{-23}$	$2.301 \times 10^{-21}$
0.7	$1.342 \times 10^{-24}$	$6.412 \times 10^{-25}$	$3.113 \times 10^{-26}$	$2.005 \times 10^{-26}$	$6.464 \times 10^{-24}$
0.8	$1.109 \times 10^{-27}$	$3.997 \times 10^{-28}$	$6.466 \times 10^{-30}$	$3.568 \times 10^{-30}$	$1.000 \times 10^{-26}$

Table (4-17): The flow charge transition rate of InAs / D149 as a function of a potential barrier  $\Delta U^{LS}$  at coupling strength of  $2 \times 10^{-2}$  eV

$\Delta U^{LS} = E_{cb} - qE^0$ (eV)	The current of electron transfer ( $\text{cm}^4\text{sec}^{-1}$ )				
	Solvent Types				
	Propanol	Butanol	Octanol	Dichloroethane	Acetonitrile
0.2	$3.441 \times 10^{-12}$	$4.219 \times 10^{-12}$	$7.655 \times 10^{-12}$	$8.189 \times 10^{-12}$	$1.957 \times 10^{-12}$
0.3	$1.505 \times 10^{-13}$	$1.736 \times 10^{-13}$	$2.490 \times 10^{-13}$	$2.573 \times 10^{-13}$	$9.817 \times 10^{-14}$
0.4	$4.191 \times 10^{-15}$	$4.441 \times 10^{-15}$	$4.579 \times 10^{-15}$	$4.508 \times 10^{-15}$	$3.309 \times 10^{-15}$
0.5	$7.428 \times 10^{-17}$	$7.054 \times 10^{-17}$	$4.760 \times 10^{-17}$	$4.404 \times 10^{-17}$	$7.499 \times 10^{-17}$
0.6	$8.379 \times 10^{-19}$	$6.962 \times 10^{-19}$	$2.798 \times 10^{-19}$	$2.399 \times 10^{-19}$	$1.142 \times 10^{-18}$
0.7	$6.015 \times 10^{-21}$	$4.268 \times 10^{-21}$	$9.298 \times 10^{-22}$	$7.287 \times 10^{-22}$	$1.169 \times 10^{-20}$
0.8	$2.749 \times 10^{-23}$	$1.625 \times 10^{-23}$	$1.746 \times 10^{-24}$	$1.234 \times 10^{-24}$	$8.053 \times 10^{-23}$

Table (4-18): The flow charge transition rate of InAs/D149 as a function of a potential barrier  $\Delta U^{LS}$  and a coupling strength of  $7 \times 10^{-2}$  eV

$\Delta U^{LS} = E_{cb} - qE^0$ (eV)	The current of electron transfer ( $\text{cm}^4\text{sec}^{-1}$ )				
	Solvent Types				
	Propanol	Butanol	Octanol	Dichloroethane	Acetonitrile
0.2	$1.204 \times 10^{-11}$	$1.476 \times 10^{-11}$	$2.679 \times 10^{-11}$	$2.866 \times 10^{-11}$	$6.852 \times 10^{-12}$
0.3	$5.269 \times 10^{-13}$	$6.018 \times 10^{-13}$	$8.715 \times 10^{-13}$	$9.005 \times 10^{-13}$	$3.436 \times 10^{-13}$
0.4	$1.467 \times 10^{-14}$	$1.554 \times 10^{-14}$	$1.602 \times 10^{-14}$	$1.577 \times 10^{-14}$	$1.158 \times 10^{-14}$
0.5	$2.599 \times 10^{-16}$	$2.469 \times 10^{-16}$	$1.666 \times 10^{-16}$	$1.541 \times 10^{-16}$	$2.624 \times 10^{-16}$
0.6	$2.932 \times 10^{-18}$	$2.436 \times 10^{-18}$	$9.793 \times 10^{-19}$	$8.396 \times 10^{-19}$	$3.998 \times 10^{-18}$
0.7	$2.105 \times 10^{-20}$	$1.493 \times 10^{-20}$	$3.254 \times 10^{-21}$	$2.550 \times 10^{-21}$	$4.094 \times 10^{-20}$
0.8	$9.621 \times 10^{-21}$	$5.688 \times 10^{-23}$	$6.114 \times 10^{-24}$	$4.319 \times 10^{-24}$	$2.818 \times 10^{-22}$

Table (4-19): The flow charge transition rate of InAs/D149 as a function of a potential barrier  $\Delta U^{LS}$  and a coupling strength of  $1.2 \times 10^{-3}$  eV

$\Delta U^{LS} = E_{cb} - qE^0$ (eV)	The current of electron transfer ( $\text{cm}^4\text{sec}^{-1}$ )				
	Solvent Types				
	Propanol	Butanol	Octanol	Dichloroethane	Acetonitrile
0.2	$2.065 \times 10^{-13}$	$2.531 \times 10^{-13}$	$4.593 \times 10^{-13}$	$4.913 \times 10^{-13}$	$1.174 \times 10^{-13}$
0.3	$9.033 \times 10^{-15}$	$1.042 \times 10^{-14}$	$1.494 \times 10^{-14}$	$1.543 \times 10^{-14}$	$5.890 \times 10^{-15}$
0.4	$2.515 \times 10^{-16}$	$2.664 \times 10^{-16}$	$2.747 \times 10^{-16}$	$2.704 \times 10^{-16}$	$1.985 \times 10^{-16}$
0.5	$4.457 \times 10^{-18}$	$5.232 \times 10^{-18}$	$2.856 \times 10^{-18}$	$2.642 \times 10^{-18}$	$4.499 \times 10^{-18}$
0.6	$5.027 \times 10^{-20}$	$4.177 \times 10^{-20}$	$1.678 \times 10^{-20}$	$1.439 \times 10^{-20}$	$6.854 \times 10^{-20}$
0.7	$3.609 \times 10^{-22}$	$2.560 \times 10^{-22}$	$5.579 \times 10^{-23}$	$4.372 \times 10^{-23}$	$7.018 \times 10^{-22}$
0.8	$1.649 \times 10^{-23}$	$9.752 \times 10^{-25}$	$1.048 \times 10^{-25}$	$7.405 \times 10^{-26}$	$4.831 \times 10^{-24}$

Table (4-20): The flow charge transition rate of InAs/D149 as a function of a potential barrier  $\Delta U^{LS}$  and a coupling strength of  $1.7 \times 10^{-4}$  eV

$\Delta U^{LS} = E_{cb} - qE^0$ (eV)	The current of electron transfer ( $\text{cm}^4\text{sec}^{-1}$ )				
	Solvent Types				
	Propanol	Butanol	Octanol	Dichloroethane	Acetonitrile
0.2	$2.925 \times 10^{-14}$	$3.586 \times 10^{-14}$	$6.507 \times 10^{-14}$	$6.960 \times 10^{-14}$	$1.664 \times 10^{-14}$
0.3	$1.279 \times 10^{-15}$	$1.476 \times 10^{-15}$	$2.116 \times 10^{-15}$	$2.187 \times 10^{-15}$	$8.344 \times 10^{-16}$
0.4	$3.563 \times 10^{-17}$	$3.774 \times 10^{-17}$	$3.892 \times 10^{-17}$	$3.831 \times 10^{-17}$	$2.812 \times 10^{-17}$
0.5	$6.314 \times 10^{-19}$	$5.996 \times 10^{-19}$	$4.046 \times 10^{-19}$	$3.743 \times 10^{-19}$	$6.374 \times 10^{-19}$
0.6	$7.122 \times 10^{-21}$	$5.917 \times 10^{-21}$	$2.378 \times 10^{-21}$	$2.039 \times 10^{-21}$	$9.710 \times 10^{-21}$
0.7	$5.113 \times 10^{-23}$	$3.627 \times 10^{-23}$	$7.903 \times 10^{-24}$	$6.194 \times 10^{-24}$	$9.943 \times 10^{-23}$
0.8	$2.336 \times 10^{-25}$	$1.381 \times 10^{-25}$	$1.484 \times 10^{-26}$	$1.049 \times 10^{-26}$	$6.845 \times 10^{-25}$

Table (4-21): The flow charge transition rate of InAs/D149 as a function of a potential barrier  $\Delta U^{LS}$  and a coupling strength of  $2.2 \times 10^{-4}$  eV

$\Delta U^{LS} = E_{cb} - qE^0$ (eV)	The current of electron transfer ( $\text{cm}^4\text{sec}^{-1}$ )				
	Solvent Types				
	Propanol	Butanol	Octanol	Dichloroethane	Acetonitrile
0.2	$3.786 \times 10^{-14}$	$4.671 \times 10^{-14}$	$8.421 \times 10^{-14}$	$9.007 \times 10^{-14}$	$2.153 \times 10^{-14}$
0.3	$1.656 \times 10^{-15}$	$1.927 \times 10^{-15}$	$2.739 \times 10^{-15}$	$2.830 \times 10^{-15}$	$1.079 \times 10^{-15}$
0.4	$4.611 \times 10^{-17}$	$4.941 \times 10^{-17}$	$5.037 \times 10^{-17}$	$4.958 \times 10^{-17}$	$3.640 \times 10^{-17}$
0.5	$8.171 \times 10^{-19}$	$7.872 \times 10^{-19}$	$5.236 \times 10^{-19}$	$4.844 \times 10^{-19}$	$8.249 \times 10^{-19}$
0.6	$9.217 \times 10^{-21}$	$7.794 \times 10^{-21}$	$3.077 \times 10^{-21}$	$2.639 \times 10^{-21}$	$1.256 \times 10^{-20}$
0.7	$6.617 \times 10^{-23}$	$4.795 \times 10^{-23}$	$1.022 \times 10^{-23}$	$8.015 \times 10^{-24}$	$1.286 \times 10^{-22}$
0.8	$3.023 \times 10^{-25}$	$1.833 \times 10^{-25}$	$1.921 \times 10^{-26}$	$1.357 \times 10^{-26}$	$8.858 \times 10^{-25}$

Table (4-22): The flow charge transition rate of MgO/N749 as a function of a potential barrier  $\Delta U^{LS}$  and a coupling strength of  $2 \times 10^{-2}$  eV

$\Delta U^{LS} = E_{cb} - qE^0$ (eV)	The current of electron transfer ( $\text{cm}^4\text{sec}^{-1}$ )				
	Solvent Types				
	Propanol	Butanol	Octanol	Dichloroethane	Acetonitrile
0.2	$6.255 \times 10^{-12}$	$7.236 \times 10^{-12}$	$1.108 \times 10^{-11}$	$1.170 \times 10^{-11}$	$4.173 \times 10^{-12}$
0.3	$2.503 \times 10^{-13}$	$2.751 \times 10^{-13}$	$3.492 \times 10^{-13}$	$3.580 \times 10^{-13}$	$1.883 \times 10^{-13}$
0.4	$6.155 \times 10^{-15}$	$6.294 \times 10^{-15}$	$6.140 \times 10^{-15}$	$6.041 \times 10^{-15}$	$5.478 \times 10^{-15}$
0.5	$9.295 \times 10^{-17}$	$8.665 \times 10^{-17}$	$6.026 \times 10^{-17}$	$5.622 \times 10^{-17}$	$1.027 \times 10^{-16}$
0.6	$8.622 \times 10^{-19}$	$7.179 \times 10^{-19}$	$3.301 \times 10^{-19}$	$2.886 \times 10^{-19}$	$1.240 \times 10^{-18}$
0.7	$4.912 \times 10^{-21}$	$3.579 \times 10^{-21}$	$1.009 \times 10^{-21}$	$8.175 \times 10^{-22}$	$9.663 \times 10^{-21}$
0.8	$1.719 \times 10^{-23}$	$1.073 \times 10^{-23}$	$1.722 \times 10^{-24}$	$1.277 \times 10^{-24}$	$4.850 \times 10^{-23}$

Table (4-23): The flow charge transition rate of MgO/N749 as a function of a potential barrier  $\Delta U^{LS}$  and a coupling strength of  $7 \times 10^{-2}$  eV

$\Delta U^{LS} = E_{cb} - qE^0$ (eV)	The current of electron transfer ( $\text{cm}^4\text{sec}^{-1}$ )				
	Solvent Types				
	Propanol	Butanol	Octanol	Dichloroethane	Acetonitrile
0.2	$2.189 \times 10^{-11}$	$2.532 \times 10^{-11}$	$3.880 \times 10^{-11}$	$4.097 \times 10^{-11}$	$1.460 \times 10^{-11}$
0.3	$8.763 \times 10^{-13}$	$9.628 \times 10^{-13}$	$1.222 \times 10^{-12}$	$1.253 \times 10^{-12}$	$6.592 \times 10^{-13}$
0.4	$2.154 \times 10^{-14}$	$2.202 \times 10^{-14}$	$2.149 \times 10^{-14}$	$2.114 \times 10^{-14}$	$1.917 \times 10^{-14}$
0.5	$3.253 \times 10^{-16}$	$3.032 \times 10^{-16}$	$2.109 \times 10^{-16}$	$1.967 \times 10^{-16}$	$3.594 \times 10^{-16}$
0.6	$3.017 \times 10^{-18}$	$2.512 \times 10^{-18}$	$1.155 \times 10^{-18}$	$1.010 \times 10^{-18}$	$4.343 \times 10^{-18}$
0.7	$1.719 \times 10^{-20}$	$1.252 \times 10^{-20}$	$3.533 \times 10^{-21}$	$2.861 \times 10^{-21}$	$3.382 \times 10^{-20}$
0.8	$6.018 \times 10^{-23}$	$3.758 \times 10^{-23}$	$6.030 \times 10^{-24}$	$4.469 \times 10^{-24}$	$1.697 \times 10^{-22}$



Table (4-24): The flow charge transition rate of MgO/N749 as a function of a potential barrier  $\Delta U^{LS}$  and a coupling strength of  $1.2 \times 10^{-3}$  eV

$\Delta U^{LS} = E_{cb} - qE^0$ (eV)	The current of electron transfer ( $\text{cm}^4\text{sec}^{-1}$ )				
	Solvent Types				
	Propanol	Butanol	Octanol	Dichloroethane	Acetonitrile
0.2	$3.753 \times 10^{-13}$	$4.341 \times 10^{-13}$	$6.651 \times 10^{-13}$	$7.023 \times 10^{-13}$	$2.504 \times 10^{-13}$
0.3	$1.502 \times 10^{-14}$	$1.650 \times 10^{-14}$	$2.095 \times 10^{-14}$	$2.148 \times 10^{-14}$	$1.130 \times 10^{-14}$
0.4	$3.693 \times 10^{-16}$	$3.776 \times 10^{-16}$	$3.684 \times 10^{-16}$	$3.624 \times 10^{-16}$	$3.287 \times 10^{-16}$
0.5	$5.577 \times 10^{-18}$	$5.199 \times 10^{-18}$	$3.615 \times 10^{-18}$	$3.373 \times 10^{-18}$	$6.162 \times 10^{-18}$
0.6	$5.173 \times 10^{-20}$	$4.307 \times 10^{-20}$	$1.980 \times 10^{-20}$	$1.731 \times 10^{-20}$	$7.445 \times 10^{-20}$
0.7	$2.947 \times 10^{-22}$	$2.147 \times 10^{-22}$	$6.056 \times 10^{-23}$	$4.905 \times 10^{-23}$	$5.790 \times 10^{-22}$
0.8	$1.031 \times 10^{-24}$	$6.443 \times 10^{-25}$	$1.033 \times 10^{-25}$	$7.662 \times 10^{-26}$	$2.910 \times 10^{-24}$

Table (4-25): The flow charge transition rate of MgO/N749 as a function of a potential barrier  $\Delta U^{LS}$  and a coupling strength of  $1.7 \times 10^{-4}$  eV

$\Delta U^{LS} = E_{cb} - qE^0$ (eV)	The current of electron transfer ( $\text{cm}^4\text{sec}^{-1}$ )				
	Solvent Types				
	Propanol	Butanol	Octanol	Dichloroethane	Acetonitrile
0.2	$5.317 \times 10^{-14}$	$6.150 \times 10^{-14}$	$9.423 \times 10^{-14}$	$9.950 \times 10^{-14}$	$3.547 \times 10^{-14}$
0.3	$2.218 \times 10^{-15}$	$2.338 \times 10^{-15}$	$2.968 \times 10^{-15}$	$3.043 \times 10^{-15}$	$1.600 \times 10^{-15}$
0.4	$5.231 \times 10^{-17}$	$5.349 \times 10^{-17}$	$5.219 \times 10^{-17}$	$5.134 \times 10^{-17}$	$4.656 \times 10^{-17}$
0.5	$7.900 \times 10^{-19}$	$7.365 \times 10^{-19}$	$5.122 \times 10^{-19}$	$4.779 \times 10^{-19}$	$8.730 \times 10^{-19}$
0.6	$7.328 \times 10^{-21}$	$6.102 \times 10^{-21}$	$2.806 \times 10^{-21}$	$2.453 \times 10^{-21}$	$1.054 \times 10^{-20}$
0.7	$4.175 \times 10^{-23}$	$3.042 \times 10^{-23}$	$8.580 \times 10^{-24}$	$6.948 \times 10^{-24}$	$8.214 \times 10^{-23}$
0.8	$1.461 \times 10^{-25}$	$9.128 \times 10^{-26}$	$1.464 \times 10^{-26}$	$1.085 \times 10^{-26}$	$4.122 \times 10^{-25}$

Table (4-26): The flow charge transition rate of MgO/N749 as a function of a potential barrier  $\Delta U^{LS}$  and a coupling strength of  $2.2 \times 10^{-4}$  eV

$\Delta U^{LS} = E_{cb} - qE^0$ (eV)	The current of electron transfer ( $\text{cm}^4\text{sec}^{-1}$ )				
	Solvent Types				
	Propanol	Butanol	Octanol	Dichloroethane	Acetonitrile
0.2	$6.881 \times 10^{-14}$	$7.959 \times 10^{-14}$	$1.219 \times 10^{-13}$	$1.287 \times 10^{-13}$	$4.590 \times 10^{-14}$
0.3	$2.754 \times 10^{-15}$	$3.026 \times 10^{-15}$	$3.841 \times 10^{-15}$	$3.938 \times 10^{-15}$	$2.071 \times 10^{-15}$
0.4	$6.770 \times 10^{-17}$	$6.923 \times 10^{-17}$	$6.754 \times 10^{-17}$	$6.645 \times 10^{-17}$	$6.026 \times 10^{-17}$
0.5	$1.022 \times 10^{-18}$	$9.532 \times 10^{-19}$	$6.629 \times 10^{-19}$	$6.184 \times 10^{-19}$	$1.129 \times 10^{-18}$
0.6	$9.484 \times 10^{-21}$	$7.897 \times 10^{-21}$	$3.631 \times 10^{-21}$	$3.175 \times 10^{-21}$	$1.365 \times 10^{-20}$
0.7	$5.404 \times 10^{-23}$	$3.937 \times 10^{-23}$	$1.110 \times 10^{-23}$	$8.992 \times 10^{-24}$	$1.063 \times 10^{-22}$
0.8	$1.891 \times 10^{-25}$	$1.181 \times 10^{-25}$	$1.895 \times 10^{-26}$	$1.404 \times 10^{-26}$	$5.335 \times 10^{-25}$

Table (4-27): The flow charge transition rate of MgO/D149 as a function of a potential barrier  $\Delta U^{LS}$  and a coupling strength of  $2 \times 10^{-2}$  eV

$\Delta U^{LS} = E_{cb} - qE^0$ (eV)	The current of electron transfer ( $\text{cm}^4\text{sec}^{-1}$ )				
	Solvent Types				
	Propanol	Butanol	Octanol	Dichloroethane	Acetonitrile
0.2	$1.082 \times 10^{-12}$	$1.398 \times 10^{-12}$	$2.773 \times 10^{-12}$	$3.048 \times 10^{-12}$	$5.684 \times 10^{-13}$
0.3	$6.343 \times 10^{-14}$	$7.959 \times 10^{-14}$	$1.378 \times 10^{-13}$	$1.484 \times 10^{-13}$	$3.620 \times 10^{-14}$
0.4	$2.660 \times 10^{-15}$	$3.199 \times 10^{-15}$	$4.592 \times 10^{-15}$	$4.804 \times 10^{-15}$	$1.705 \times 10^{-15}$
0.5	$7.986 \times 10^{-17}$	$9.078 \times 10^{-17}$	$1.024 \times 10^{-16}$	$1.032 \times 10^{-16}$	$5.944 \times 10^{-17}$
0.6	$1.715 \times 10^{-18}$	$1.818 \times 10^{-18}$	$1.531 \times 10^{-18}$	$1.475 \times 10^{-18}$	$1.532 \times 10^{-18}$
0.7	$2.636 \times 10^{-20}$	$2.573 \times 10^{-20}$	$1.534 \times 10^{-20}$	$1.400 \times 10^{-20}$	$2.922 \times 10^{-20}$
0.8	$2.899 \times 10^{-22}$	$2.570 \times 10^{-22}$	$1.029 \times 10^{-22}$	$8.830 \times 10^{-23}$	$4.123 \times 10^{-22}$

Table (4-28): The flow charge transition rate of MgO/D149 as a function of a potential barrier  $\Delta U^{LS}$  and a coupling strength of  $7 \times 10^{-2}$  eV

$\Delta U^{LS} = E_{cb} - qE^0$ (eV)	The current of electron transfer ( $\text{cm}^4\text{sec}^{-1}$ )				
	Solvent Types				
	Propanol	Butanol	Octanol	Dichloroethane	Acetonitrile
0.2	$3.787 \times 10^{-12}$	$4.788 \times 10^{-12}$	$9.706 \times 10^{-12}$	$1.067 \times 10^{-11}$	$2.019 \times 10^{-12}$
0.3	$2.220 \times 10^{-13}$	$2.709 \times 10^{-13}$	$4.825 \times 10^{-13}$	$5.196 \times 10^{-13}$	$1.291 \times 10^{-13}$
0.4	$9.313 \times 10^{-15}$	$1.081 \times 10^{-14}$	$1.607 \times 10^{-14}$	$1.681 \times 10^{-14}$	$6.109 \times 10^{-15}$
0.5	$2.795 \times 10^{-16}$	$3.046 \times 10^{-16}$	$3.586 \times 10^{-16}$	$3.614 \times 10^{-16}$	$2.138 \times 10^{-16}$
0.6	$6.004 \times 10^{-18}$	$6.054 \times 10^{-18}$	$5.361 \times 10^{-18}$	$5.163 \times 10^{-18}$	$5.541 \times 10^{-18}$
0.7	$9.228 \times 10^{-20}$	$8.489 \times 10^{-20}$	$5.370 \times 10^{-20}$	$4.901 \times 10^{-20}$	$1.062 \times 10^{-19}$
0.8	$1.014 \times 10^{-21}$	$8.398 \times 10^{-22}$	$3.603 \times 10^{-22}$	$3.090 \times 10^{-22}$	$1.507 \times 10^{-21}$

Table (4-29): The flow charge transition rate of MgO/D149 as a function of a potential barrier  $\Delta U^{LS}$  and a coupling strength of  $1.2 \times 10^{-3}$  eV

$\Delta U^{LS} = E_{cb} - qE^0$ (eV)	The current of electron transfer ( $\text{cm}^4\text{sec}^{-1}$ )				
	Solvent Types				
	Propanol	Butanol	Octanol	Dichloroethane	Acetonitrile
0.2	$6.492 \times 10^{-14}$	$8.208 \times 10^{-14}$	$1.663 \times 10^{-13}$	$1.829 \times 10^{-13}$	$3.462 \times 10^{-14}$
0.3	$3.806 \times 10^{-15}$	$4.644 \times 10^{-15}$	$8.272 \times 10^{-15}$	$8.908 \times 10^{-15}$	$2.213 \times 10^{-15}$
0.4	$1.596 \times 10^{-16}$	$1.854 \times 10^{-16}$	$2.755 \times 10^{-16}$	$2.882 \times 10^{-16}$	$1.047 \times 10^{-16}$
0.5	$4.792 \times 10^{-18}$	$5.223 \times 10^{-18}$	$6.148 \times 10^{-18}$	$6.197 \times 10^{-18}$	$3.666 \times 10^{-18}$
0.6	$1.029 \times 10^{-19}$	$1.037 \times 10^{-19}$	$9.191 \times 10^{-20}$	$8.852 \times 10^{-20}$	$9.500 \times 10^{-20}$
0.7	$1.581 \times 10^{-21}$	$1.455 \times 10^{-21}$	$9.205 \times 10^{-22}$	$8.401 \times 10^{-22}$	$1.821 \times 10^{-21}$
0.8	$1.739 \times 10^{-23}$	$1.439 \times 10^{-23}$	$6.176 \times 10^{-24}$	$5.298 \times 10^{-24}$	$2.584 \times 10^{-23}$

Table (4-30): The flow charge transition rate of MgO/D149 as a function of a potential barrier  $\Delta U^{LS}$  and a coupling strength of  $1.7 \times 10^{-4}$  eV

$\Delta U^{LS} = E_{cb} - qE^0$ (eV)	The current of electron transfer ( $\text{cm}^4\text{sec}^{-1}$ )				
	Solvent Types				
	Propanol	Butanol	Octanol	Dichloroethane	Acetonitrile
0.2	$9.198 \times 10^{-15}$	$1.162 \times 10^{-14}$	$2.357 \times 10^{-14}$	$2.591 \times 10^{-14}$	$4.831 \times 10^{-15}$
0.3	$5.391 \times 10^{-16}$	$6.579 \times 10^{-16}$	$1.171 \times 10^{-15}$	$1.261 \times 10^{-15}$	$3.077 \times 10^{-16}$
0.4	$2.261 \times 10^{-17}$	$2.626 \times 10^{-17}$	$3.903 \times 10^{-17}$	$4.083 \times 10^{-17}$	$1.449 \times 10^{-17}$
0.5	$6.788 \times 10^{-19}$	$7.399 \times 10^{-19}$	$8.710 \times 10^{-19}$	$8.779 \times 10^{-19}$	$5.053 \times 10^{-19}$
0.6	$1.458 \times 10^{-20}$	$1.470 \times 10^{-20}$	$1.302 \times 10^{-20}$	$1.254 \times 10^{-20}$	$1.302 \times 10^{-20}$
0.7	$2.241 \times 10^{-22}$	$2.061 \times 10^{-22}$	$1.304 \times 10^{-22}$	$1.190 \times 10^{-22}$	$2.484 \times 10^{-22}$
0.8	$2.464 \times 10^{-24}$	$2.039 \times 10^{-24}$	$8.750 \times 10^{-25}$	$7.505 \times 10^{-25}$	$3.504 \times 10^{-24}$

Table (4-31): The flow charge transition rate of MgO/D149 as a function of a potential barrier  $\Delta U^{LS}$  and a coupling strength of  $2.2 \times 10^{-4}$  eV

$\Delta U^{LS} = E_{cb} - qE^0$ (eV)	The current of electron transfer ( $\text{cm}^4\text{sec}^{-1}$ )				
	Solvent Types				
	Propanol	Butanol	Octanol	Dichloroethane	Acetonitrile
0.2	$1.190 \times 10^{-14}$	$1.504 \times 10^{-14}$	$4.050 \times 10^{-14}$	$3.353 \times 10^{-14}$	$6.252 \times 10^{-15}$
0.3	$6.977 \times 10^{-16}$	$8.515 \times 10^{-16}$	$1.516 \times 10^{-15}$	$1.633 \times 10^{-15}$	$3.982 \times 10^{-16}$
0.4	$2.926 \times 10^{-17}$	$3.399 \times 10^{-17}$	$5.051 \times 10^{-17}$	$5.284 \times 10^{-17}$	$1.876 \times 10^{-17}$
0.5	$8.785 \times 10^{-19}$	$9.575 \times 10^{-19}$	$1.127 \times 10^{-18}$	$1.136 \times 10^{-18}$	$6.539 \times 10^{-19}$
0.6	$1.887 \times 10^{-20}$	$1.902 \times 10^{-20}$	$1.685 \times 10^{-20}$	$1.622 \times 10^{-20}$	$1.685 \times 10^{-20}$
0.7	$2.900 \times 10^{-22}$	$2.668 \times 10^{-22}$	$1.687 \times 10^{-22}$	$1.540 \times 10^{-22}$	$3.215 \times 10^{-22}$
0.8	$3.189 \times 10^{-24}$	$2.639 \times 10^{-24}$	$1.132 \times 10^{-24}$	$9.713 \times 10^{-25}$	$4.535 \times 10^{-24}$

Table (4-32): The flow charge transition rate of ZnO/N749 as a function of a potential barrier  $\Delta U^{LS}$  and a coupling strength of  $2 \times 10^{-2}$  eV

$\Delta U^{LS} = E_{cb} - qE^0$ (eV)	The current of electron transfer ( $\text{cm}^4\text{sec}^{-1}$ )				
	Solvent Types				
	Propanol	Butanol	Octanol	Dichloroethane	Acetonitrile
0.26	$7.776 \times 10^{-13}$	$8.719 \times 10^{-13}$	$1.189 \times 10^{-12}$	$1.232 \times 10^{-12}$	$5.557 \times 10^{-13}$
0.34	$4.690 \times 10^{-14}$	$4.986 \times 10^{-14}$	$5.578 \times 10^{-14}$	$5.602 \times 10^{-14}$	$3.797 \times 10^{-14}$
0.40	$4.620 \times 10^{-15}$	$4.675 \times 10^{-15}$	$4.354 \times 10^{-15}$	$4.248 \times 10^{-15}$	$4.197 \times 10^{-15}$
0.57	$2.429 \times 10^{-18}$	$2.046 \times 10^{-18}$	$9.644 \times 10^{-19}$	$8.449 \times 10^{-19}$	$3.387 \times 10^{-18}$
0.66	$2.476 \times 10^{-20}$	$1.844 \times 10^{-20}$	$5.499 \times 10^{-21}$	$4.483 \times 10^{-21}$	$4.601 \times 10^{-20}$
0.77	$5.234 \times 10^{-23}$	$3.273 \times 10^{-23}$	$5.095 \times 10^{-24}$	$3.749 \times 10^{-24}$	$1.463 \times 10^{-22}$
0.88	$6.017 \times 10^{-26}$	$3.076 \times 10^{-26}$	$2.261 \times 10^{-27}$	$1.478 \times 10^{-27}$	$2.694 \times 10^{-25}$

Table (4-33): The flow charge transition rate of ZnO/N749 as a function of a potential barrier  $\Delta U^{LS}$  and a coupling strength of  $7 \times 10^{-2}$  eV

$\Delta U^{LS} = E_{cb} - qE^0$ (eV)	The current of electron transfer ( $\text{cm}^4\text{sec}^{-1}$ )				
	Solvent Types				
	Propanol	Butanol	Octanol	Dichloroethane	Acetonitrile
0.26	$2.721 \times 10^{-12}$	$3.051 \times 10^{-12}$	$4.163 \times 10^{-12}$	$4.314 \times 10^{-12}$	$1.945 \times 10^{-12}$
0.34	$7.254 \times 10^{-13}$	$1.745 \times 10^{-13}$	$1.952 \times 10^{-13}$	$1.960 \times 10^{-13}$	$1.329 \times 10^{-13}$
0.40	$1.617 \times 10^{-14}$	$1.636 \times 10^{-14}$	$1.524 \times 10^{-14}$	$1.486 \times 10^{-14}$	$1.469 \times 10^{-14}$
0.57	$8.504 \times 10^{-18}$	$7.164 \times 10^{-18}$	$3.375 \times 10^{-18}$	$2.957 \times 10^{-18}$	$1.185 \times 10^{-17}$
0.66	$8.666 \times 10^{-20}$	$6.455 \times 10^{-20}$	$1.924 \times 10^{-20}$	$1.569 \times 10^{-20}$	$1.610 \times 10^{-19}$
0.77	$1.831 \times 10^{-22}$	$1.145 \times 10^{-22}$	$1.783 \times 10^{-23}$	$1.312 \times 10^{-23}$	$5.121 \times 10^{-22}$
0.88	$2.106 \times 10^{-25}$	$1.076 \times 10^{-25}$	$7.915 \times 10^{-27}$	$5.173 \times 10^{-27}$	$9.432 \times 10^{-25}$

Table (4-34): The flow charge transition rate of ZnO/N749 as a function of a potential barrier  $\Delta U^{LS}$  and a coupling strength of  $1.2 \times 10^{-3}$  eV

$\Delta U^{LS} = E_{cb} - qE^0$ (eV)	The current of electron transfer ( $\text{cm}^4\text{sec}^{-1}$ )				
	Solvent Types				
	Propanol	Butanol	Octanol	Dichloroethane	Acetonitrile
0.26	$4.665 \times 10^{-14}$	$5.231 \times 10^{-14}$	$7.138 \times 10^{-14}$	$7.396 \times 10^{-14}$	$3.334 \times 10^{-14}$
0.34	$2.814 \times 10^{-15}$	$2.991 \times 10^{-15}$	$3.347 \times 10^{-15}$	$3.361 \times 10^{-15}$	$2.278 \times 10^{-15}$
0.40	$2.772 \times 10^{-16}$	$2.805 \times 10^{-16}$	$2.612 \times 10^{-16}$	$2.548 \times 10^{-16}$	$2.518 \times 10^{-16}$
0.57	$1.457 \times 10^{-19}$	$1.228 \times 10^{-19}$	$5.786 \times 10^{-20}$	$5.069 \times 10^{-20}$	$2.032 \times 10^{-19}$
0.66	$1.485 \times 10^{-21}$	$1.106 \times 10^{-21}$	$3.299 \times 10^{-22}$	$2.689 \times 10^{-22}$	$2.760 \times 10^{-21}$
0.77	$3.140 \times 10^{-24}$	$1.964 \times 10^{-24}$	$3.057 \times 10^{-25}$	$2.249 \times 10^{-25}$	$8.779 \times 10^{-24}$
0.88	$3.610 \times 10^{-27}$	$1.845 \times 10^{-27}$	$1.357 \times 10^{-28}$	$8.869 \times 10^{-29}$	$1.616 \times 10^{-26}$

Table (4-35): The flow charge transition rate of ZnO/N749 as a function of a potential barrier  $\Delta U^{LS}$  and a coupling strength of  $1.7 \times 10^{-4}$  eV

$\Delta U^{LS} = E_{cb} - qE^0$ (eV)	The current of electron transfer ( $\text{cm}^4\text{sec}^{-1}$ )				
	Solvent Types				
	Propanol	Butanol	Octanol	Dichloroethane	Acetonitrile
0.26	$6.610 \times 10^{-15}$	$7.411 \times 10^{-15}$	$1.011 \times 10^{-14}$	$1.047 \times 10^{-14}$	$4.724 \times 10^{-15}$
0.34	$3.986 \times 10^{-16}$	$4.238 \times 10^{-16}$	$4.742 \times 10^{-16}$	$4.762 \times 10^{-16}$	$3.227 \times 10^{-16}$
0.40	$3.927 \times 10^{-17}$	$3.974 \times 10^{-17}$	$3.701 \times 10^{-17}$	$3.611 \times 10^{-17}$	$3.568 \times 10^{-17}$
0.57	$2.065 \times 10^{-20}$	$1.739 \times 10^{-20}$	$8.197 \times 10^{-21}$	$7.182 \times 10^{-21}$	$2.879 \times 10^{-20}$
0.66	$2.104 \times 10^{-22}$	$1.567 \times 10^{-22}$	$4.674 \times 10^{-23}$	$3.810 \times 10^{-23}$	$3.910 \times 10^{-22}$
0.77	$4.449 \times 10^{-25}$	$2.782 \times 10^{-25}$	$4.331 \times 10^{-26}$	$3.186 \times 10^{-26}$	$1.243 \times 10^{-24}$
0.88	$5.114 \times 10^{-28}$	$2.614 \times 10^{-28}$	$1.922 \times 10^{-29}$	$1.256 \times 10^{-29}$	$2.290 \times 10^{-27}$

Table (4-36): The flow charge transition rate of ZnO/N749 as a function of a potential barrier  $\Delta U^{LS}$  and a coupling strength of  $2.2 \times 10^{-4}$  eV

$\Delta U^{LS} = E_{cb} - qE^0$ (eV)	The current of electron transfer ( $\text{cm}^4\text{sec}^{-1}$ )				
	Solvent Types				
	Propanol	Butanol	Octanol	Dichloroethane	Acetonitrile
0.26	$8.554 \times 10^{-15}$	$9.591 \times 10^{-15}$	$1.312 \times 10^{-14}$	$1.355 \times 10^{-14}$	$6.113 \times 10^{-15}$
0.34	$5.159 \times 10^{-16}$	$5.484 \times 10^{-16}$	$6.162 \times 10^{-16}$	$6.162 \times 10^{-16}$	$4.176 \times 10^{-16}$
0.40	$5.083 \times 10^{-17}$	$5.143 \times 10^{-17}$	$4.813 \times 10^{-17}$	$4.673 \times 10^{-17}$	$4.617 \times 10^{-17}$
0.57	$2.672 \times 10^{-20}$	$2.251 \times 10^{-20}$	$1.068 \times 10^{-20}$	$9.294 \times 10^{-21}$	$3.725 \times 10^{-20}$
0.66	$2.723 \times 10^{-22}$	$2.028 \times 10^{-22}$	$6.104 \times 10^{-23}$	$4.931 \times 10^{-23}$	$5.061 \times 10^{-22}$
0.77	$5.757 \times 10^{-25}$	$3.601 \times 10^{-25}$	$5.668 \times 10^{-26}$	$4.123 \times 10^{-26}$	$1.609 \times 10^{-24}$
0.88	$6.619 \times 10^{-28}$	$3.383 \times 10^{-28}$	$2.521 \times 10^{-29}$	$1.626 \times 10^{-29}$	$2.964 \times 10^{-27}$

Table (4-37): The flow charge transition rate of ZnO/D149 as a function of a potential barrier  $\Delta U^{LS}$  and a coupling strength of  $2 \times 10^{-2}$  eV

$\Delta U^{LS} = E_{cb} - qE^0$ (eV)	The current of electron transfer ( $\text{cm}^4\text{sec}^{-1}$ )				
	Solvent Types				
	Propanol	Butanol	Octanol	Dichloroethane	Acetonitrile
0.26	$1.694 \times 10^{-13}$	$2.104 \times 10^{-13}$	$3.999 \times 10^{-13}$	$4.354 \times 10^{-13}$	$9.207 \times 10^{-14}$
0.34	$1.505 \times 10^{-14}$	$1.804 \times 10^{-14}$	$2.998 \times 10^{-14}$	$3.193 \times 10^{-14}$	$8.907 \times 10^{-15}$
0.40	$2.123 \times 10^{-15}$	$2.460 \times 10^{-15}$	$3.611 \times 10^{-15}$	$3.769 \times 10^{-15}$	$1.358 \times 10^{-15}$
0.57	$4.226 \times 10^{-18}$	$4.327 \times 10^{-18}$	$4.008 \times 10^{-18}$	$3.880 \times 10^{-18}$	$3.620 \times 10^{-18}$
0.66	$1.052 \times 10^{-19}$	$9.918 \times 10^{-20}$	$6.744 \times 10^{-20}$	$6.206 \times 10^{-20}$	$1.096 \times 10^{-19}$
0.77	$7.922 \times 10^{-22}$	$6.633 \times 10^{-22}$	$2.907 \times 10^{-22}$	$2.489 \times 10^{-22}$	$1.090 \times 10^{-21}$
0.88	$3.942 \times 10^{-24}$	$2.880 \times 10^{-24}$	$7.605 \times 10^{-25}$	$5.994 \times 10^{-25}$	$7.478 \times 10^{-24}$

Table (4-38): The flow charge transition rate of ZnO/D149 as a function of a potential barrier  $\Delta U^{LS}$  and a coupling strength of  $7 \times 10^{-2}$  eV

$\Delta U^{LS} = E_{cb} - qE^0$ (eV)	The current of electron transfer ( $\text{cm}^4\text{sec}^{-1}$ )				
	Solvent Types				
	Propanol	Butanol	Octanol	Dichloroethane	Acetonitrile
0.26	$5.931 \times 10^{-13}$	$7.306 \times 10^{-13}$	$1.399 \times 10^{-12}$	$1.524 \times 10^{-12}$	$3.222 \times 10^{-13}$
0.34	$5.270 \times 10^{-14}$	$6.314 \times 10^{-14}$	$1.049 \times 10^{-13}$	$1.117 \times 10^{-13}$	$3.117 \times 10^{-14}$
0.40	$7.430 \times 10^{-15}$	$8.610 \times 10^{-15}$	$1.264 \times 10^{-14}$	$1.319 \times 10^{-14}$	$4.754 \times 10^{-15}$
0.57	$1.479 \times 10^{-17}$	$1.514 \times 10^{-17}$	$1.403 \times 10^{-17}$	$1.358 \times 10^{-17}$	$1.267 \times 10^{-17}$
0.66	$3.684 \times 10^{-19}$	$3.471 \times 10^{-19}$	$2.360 \times 10^{-19}$	$2.172 \times 10^{-19}$	$3.838 \times 10^{-19}$
0.77	$2.772 \times 10^{-21}$	$2.321 \times 10^{-21}$	$1.017 \times 10^{-21}$	$8.714 \times 10^{-22}$	$3.815 \times 10^{-21}$
0.88	$1.379 \times 10^{-23}$	$1.008 \times 10^{-23}$	$2.662 \times 10^{-24}$	$2.098 \times 10^{-24}$	$2.617 \times 10^{-23}$

Table (4-39): The flow charge transition rate of ZnO/D149 as a function of a potential barrier  $\Delta U^{LS}$  and a coupling strength of  $1.2 \times 10^{-3}$  eV

$\Delta U^{LS} = E_{cb} - qE^0$ (eV)	The current of electron transfer ( $\text{cm}^4\text{sec}^{-1}$ )				
	Solvent Types				
	Propanol	Butanol	Octanol	Dichloroethane	Acetonitrile
0.26	$1.016 \times 10^{-14}$	$1.202 \times 10^{-14}$	$2.399 \times 10^{-14}$	$2.612 \times 10^{-14}$	$5.524 \times 10^{-15}$
0.34	$9.035 \times 10^{-15}$	$1.082 \times 10^{-15}$	$1.798 \times 10^{-15}$	$1.916 \times 10^{-15}$	$5.344 \times 10^{-16}$
0.40	$1.273 \times 10^{-16}$	$1.476 \times 10^{-16}$	$2.167 \times 10^{-16}$	$2.261 \times 10^{-16}$	$8.150 \times 10^{-17}$
0.57	$2.535 \times 10^{-19}$	$2.596 \times 10^{-19}$	$2.405 \times 10^{-19}$	$2.328 \times 10^{-19}$	$2.172 \times 10^{-19}$
0.66	$6.315 \times 10^{-21}$	$5.951 \times 10^{-21}$	$4.046 \times 10^{-21}$	$3.723 \times 10^{-21}$	$6.579 \times 10^{-21}$
0.77	$4.753 \times 10^{-23}$	$3.980 \times 10^{-23}$	$1.744 \times 10^{-23}$	$1.493 \times 10^{-23}$	$6.540 \times 10^{-23}$
0.88	$2.365 \times 10^{-25}$	$1.728 \times 10^{-25}$	$4.563 \times 10^{-26}$	$3.596 \times 10^{-26}$	$4.487 \times 10^{-25}$



Table (4-40): The flow charge transition rate of ZnO/D149 as a function of a potential barrier  $\Delta U^{LS}$  and a coupling strength of  $1.7 \times 10^{-4}$  eV

$\Delta U^{LS} = E_{cb} - qE^0$ (eV)	The current of electron transfer ( $\text{cm}^4\text{sec}^{-1}$ )				
	Solvent Types				
	Propanol	Butanol	Octanol	Dichloroethane	Acetonitrile
0.26	$1.440 \times 10^{-15}$	$1.789 \times 10^{-15}$	$3.399 \times 10^{-15}$	$3.701 \times 10^{-15}$	$7.826 \times 10^{-16}$
0.34	$1.280 \times 10^{-16}$	$1.533 \times 10^{-16}$	$2.548 \times 10^{-16}$	$2.714 \times 10^{-16}$	$7.571 \times 10^{-17}$
0.40	$1.804 \times 10^{-17}$	$2.091 \times 10^{-17}$	$3.069 \times 10^{-17}$	$3.204 \times 10^{-17}$	$1.154 \times 10^{-17}$
0.57	$3.592 \times 10^{-20}$	$3.678 \times 10^{-20}$	$3.407 \times 10^{-20}$	$3.298 \times 10^{-20}$	$3.077 \times 10^{-20}$
0.66	$8.947 \times 10^{-22}$	$8.430 \times 10^{-22}$	$5.733 \times 10^{-22}$	$5.275 \times 10^{-22}$	$9.321 \times 10^{-22}$
0.77	$6.734 \times 10^{-24}$	$5.638 \times 10^{-24}$	$2.471 \times 10^{-24}$	$2.116 \times 10^{-24}$	$9.266 \times 10^{-24}$
0.88	$3.351 \times 10^{-26}$	$2.448 \times 10^{-26}$	$6.465 \times 10^{-27}$	$5.095 \times 10^{-27}$	$6.356 \times 10^{-26}$

Table (4-41): The flow charge transition rate of ZnO/D149 as a function of a potential barrier  $\Delta U^{LS}$  and a coupling strength of  $2.2 \times 10^{-4}$  eV

$\Delta U^{LS} = E_{cb} - qE^0$ (eV)	The current of electron transfer ( $\text{cm}^4\text{sec}^{-1}$ )				
	Solvent Types				
	Propanol	Butanol	Octanol	Dichloroethane	Acetonitrile
0.26	$1.864 \times 10^{-15}$	$2.315 \times 10^{-15}$	$4.399 \times 10^{-15}$	$4.789 \times 10^{-15}$	$1.012 \times 10^{-15}$
0.34	$1.656 \times 10^{-16}$	$1.984 \times 10^{-16}$	$3.298 \times 10^{-16}$	$3.512 \times 10^{-16}$	$9.798 \times 10^{-17}$
0.40	$2.335 \times 10^{-17}$	$2.706 \times 10^{-17}$	$3.972 \times 10^{-17}$	$4.146 \times 10^{-17}$	$1.494 \times 10^{-17}$
0.57	$4.649 \times 10^{-20}$	$4.760 \times 10^{-20}$	$4.409 \times 10^{-20}$	$4.268 \times 10^{-20}$	$3.982 \times 10^{-20}$
0.66	$1.157 \times 10^{-21}$	$1.091 \times 10^{-21}$	$7.419 \times 10^{-22}$	$6.826 \times 10^{-22}$	$1.206 \times 10^{-21}$
0.77	$8.714 \times 10^{-24}$	$7.296 \times 10^{-24}$	$3.198 \times 10^{-24}$	$2.738 \times 10^{-24}$	$1.199 \times 10^{-23}$
0.88	$4.336 \times 10^{-26}$	$3.168 \times 10^{-26}$	$8.366 \times 10^{-27}$	$6.593 \times 10^{-27}$	$8.226 \times 10^{-26}$

## 4.6 Discussion

### 4.6.1 Theoretical Model of Charge Transfer at Semiconductor/Molecule

#### Interface.

The flow charge transfer rate yields at the interface of a semiconductor/molecule system under a continuum hypothesis for a polar media has been theoretically studied and evaluated. The flow charge transfer rate was calculated according to Marcus model for the donor acceptor systems of InAs/D149, ZnO/D149, MgO/D149, InAs/N749, ZnO/N749 and MgO/N749 depending on the quantum consideration theory. The flow charge transfer rate of these systems is very useful in selecting the suitable system for applied technology, Such as photonic cell.

The flow charge rate is a good tool in theoretical studies of the electric properties of material devices.

### 4.6.2 Modeling of the Charge Transfer Mechanism

The flow charge rate  $\mathcal{F}_{S-L}$  of InAs/D149, ZnO/D149, MgO/D149, InAs/N749, ZnO/N749 and MgO/N749 systems was theoretical studied and evaluated as a function of the solvent medium polarity using a simple theoretical model based on a quantum transport theory. In order to evaluate and study the flow charge rate systems, several parameters such as the reorientation transition energy, potential barrier, strength coupling coefficient and flow charge rate transition were studied at room temperature. Due to this model, the electronic states in both semiconductor and sensitized dye materials were assumed to be continuum for electrons transition over the potential barrier height at the interface region when the two wave functions for the acceptor semiconductor state and donor sensitized dye molecule state are overlapping with each other.

The probability of the flow electronic transition rate that yields at a polar media  $\mathcal{F}_{SL}(\text{sec}^{-1})$  in Eq.(3-48) depends on the reorientation transition energy  $\mathcal{T}_S^L$  (eV),

potential barrier and the strength coupling coefficient  $\mathbb{C}_{S/L}$  (eV), density of electronic state  $D_S(\epsilon)$ , the driving force energy, and the absorption energy of the dye and some structure parameters of materials in devices. In order to discuss the flow charge rate of electrons that transfer from donor to acceptor states in a system, It is important to understand and calculate the electron transfer parameters that describe the behavior of electron in such devices. The reorientation transition energy  $\mathcal{T}_S^L$  (eV) at a semiconductor/molecule dye was evaluated according to classical Marcus theory. The continuum Marcus theory approaches were introduced according to optical dielectric constant, refractive index, static dielectric constant and radii of donor and acceptor materials. The values of the refractive index and dielectric constants of the dyes that used in all calculations were taken from the experimental results of ref. [124]. The simplicity and the natures of semiconductor and sensitized molecule interface help in predicting the typical order of the reorientation energies  $\mathcal{T}_S^L$  and flow charge rate  $\mathcal{F}_{S-L}$  of the electronic transition in the solvent media. The electron transfer reaction at semiconductor/molecule dye interface was effected by the polarity of the molecules solvent, and the sensitized molecule dye has both static and optical dielectric constants properties. Furthermore, one of the most important factor in the probability flow charge rate is the strength coupling coefficient  $\mathbb{C}_{S/L}(\epsilon)$ , which investigated by the overlapping in quantum space of wave functions between semiconductor and molecule dye state at interfaces system. From the values of the strength coupling coefficient of the charge transfer rate, it has been distinguished the type of the electrons transfer (adiabatic or/and non-adiabatic transition). The current rate of the electronic transition reaction was found to be proportional to square value of the effective strength coupling coefficient  $|\mathbb{C}_{S/L}(\epsilon)|^2$ . The square value of the effective strength coupling coefficient  $|\mathbb{C}_{S/L}(\epsilon)|^2$  has been controlled the mechanism of the charge transfer between donor and acceptor systems. The electronic properties

of the molecules were strongly affected by the closeness of the solid surfaces, due to strength of the semiconductor-molecule reaction [128]. The electronic strength coupling of the electronic transfer from donor to acceptor states at the interfaces has been evidently reflected to transfer ability of electrons. Moreover, it is well known that the potential barriers energy was theoretically calculated from Eq.(3-49), which refers to the relation of absorbed light by sensitized molecule dye and the reorientation transition energy. It also depends on both the refractive index and the dielectric constant of the media. It has been calculated based on Eq.(3-50). So far, we can study and evaluation the most of an important coefficients of charge transfer that is reorientation transition energy under the postulate of Marcus oxidants or reductions state. On the other hand, we can show a theoretical analysis of the results have been performed for the determination of the reorientation transition energy, potential barrier, strength coupling and some other parameters of two material N749 and D149 such as, density of electronic distribution  $\rho_{S-L}(\epsilon)$ , the density of electronic states in the semiconductor  $D_S$ , the effective coupling length  $l_{ecl}$ , the atomic density of semiconductor  $\rho_a$ , penetration depth  $\beta_S$ , the conduction energy band  $E_{cb}$ , the electrochemical potential of dye  $qE^0$  and room temperature. As expected, the results of the flow charge transfer rate show the behavior of the electronic transfer in non-scale limit, and the electron transfer reaction in semiconductor/molecule dye system is non-adiabatic according to the results of the strength coupling coefficient  $C_{S/L}(\epsilon)$ , (eV) at the interface between semiconductor and molecule dye states. Tables (4-12) to (4-41) for all the six systems show that the flow charge transfer rate is small for the weak strength coupling coefficient of semiconductor/molecule dye system, and it increased with increasing the strength coupling. The maximum flow charge transfer rate was found in a semiconductor/molecule systems with dichloroethane solvent for all the six systems along with lowering potential barrier height in tables (4-11) to (4-

16). Also, the flow charge rate increases for a low polarity of the dichloroethane solvent (0.383) [124], and decreases for a high polarity of propanol solvent (0.528). On the other hand, the reorientation transition energy is small for low polarity solvent and large for high polarity solvents as seen in table (4-5), this indicates that electrons probably transfer for a system with low reorientation transition energy. Moreover, the flow charge rate of transition constant  $\mathcal{F}_{SL}(\text{sec}^{-1})$  for InAs/D149, ZnO/D149 and MgO/D149 systems are higher than the flow charge rate for InAs/N749, ZnO/N749 and MgO/N749 systems which indicates that the D149 is more active than N749 and electrons activity transfer with low polar solvents.

#### **4.6.3 Influence of Reorientation Transition Energy $\mathcal{T}_S^L$ (eV) on the Flow Charge Transition Rate**

One of the most important parameters for charge transfer rate is the reorientation transition energy  $\mathcal{T}_S^L$  (eV), and it is widely used in the quantum transition theory to investigate the transfer of electrons in polar and/or non-polar region. It is predicted the refractive index and dielectric constant of the solvent and semiconductor according to Marcus continuum model. However, the understanding of the charge transfer reaction should be considered as a starting points for studying the behavior of reorientation transition energy at semiconductor/molecule interface devices. However, the reorientation transition energy  $\mathcal{T}_S^L$  (eV) of the charge transition could be affected the flow charge transition rate  $\mathcal{F}_{SL}(\text{sec}^{-1})$  at semiconductor/molecule dye system. We present evidence that the flow charge transition rate depends on the nature of material, surround the solvent the polarity of both the solvent and the system as well as the radii of materials. The reorientation transition energy is governed by polarity of the solvent.

A Marcus continuum model of donor-acceptor system reactions facilitate the calculation of the electronic reorientation transition energy before the charge

transition  $\mathcal{T}_S^L$ (eV) at a semiconductor/molecule interface system due to the limitation of the charge transfer by both the refractive index, and the static dielectric constant for a donor-acceptor system.

#### **4.6.4 Influence of Polarity Solvents on the Flow Charge Rate**

At a fixed sensitized molecule dye, the reorientation transition energy decreases with decreasing the polarity of solvents. For example, propanol with a high polarity of (0.473) leads to large reorientation transition energy in all systems, Octanol a polarity of (0.393) lower than propanol results to reorientation transition energy, Butanol has polarity equal (0.453) lower than while dichloroethane with a polarity of (0.383) has the lowest reorientation transition energy. However, Acetonitrile a high reorientation transition energy despite its polarity of (0.528) that lies in the middle of other solvent values dielectric constant value (37.5). From the discussion of the reorientation transition energy results for as a function of solvents and molecule dyes, it is clear that the reorientation transition energy is high for InAs/D149, ZnO/D149, and MgO/D149 systems, while it is low for InAs/N749, ZnO/N749 and MgO/N749 systems. This is related to the structure of both D149 and N749 dyes and their molecular weights, The D149 dye has a molecular weight of (741.94 g/mol), and a mass density of (2.141 g/cm<sup>3</sup>) [86], while the N749 dye has a molecular weight of (781.73 g/mol), and a mass density of (0.749 g/cm<sup>3</sup>) and their radii are (5.16 Å) and (7.45 Å) respectively. By comparing the results of reorientation transition energy in table (4-5) and the results of flow charge rate in tables (4-12) to (4-41), we find that the flow charge rate increases with decreasing both the reorientation transition energy and the polarity of solvents in lower potential region and vice versa due to the effect of potential height .

#### **4.6.5 Effect of Polarity Function on the Flow Charge Transfer**

One important critical parameter that effected on the reorientation transition energy  $\mathcal{T}_S^L(\text{eV})$  in all the six semiconductor/molecule systems is the polarity function. The polarity function has a strong impact on the flow charge transfer through effecting the distribution of electrons in semiconductor/molecule systems. In the charge transfer reaction in semiconductor/molecule devices, the behavior of electrons was limited by the polarity function of the solvent media which then effected the reorientation transition energy. Hence the polarity function that effects on the electronic transition interactions at the semiconductor/molecule interface way effected by both the refractive index and the dielectric constant. According to the results in table (4-5), we can see that the orientation transition energy increases with increasing the polarity function  $\delta(n, \epsilon)$  and the calculated results are 0.473, 0.453, 0.393, 0.383 and 0.528 for Propanol, Butanol, octanol, Dichloroethane and Acetonitrile respectively. Therefore, it is useful to calculate the polarity function according to a continuum approximation method in Eq.(3-51) which indicates that the optical properties is effected on the charge transfer rate as shown in table (4-5). The theoretical results of the electronic rate production were made for six different system. On the other hand, the reorientation transition energy  $\mathcal{T}_S^L(\text{eV})$  of the electronic transition is limited the probabilities of the flow charge rate constant  $\mathcal{F}_{SL}(\text{sec}^{-1})$  at semiconductor/molecule system. For all the six systems of InAs/D149, ZnO/D149, MgO/D149, InAs/N749, ZnO/N749 and MgO/N749, with different solvents such as propanol, butanol, octanol, dichloroethane and acetonitrile are that listed in table (4-3), the reorientation transition energy for these systems were affected by refractive index ( $n$ ), dielectric constant ( $\epsilon_{so}$ ) and the polarity function of the solvent as seen in table (4-5). By comparing the results in table (4-5) and estimation the polarity function  $\delta(n, \epsilon)$ , we see that the reorientation transition energy is high for a large polarity function and vice versa. This indicates that the

reorientation transition energies are dependent on the polarity function of the system. It is well known that the probability of the flow charge transition across the semiconductor/molecule interface  $\mathcal{F}_{SL}(\text{sec}^{-1})$  can be evaluated according to the quantum method as a results of the orientation transition energy of the system. The reorientation transition energy of the system makes the system reformed its configuration to start the transition and each one needs an energy differ than another system.

#### **4.6.6 Influence of the Experimental Potential Force on Flow Charge Rate**

Two types of potential were used in this study. The experimental values of potential were used to calculate the flow charge rate while the other theoretical results of potential were calculated according to absorption energy from spectrum of dyes and the reorientation transition energy. The experimental potential ( $\mathcal{U}^{LS}$ ) depends on the conduction band energies ( $E_{cb}$ ) of InAs, ZnO and MgO semiconductors and on the electrochemical potential ( $qE^0$ ) of the dye. Experimental potential data were taken from ref. [8] and they analyzes through our model. From tables (4-12) to (4-41), we can see that the effect of the experimental data of the potential  $\Delta\mathcal{U}^{LS}(\text{eV})$  on the flow charge rate for InAs/D149, ZnO/D149, MgO/D149, InAs/N749, ZnO/N749 and MgO/N749 systems with respect to the conduction band energy  $E_{cb}$  and electrochemical potential  $qE^0$  of dye. The experimental data of the potential for both InAs and MgO both dyes are were ( 0.2, 0.3, 0.4, 0.5, 0.6, 0.7 and 0.8) eV, while they were ( 0.26, 0.34, 0.40, 0.57, 0.66, 0.77 and 0.88 ) eV for ZnO semiconductors. The results of the flow charge transfer rate in tables (4-12) to (4-41) show that the transfer of electrons decreases with increasing experimental potential and vice versa. On the other hand, we found that the experimental value of the potential at a specific value of the conduction band energy decreases with increasing the electrochemical potential of the dye. While, the flow charge transition



rate decreases with increasing the electrochemical potential. this means that the dye appears high electrochemical potential leading to more electrons transfer.

#### **4.6.7 Influence of Theoretical Potential Barrier Height $\Delta\mathcal{U}^{LS}$ (eV) on the Flow**

##### **Charge Transfer**

The behavior of electronic transfer across the interface of semiconductor /molecule dye depends on the theoretical value of the potential (potential barrier height). The theoretical potential reflected the ability of electrons to transfer from donor to acceptor states. The potential barrier height is created at the interface region between semiconductor and molecule material. At the interface, it is possible to discuss and study the influence of the potential barrier height on the electronic transition phenomena at semiconductor/molecule devices. Tables (4-6) to (4-11), show the theoretical potential barrier height values of InAs/D149, ZnO/D149, MgO/D149, InAs/N749, ZnO/N749 and MgO/N749 systems that resulted due to Marcus formula in Eq.(3-49) along the results of the reorientation transition energies and the absorption energy of different solvents. For the semiconductor/molecule devices interface, the theoretical potential barrier height value is formed due to the differences in the energy level according to the properties of semiconductor, molecule and solvent, which hinder the transition of more electron from donors to acceptor states. Theoretical potential barrier height is a function of the absorption energy by N749 and D149 dyes and the reorientation transition energy. Both N749 and D149 dyes have special absorption spectrum which reflected the working region of the dye. For example, the active area for N749 is in the range of (450-800) nm, while that for D149 is in the range of (400-800). The potential barrier height for all systems increases with increasing the absorption energies and decreasing the wave length. Also, the potential barrier increases with decreasing the reorientation transition energy and vice versa. However, the flow charge transition rate for

electronic transition in semiconductor/molecule devices increases with decreasing the potential barrier height. Also the electronic density distribution of energy state at semiconductor and the electronic at energy levels at HOMO LUMO state cooperation to creates a potential barrier at interface of semiconductor/molecule systems. The energy states founded close to the HOMO levels in the system for both molecules are due to the semiconductor energy states arised from the hybridization of the energy states of semiconductor with the occupied molecular states. This indicates that save of the absorption energies by dyes used to reform the configuration of the system before the electrons transfer and others lead to drive more electrons to transition from donor to acceptor over the potential barrier height. Theoretical potential barrier results in this model are consistent with the observed flow charge rate constant [104]. From tables (4-6) to (4-11) we can see that the flow charge rate for electronic transfer increases with decreasing the potential barrier height for all systems. due to hindering the electrons transition by potential barrier height.

#### **4.6.8 Influence of the Coupling Strength Coefficient $C_{S/L}(\epsilon)$ (eV) on the Flow**

##### **Charge Transfer Rate**

Due to the electronic transition processes for semiconductor/molecule dye systems the flow charge transfer for system has evaluated due to coupling strength  $2 \times 10^{-2}$  eV to  $2.2 \times 10^{-4}$  eV. The flow charge transfer rate is controlled by to the coupling strength and it is proportional to the square value of the coupling strength parameters. The coupling strength shows the mechanisms of the overlapping reactions between the electronic wave functions of semiconductor and molecule states. From Eq.(3-47), it is seen that the strength coupling coefficient was used to evaluate the flow charge rate constant using Eq.(3-48). We discussion the strength coupling for the electronic through interface of heterostructures devices InAs/D149, ZnO/D149, MgO/D149, InAs/N749, ZnO/N749 and MgO/N749 systems. It can discussion the overlapping of two wave function of electronic state for electrons at conduction band and wave function of electronic at molecule to creation the strength coupling between the energy levels of two material. The strength coupling of

electronic in semiconductor/molecule has evidently indicated the system have capable to transfer more charge when the energy levels state are alignment for semiconductor and molecules. The strength coupling of electronic give the system enough strong to pulling down the energy levels of molecule and leading to alignment with semiconductor levels. In conclusion, the semiconductor is bounded to the molecules surface chemisorption, and the charged cross from molecules to semiconductor cross interface, that's taken in the range be  $|C_{S/L}(\epsilon)|^2 \approx 2 \times 10^{-2}$  eV,  $7 \times 10^{-2}$  eV,  $1.2 \times 10^{-3}$  eV,  $1.7 \times 10^{-4}$  eV and  $2.2 \times 10^{-4}$  eV [127] for semiconductor to molecule system depending on the experimental data. At interface between semiconductor and molecule, the wave functions for semiconductor and molecule overlapping and electrons can cross the potential barrier height to transfer from donor to acceptor. However, the transfer of electrons occurs when the energy levels of electron and final electronic energy states should be equally by energies under assume continuum energy of electronic states at interfaces.

On the other hand, these electronic states became resonance due to fluctuations of polarity function for solvent surrounding medium. From tables (4-12) to (4-41) for InAs/D149, ZnO/D149, MgO/D149, InAs/N749, ZnO/N749 and MgO/N749 systems. we show that flow charge rate of electronic transition are increasing with increasing strength coupling and vice versa.

**Chapter Five**  
**Conclusions**  
**And**  
**Suggested Future**  
**works**

## Chapter Five

### 5.1 Conclusions

A simple model for the charge transfer based on the quantum mechanics and Marcus continuity theory was used to study the electronic behavior in semiconductor/molecule system. Studying the flow charge transfer rate for electronic transition in semiconductor/molecule system helps in choosing the suitable system in the technology. Also the flow charge transfer rate of the electronic from donor to acceptor states at semiconductor/molecule interface was studied according to quantum theory and the theory of continuity. The results can be summarized in the following points:

- 1- The flow charge transfer rate from donor to acceptor states is proportional to both material structure and the solvent polarity.
- 2- Orientation transition energy of the charge transition affects the constant rate of the transition probability in semiconductor/molecule system, and the flow charge transfer rate increases along with decreases of the orientation transition energy.
- 3- Electronic transition reactions is clearly depends on the solvents polarity that affected the flow charge transfer rate and orientation transition energy.
- 4- The strength coupling of overlapped wave functions for both semiconductor and molecule controls the type of charge transfer rate.
- 5- The flow charge transfer rate for electronic transitions increases with decreases the potential barrier height .

## **5.2 Suggested Future works**

According to the present results, we may suggest the following points as future works:

- 1- Theoretical study on the effect of the tunneling barrier on the flow electronic transition at solid/solid interface.
- 2- Theoretical study on the influence of the density of state on the behavior of electronic transition interaction at solid/liquid system.
- 3- Study the effect of electronic-hole interaction on the charge transfer in solid material.

## References

- 1- Zeman M. 2003 “Introduction to Photovoltaic Solar Energy” solar cells college material.
- 2- Fox M.A. ;Chanon, M. 1988 “Photoinduced Electron Transfer” Elsevier, Amsterdam, PP 117-205.
- 3- Gray H.B., and Ellis W.R, Valentine 1994 “Electron Transfer Theory” JS Eds University Science Book Mill Valley CA, PP 315-363.
- 4- Juris, A.; Balzani, V.; Barigelletti, F.; Campagna, S.; Belser, P.; von Zelewsky, A. 1988 “Ru (II) Polypyridine Complexes: Photophysics, Photochemistry, Electrochemistry, and Chemiluminescence” Coord Chem. Rev. 84, 85.
- 5- Demas,J. N.; DeGraff, B. A. 2001 “Applications of Luminescent Transition Platinum Group Metal Complexes to Sensor Technology and Molecular Probes” Coord. Chem. Rev. 211, 317.
- 6- Mejiritski, A.; Polykarpov, A. Y.; Sarker, A. M.; Neckers, D. C. 1996 “Novel Photoimaging System Based on Photoinduced Electron Transfer in Polymers Containing Pendant Benzophenone-Borate Salts” Chem. Mat. 8, 1360.
- 7- Kim,Y.; Teshima,K. ; Kobayashi,N. 2000 “Improvement of Reversible Photoelectrochromic Reaction of Polyaniline in Polyelectrolyte Composite Film with the Dichloroethane Solution System” Electrochimica Acta, 45, 1549.

- 8- Hopfield, J. J.; Onuchic, J. N.; Beratan, D. N. 1989 “Electronic Shift Register Memory Based on Molecular Electron-Transfer Reactions” *J. Phys. Chem.* 93, 6350.
- 9- Hoffman, M. R.; Martin, S. T.; Choi, W.; Bahnemann, D. W. “Environmental Applications of Semiconductor Photocatalysis” *Chem.Rev.* 1995, 95, 69.
- 10- Homlin, R. E.; Stemp, E. D. A; Barton, J. K. 2000 “Ground and Excited State Electron Transfer Dynamics” *Inorg. Chini. Acta*, 297, 88 .
- 11- Nazeeruddin , M. K.; Kay, A.; Rodicio, I.; Humphry-Baker, R.Muller, E.; Liska, P.; Vlachopoulos, N.; Grätzel, M. 1993 “Conversion of Light to Electricity by cis-X<sub>2</sub>bis (2, 2'-bipyridyl-4, 4'-Dicarboxylate) Ruthenium(II)Charge-Transfer Sensitizers(X=Cl-, Br-, I-, CN-, and SCN-) on ...” *J. Am. Chem. Soc.*, 115, 6382.
- 12- Sheehan SW, Thomsen JM, Hintermair U, Crabtree RH, Brudvig GW, Schmittenmaer CA. 2015 “A Molecular Catalyst for Water Oxidation. that Binds to Metal Oxide Surfaces”. *Nature communications.* 6. 6469
- 13- Panwar N.,Kothari S. 2011 “Role of Renewable Energy Source in Environmental Protection” :areview renewable and sustainable energy reviews 15, PP 1513-1524
- 14- Compano, R., Molenkamp L., Paul, D., J. 2000 “Technology Roadmap for Nanoelectronics” ; European Commission, IST Programme, Future and Emerging Technologies.



- 15- Hanning Chen, Mark A. Ratner, and George C. Schatz 2011 “Time-Dependent Theory of the Rate of Photo-Induced Electron Transfer” *J. Phys. Chem. C*, 115, 18810-18821.
- 16- Andrew S. Leathers, David A. Micha, and Dmitri S. Kilin 2010 “Direct and Indirect Electron Transfer at a Semiconductor Surface with an Adsorbate: Theory and Application to  $\text{Ag}_3\text{Si}(111):\text{H}$ ” *The Journal of Chemical Physics* 132, 114702.
- 17- N. P. Guisinger, M. E. Greene, R. Basu, A. S. Baluch, and M. C. Hersam, 2004 “Room Temperature Negative Differential Resistance Through Individual Organic Molecules on Silicon Surfaces” *Nano Letters*, Vol. 4(1), P 55-59.
- 18- G. Ashkenasy et al, 2002 “Molecular Engineering of Semiconductor Surfaces and Devices” *Acc. Chem. Res.* Vol. 35, p. 121.
- 19- Linjun Wang and David Beljonne 2013 “Charge Transport in Organic Semiconductors: Assessment of the Mean Field Theory in the Hopping Regime” *J. Chem. Phys.* 139, P20-P064316-1 to 064316-12.
- 20- Ji Won Ha, T. Purnima A. Ruberu, Rui Han, Bin Dong, Javier Vela, and Ning Fang 2014 “Super-Resolution Mapping of Photogenerated Electron And Hole Separation in Single Metal–Semiconductor Nanocatalysts” *J. Am. Chem. Soc.* 136, 1398-1408.
- 21- Anna Reynal, Fezile Lakadamyali, Manuela A. Gross, Erwin Reisner and James R. Durrant. 2013 “Parameters Affecting Electron Transfer Dynamics from Semiconductors to Molecular Catalysts for the Photochemical

- Reduction of Protons” Energy & Environmental Science, 6.11,3291-3300
- 22- Wörner, H. J., Arrell, C. A., Banerji, N., Cannizzo, A., Chergui, M., Das, A. K., ...& Lopez-Tarifa, P.(2017). “Charge migration and charge transfer in molecular systems”. Structural dynamics, 4(6), 061508.
- 23- Yi Qin Gao, Yuri Georgievskii, and R. A. Marcus. 2000 “On the Theory of Electron Transfer Reactions at Semiconductor Electrode Liquid Interfaces” Journal of Chemical Physics Volume 112, Number 7,PP 3358- 3369.
- 24- John B. Asbury, Encai Hao, Yongqiang Wang, Hirendra N. Ghosh, and Tianquan Lian. 2001 “Ultrafast Electron Transfer Dynamics from Molecular Adsorbates to Semiconductor Nanocrystalline Thin Films” J. Phys. Chem. B, 105, 4545-4557.
- 25- Ayelet Vilan and David Cahen 2002 “How Organic Molecules can Control Electronic Devices” Trends in Biotechnology Vol.20. No.1 January.
- 26- Yuri A. Berlin, Geoffrey R. Hutchison, Pawel Rempala, Mark A. Ratner, and Josef Michl 2003“Charge Hopping in Molecular Wires as A Sequence of Electron-Transfer Reactions”J. Phys. Chem. A, 107, 3970-3980.
- 27- Francois O. Laforge, Takashi Kakiuchi, Fumiko Shigematsu, and Michael V. Mirkin, 2004 “Comparative Study of Electron Transfer Reactions at the Ionic Liquid/Water and Organic/Water Interfaces” J. AM. CHEM. SOC, 126, 15380-15381

- 28- Neil A. Anderson and Tianquan Lian 2005 “Ultrafast Electron Transfer at the Molecule-Semiconductor Nanoparticle Interface” *Annu. Rev. Phys. Chem.* 56: 491-519.
- 29- Sumanta Bhattacharya , Soumyaditya Mula , Subrata Chattopadhyay and Manas Banerjee. 2006 “Charge Transfer in the Electron Donor-Acceptor Complexes” *J Solution Chem.* 35:1255-1269.7
- 30- Veaceslav Coropceanu, Je ro me Cornil, Demetrio A. da Silva Filho, Yoann Olivier, Robert Silbey, and Jean-Luc Bre das. 2007 “Charge Transport in Organic Semiconductors” *Chem. Rev.* 107, 926-952
- 31- Krause S., Casu M. B, A Scholl and Umbach E. 2008 “Determination of Transport Levels of Organic Semiconductors by UPS and IPS” *New Journal of Physics* 10. 085001 IOP Publishing Ltd and Deutsche Physikalische Gesellschaft
- 32- Jaehyung Hwang, Alan Wan and Antoine Kahn 2009 “Energetics of Metal-Organic Interfaces: New Experiments and Assessment of the Field” *Materials Science and Engineering R* 64. 1-31.
- 33- J. Aguiar, Q. M. Ramasse, M. Arredondo, F. Sandiumenge, P. Abellan, N. Valanoor and N.D. Browning 2011 “Charge Transfer in Magnetic Heterostructures from Atomic Resolution EELS” *Microsc. Microanal.* 17 (Suppl 2), PP1404-1405
- 34- Carina Faber, Ivan Duchemin, Thierry Deutsch, Claudio Attaccalite, Valerio Olevano and Xavier Blase 2012 “Electron-Phonon Coupling and Charge-Transfer Excitations in Organic Systems from Many-Body

- Perturbation Theory” *J Mater Sci.* 47:7472-748.
- 35- Benlin He, Qunwei Tang, Jinghuan Luo, Qinghua Li, Xiaoxu Chen and Hongyuan Cai (2014) “Rapid Charge-Transfer in Polypyrrole/single Wall Carbon Nanotube Complex Counter Electrodes: Improved Photovoltaic Performances of Dye-Sensitized Solar Cells” *Journal of Power Sources* Vol.256, PP170-177
- 36- Dorine Ameline, St´ ephane Diring, Yoann Farre, Yann Pellegrin, Gaia Naponiello, Errol Blart, Benoˆ it Charrier, Danilo Dini, Denis Jacquemin and Fabrice Odobel (2015) “Isoindigo Derivatives for Application in P-Type Dye Sensitized Solar Cells” *The Royal Society of Chemistry RSC Adv.* 5, 85530-85539
- 37- Hyunwoong Park, Hyoung-il Kim, Gun-hee Moon and Wonyong Choi 2016 “Photoinduced Charge Transfer Processes in Solar Photocatalysis Based on Modified TiO<sub>2</sub>” *Energy & Environmental Science*, 9, 411-433
- 38- Hadi J.M Al-agealy, Mohsin A. Hassooni, Ahmed M. Ashweik, B. Alshafaay, Raad H. Mjeed and Abbas K. Sadoon 2017 “Theoretical Study of Electronic Transfer rate constant At Solar Cell” *Mesop. environ. j. Special Issue C.*;24-33
- 39- Hadi J. M. AL-Agealy, Taif Saad AlMaadhede, Mohsin A.Hassooni, Abbas K.Sadoon, Ahmed M.Ashweik, Hind Abdlmajeed Mahdi, and Rawnaq Qays Ghadhban 2018 “Theoretical Study of Electronic Transfer Current Rate at Dye-Sensitized Solar Cells” *AIP Conference*

Proceedings 1968, 030055.

- 40- Timothy D.K.,2012 “Excited State and Electron Transfer in Solution, Model Based on Density Function Theory” PhD dissertation, Massachusetts institute of technology.
- 41- Bobisch, C. Th.and Wagner, A. Bannani, and R. MÄoller.2003 “Ordered Binary Monolayercomposed of Two Organic Molecules: Copper-Phthalocyanine and 3,4,9,10-Perylene-Tetra-Carboxylic-Dianhydride on Cu(111)”. *Journal of Chemical Physics*,119(18):9804-9408.
- 42- Walter R. Duncan and Oleg V. Prezhdo, 2007 “Theoretical Studies Of Photoinduced Electron Transfer in Dye-Sensitized TiO<sub>2</sub>” *Annu. Rev. Phys. Chem.*.Vol.58:143-84
- 43- Ellenbogen J. C, and love, J.Cerog. *IEEE.*, 2000. “Architectures for Molecular Electronic Computers. I. Logic Structures and an Adder Designed from Molecular Electronic Diodes” Vol.88, pp. 386-426.
- 44- Schmickler F., 1996 “Interfacial Electrochemistry” Book (Oxford University Press, Oxford).
- 45- Jing H., 2006 “Design, Characterization, and Electron Transfer Properties of Synthetic Metalloproteinase” Ph.D thesis, Graduate College of Bowling Green State University.
- 46- Wibren. Du., W. and Gispen.W., H., 2002 “Electron Transfer in Donor-Bridge-Acceptor System and Derived Materials” Ph. D. thesis, Debye Institute and University of Utrecht, Chapter (1), p (1-10).
- 47- Paulus A. and Van H.2003 “Photo physics of Molecules and Materials for Polymer Solar Cells” , Eindhoven: Technische Universities Eindhoven.
- 48- Hussien K. M., 2012 “A Quantum Mechanical for Electron Transfer at Metal Semiconductor Interface” MsC Thesis College of Education Ibn

AL-Haitham of Baghdad University.

- 49- Minoia A. 2008 “Marcus Theory for Electron Transfer a Short Introduction” MPIP-Journal Club-Mainz-29, Article, pp.7,8. Institute of Technology Pasadena, California.
- 50- Shachi S. G. 2002 “Electron Transfer at Metal Surfaces” Ph.D. Thesis, California, 6006.
- 51- Ásgeir E. Konráðsson, 2004 “Adiabatic Electron Transfer in Aromatic Bridged bishydrazine Radical Cations” Ph D. thesis University of Wisconsin-Madison.
- 52- Marcus RA. 1965. “On the Theory of Electron-Transfer Reactions. VI. Unified Treatment for Homogeneous and Electrode Reactions” J. Chem. Phys. 43: 679–701
- 53- Gerischer H. 1970. “Photoelectrochemistry: Applications to Solar Energy Conversion” See Ref. 167, pp. 463–542
- 54- Levich VG. 1970. “Electron Transfer in Proteins” See Ref. 167, pp. 985–1074
- 55- Gao, Y. Q., & Marcus, R. A. (2000). “On the theory of electron transfer reactions at semiconductor/liquid interfaces. II. A free electron model” The Journal of Chemical Physics, 113(15), 6351- 6360.
- 56- Antoine Van Voren 2009 “Theoretical Characterization of the Dynamics of Charge Transfer Processes in Donor-Bridge-Acceptor Architecture” PhD Thesis ,University of Mons.
- 57- Paul F. Barbara ,Thomas J. Meyer nand Mark A. Ratner, 1996 “Contemporary Issues in Electron Transfer Research” J. Phys. Chem. 100, 13148 13168.

- 58- Henriksen, N. E.; Hansen, F. Y. 2008 “Theories of Molecular Reaction Dynamics”, 1st ed.; Oxford University Press.
- 59- Ceroni P. 2011 “The Exploration of Supramolecular Systems and Nanostructures Byphotochemical Techniques”. vol. 78. Springer Science & Business Media.
- 60- Saavedra Becerril V. 2015 “Studies of Charge Separation in Molecular and Molecular-Inorganic Materials Assemblies for Solar Energy Conversion”.
- 61- Malin L. A., 2001 “Electron Transfer in Ruthenium Manganese Complex for Artificial Photo Synthesis” Ph.D. thesis, University of Uppsala, Sweden, chapter 2, pp 15-16.
- 62- Marcus.R.A.,and Sutin. N., 1985 “Electron Transfer in Chemistry and Biology” , Biochim. Biophys. Acta. Vol 811, pp 265–322.
- 63- Stephen Fletcher, 2007 “A non-Marcus Model for Electrostatic Fluctuations In Long Range Electron Transfer” J Solid State Electrochem 11:965-969
- 64- Mikael.A, 2002“Tunning ET Reaction by Selective Excitation in Porphyrin-Acceptor Assemblies” Ph. D, Thesis Actauniversity, Uppsala.
- 65- Fox. L.S, Kozik. M.,Winkler.J.R., Gray. H. B., and Gausson. F. 1990 “Free Energy Dependence of Electron Transfer Rates in Iridium Complexes”, Science. Vol 247, p 4946.
- 66- Sebastiao J. Formosinho and Luis G. Arnaut 2001“Theory of Electron Transfer Reactions in Blue-Copper Proteins” Res. Chem. Intermed. Vol. 27, No. 1,2, PP. 103–124. VSP.
- 67- Lindstrom C. D. and Zhu X.-Y. 2006 “Photoinduced Electron

- Transfer at Molecule Metal Interfaces” Chem. Rev., Vol.106, 4281-4300.
- 68- Zhu X.-Y. 2002 “Electron Transfer at Molecule-Metal Interfaces: a Two-Photon Photoemission Study” Annu. Rev. Phys. Chem. 53:221-47.
- 69- Al-agealy, H. J, (2004) “Quantum Mechanical Model for Electron Transfer in Q-Swiched Dye for Solid State Laser” thesis, ph. D, Baghdad university.
- 70- Chérubin, 2009 “Noumissing Sao Dye-Sensitized Solar Cells Based on Perylene Derivatives” PhD Thesis, University of Kassel, Kassel.
- 71- B. A. Gregg, 2003 “Excitonic Solar Cells” J. Phys. Chem. 107,4688.
- 72- L.M.Peter 2007 “Characterization and Modeling of Dye-Sensitized Solar Cells” J. Phys. Chem. 111, 6601.
- 73- J. R. Durrant, Y. Tachibana, I. Mercer, Z Phys. 1999 “Chemie-Int. the Excitation Wavelength and Solvent Dependence of the Kinetics of Electron Injection in Ru (dcbpy) 2 (NCS) 2 Sensitized Nanocrystalline TiO2 Films” J. Res. Phys. Chem Chem Phys. 1999, 212, 93.
- 74- J. B. Asbury, E. Hao, Y. Wang, T. Lian, 2000 “Applications of Functionalized Transition Metal Complexes in Photonic and Optoelectronic Devices” J. Phys. Chem. B 2000, 104, 11957.



- 75- K. Kalyanasundaram, M. Grätzel, Coord. 1998 “Applications of Functionalized Transition Metal Complexes in Photonic and Optoelectronic Devices” Chem. Rev. 177, 347.
- 76- B. T. Langdon, V. J. MacKenzie, D. J. Asunskis, D. F. Kelley 1999 “Electron Injection Dynamics of Ru (4,4-dicarboxy-2,2- bipyridine) (NCS) Adsorbed on MoS<sub>2</sub> Nanoclusters” J.Phys. Chem. 103, 11176.
- 77- R. A. Marcus, Ann. Rev. 1964 “On the Theory of Electron-Transfer Reactions. VI. Unified Treatment for Homogeneous and Electrode Reactions” Phys. Chem. 15, 155.
- 78- R. Memming, F. Schroppel, U. Bringmann. 1979 “Sensitized Oxidation of Water by Tris (2,2'-bipyridyl) Ruthenium at SnO<sub>2</sub> Electrodes” J. Electroanal. Chem. 100, 307.
- 79- D. Shi, N. Pootrakulchote, R. Li, J. Guo, Y. Wang, S. M. Zakeeruddin, M. Grätzel, P. Wang, Shi, Dong, et al. 2008 “New Efficiency Records for Stable Dye-Sensitized Solar Cells With Low-volatility and ionic liquid electrolytes.” The Journal of Physical Chemistry C 112.44: 17046-17050.
- 80- Q. Yu, S. Liu, M. Zhang, N. Cai, Y. wang, P. Wang, 2009 “An Extremely High Molar Extinction Coefficient Ruthenium Sensitizer in Dye-Sensitized Solar Cells: The Effects of  $\pi$ -Conjugation Extension” J. Phys. Chem. C, 113, 14559.

- 81- T. Horiuchi, H. Miura, K. Sumioka, S. Uchida, J. Am. 2004 “High Efficiency of Dye-Sensitized Solar Cells Based on Metal-Free Indoline Dyes” Chem. Soc. 126, 12218.
- 82- N. Koumura, Z. S. Wang, S. Mori, M. Miyashita, E. Suzuki, K. Hara, J. Am. 2006 “Alkyl-Functionalized Organic Dyes for Efficient Molecular Photovoltaics Solar Cells” Chem. Soc. 128,14256.
- 83- M. K. Nazeeruddin, P. Pechy, T. Renouard, S. M. Zakeeruddin, R. Humphry-Baker, P. Comte, P. Liska, L. Cevey, E. Costa, V. Shkloer, L. Spiccia, G. B. Deacon, C. A. Bignozzi, M. Grätzel, J. 2001 “Engineering of Efficient Panchromatic Sensitizers for Nanocrystalline TiO<sub>2</sub>-Based” Am. Chem. Soc., 123, 1613
- 84- Y. Chiba, A. Islam, Y. Wanatobe, R. Komiya, N. Koide, L.Y.Han, 2006 “Dye-Sensitized Solar Cells with Conversion Efficiency of 11.1%” Jpn. J. Appl. Phys., 45, 638
- 85- So Yeon Bang, Min Jae Koa, Kyungkon Kim, Jong Hak Kim, In-Hyuk Jangd and Nam-Gyu Parkd, 2012 “Evaluation of Dye Aggregation and Effect of Deoxycholic Acid Concentration on Photovoltaic Performance of N749-Sensitized Solar Cell” Synthetic Metals 162. 1503-1507
- 86- Anna Reynal, Amparo Forneli and Emilio Palomares. 2010 “Dye Structure-Charge Transfer Process Relationship in Efficient Ruthenium-Dye Based Dye Sensitized Solar Cells” Energy Environ. Sci. 3, 805–812

- 87- H.J. Snaith, 2010 “Estimating the Maximum Attainable Efficiency in Dye-Densitized Solar Cells” *Advanced Functional Materials* p13-19.
- 88- Green, M. A., Emery, K., Hishikawa, Y., Warta, W., & Dunlop, E. D. (2012). “NIMS Sets a New World Record for the Highest Conversion Efficiency in Dye-Sensitized Solar Cells”. *Progress In Photovoltaics Research and Applications*, 20, 12-20.
- 89- M. Fakis, E. Stathatos, G. Tsigaridas, V. Giannetas, and P. Persephonis 2011 “Femtosecond Decay and Electron Transfer Dynamics of the Organic Sensitizer D149 and Photovoltaic Performance in Quasi-Solid-State Dye-Sensitized Solar Cells” *J. Phys. Chem. C*, 115, 13429–13437
- 90- Wang, H.; Peter, L. M. 2012 “Influence of Electrolyte Cations on Electron Transport and Electron Transfer in Dye-Sensitized Solar Cells”. *J. Phys. Chem. C*, 116, 10468–10475.
- 91- Bai Y, Mora-Seró I, De Angelis F, Bisquert J, Wang P. 2014 “Titanium Dioxide Nano-Materials for Photovoltaic Applications” *Chemical reviews*. 114(19):PP.10095-10130.
- 92- Kittel C. 2005 “Introduction to Solid State Physics”. Wiley.
- 93- Bard AJ, Faulkner LR. 2001 “Fundamentals and Applications” *Electrochemical Methods*, 2. p 482
- 94- M. A. Alzamil 2011 “Electron Mobility Calculations of n-InAs” *Digest Journal of Nanomaterials and Biostructures*, Vol. 6, No 2, April-June, PP. 725-729

- 95- W. Wei, C. Jin, J. Narayan, R. J. Narayan, 2010 “Optical and Electrical Properties of Gallium Doped  $Mg_xZn_{1-x}O$ ” *J. Appl. Phys.* 107,p 013510.
- 96- D. L. Li, Q. L. Ma, S. G. Wang, R. C. C. Ward, T. Hesjedal, X. G. Zhang, A. Kohn, E Amsellem, G. Yang, J. L. Liu, J. Jiang, H. X. Wei, X. F. Han, 2014 “Controlling Spin-Dependent Tunneling by Band Gap Tuning in Epitaxial Rocksalt  $MgZnO$  Films” *Sci. Rep.* 4 7277.
- 97- Cohen, R., Bastide, S., Cahen, D., Libman, J., Shanzer, A., Rosenwaks, Y. 1998 “Controlling Surfaces and Interfaces of Semiconductors Using Organic Molecules” *Opt. Mater.*, Vol.9, p. 394.
- 98- N. P. Guisinger, M. E. Greene, R. Basu, A. S. Baluch, and M. C. Hersam, (2004) “Room Temperature Negative Differential Resistance Through Individual Organic Molecules on Silicon Surfaces” *Nano Lett.*, Vol. 4, p. 20.
- 99- J. M. Buriak, 1999 “Organometallic chemistry on silicon surfaces: formation of functional monolayers bound through Si-C bonds” *Chem. Commun. (Cambridge)*, p. 1051.
- 100- W. Wang, T. Lee, M. Kamdar, M. A. Reed, M. P. Stewart, J.-J. Hwang, and J.M. Tour, 2003 “Electrical Characterization of Metal-Molecule-Silicon Junctions” *Superlattices Microstruct.* Vol.33, p.217.
- 101- Y.-L. Loo, D. V. Lang, J. A. Rogers, and J. W. P. Hsu, *Nano.* 2003 “Electrical Contacts to Molecular Layers by Nanotransfer Printing”,

Vol. 3, p. 913.

- 102- Raymond T. Tung, (2001) “Recent Advances in Schottky Barrier Concepts” Sci. Eng. Volume 35, Issues 1–3, Pages 1-138-51.
- 103- A. Salomon, T. Boecking, C. K. Chan, F. Amy, O. Girshevitz, D. Cahen, and A. Kahn, 2005 “How Do Electronic Carriers Cross Si-Bound Alkyl Monolayers” Phys. Rev. Lett. Vol. 95, P 266807.
- 104- Hadi, J. M, Al-agealy, Hazim, H. D. Al Hasan.2019 “Investigation the Flow Charge Rate at InAs/D149 and ZnO/D149 System Using Theoretical Quantum Model” AIP Conference Proceedings (Vol. 2123, No. 1, p. 020055). AIP Publishing.
- 105- Michel Le Bellac 2006 “Quantum Physics” Book, Cambridge University Press.
- 106- Charles E. Burkhardt · Jacob J. Leventhal 2008 “Foundations of Quantum Physics” Book, Springer Science and Business Media, LLC.
- 107- David J.Griffths 1995 “Intrduction to Quantum Mechanics” Book, Hall, Inc Publishing.
- 108- J. C. Garrison and R. Y. Chiao 2008 “Quantum Optics” Book, Oxford University Press.
- 109- David K Ferry 2001 “Quantum Mechanics” Book, IOP Publishing Ltd
- 110- Levi, A., F., J. 2003 “Applied Quantum Mechanics” Published in the United States of America by Cambridge University Press, New York.

- 111- Hadi, J. M. Al-Agealy; Salih, Waleed Bdaiwi, TAIF, S. Murdhi.2013  
 “Effects of Driving Force Energy on the Rates of Electron-Transfer  
 Reactions at Metal/LiquidInterface” Jurnal of Madenat Al Elem  
 College, 5.2, P 31-39.
- 112- Hadi J.M Al-Agealya, Taif Saad Al MaadhedeB, B. AlShafaayc,  
 RaadH. Mjeeda, Ahmed M.Ashweikb 2017 “Theoretical Study of Charge  
 Transfer Simulation At Fe Metal with Ge and ZnO Semiconductors  
 Nano Devices Material” Energy Procedia 119, PP325-331.
- 113- Fedir T. Vasko and Oleg E. Raichev 2005 “Quantum Kinetic  
 Theory and Applications” Book, Springer Science and Business  
 Media, Inc.
- 114- William J. Royea, Arnel M. Fajardo, and Nathan S. Lewis 1997  
 “Fermi Golden Rule Approach to Evaluating Outer-Sphere Electron-  
 Transfer Rate Constants at Semiconductor/Liquid Interfaces” J.  
 Phys. Chem. B, 101, P 11152-11159
- 115- Steven H. Simon 2013 “The Oxford Solid State Basics” Book,  
 Oxford University Press , UK.
- 116- Thomas W. Hamann, Florian Gstrein, Bruce S. Brunschwig, and  
 Nathan S. Lewis 2005 “Measurement of the Free-Energy  
 Dependence of Interfacial Charge-Transfer Rate Constants Using  
 ZnO/H<sub>2</sub>O Semiconductor/Liquid Contacts” J. AM. CHEM. SOC.  
 127, P 7815-7824.
- 117- Sze, S. M. 1981 “The Physics of Semiconductor Devices” 2nd ed;

Wiley & Sons, 15, 43.

- 118- Fonash, S. J. 1981 "Solar Cell Device" Physics; Academic: New York,
- 119- Blakemore, J. S. 1987 "Semiconductor Statistics" Dover Publications,  
Inc.:New York.
- 120- Garol, C., Bruce, S. R., and Sutan, N. 2006. "Interfacial Charge  
Transfer Absorption" Am. Chem. Soc. 1 (1): PP 3425-3436.
- 121- Al-Agealy, H. J. M., and Hassooni, M. A. 2014. "Effect of  
Semiconductors Types on Electron Transmission at Metal/  
Semiconductor Interface" J. Chem. Bio. Phys. SCI. Sec. C. 4(3).
- 122- Bart J. Van Zeghbroeck 1996 "Principles of Electronic Devices"  
Book.
- 123- Sujuan Wu, Hongwei Han, Qidong Tai, Jing Zhang, Sheng Xu,  
Conghua Zhou, Ying Yang, Hao Hu, BoLei Chen, Bobby Sebo  
And Xing-Zhong Zhao(2008) "Enhancement in Dye-Sensitized  
Solar Cells Based on MgO-Coated TiO<sub>2</sub> Electrodes by Reactive DC  
Magnetron Sputtering" Nanotechnology 19 215704 (6pp)  
doi:10.1088/0957-4484/19/21/215704
- 124- Ian M. Smallwood 1998 "Handbook of Organic Solvent Properties"  
Copublished in the Americas by Halsted Pres. 21.
- 125- M d. Akhtaruzzaman, Ashraful Islam, Mohammad Rezaul Karim,  
A. K. Mahmud Hasan, and Liyuan Han 2013 "Improving the  
Spectral Response Black Dye by Cosensitization with a Simple  
Indoline Based Dye in Dye-Sensitized Solar Cell" Hindawi

Publishing Corporation Journal Chemistry Volume, Article ID

910527, 5 pages

- 126- Wang, H.; Peter, L. M. 2012 “Influence of Electrolyte Cations on Electron Transport and Electron Transfer in Dye-Sensitized Solar Cells” J. Phys. Chem. 116, PP 10468–10475.
- 127- Nathan S. Lewis 1998 “Progress in Understanding Electron-Transfer Reactions at Semiconductor/Liquid Interfaces” J. Phys. Chem. B, Vol. 102, No. 25.
- 128- Braun S., Salaneck W. R., and Fahlman M., 2009 “Energy-Level Alignment at Organic/Metal and Organic/Organic Interfaces” Adv. Mater., Vol. 21, PP.1450–1472.
- 129- Levi A. F. J. 2003 “Applied Quantum Mechanics” Cambridge University Press.
- 130- David K F., 2001 “Quantum Mechanics” Book, IOP Publishing Ltd.
- 131- Axel G., 2002 “Theoretical Physics III Quantum Mechanics” Book  
13 October 2002, München Springer publisher.



## الخلاصة

في هذه الدراسة، أُستخدم نموذج نظري بسيط لنظرية ماركوس لدراسة معدل فيض الشحنة عبر نظام شبه موصل - سائل ، حيث طُبقت نظرية الميكانيك الكمي لتحقيق وحساب معدل فيض الشحنة في نظام مانح- مستقبل . حيث بحثنا في آلية الانتقال لفيض الشحنة لواجهات نظام شبه موصل - سائل استناداً الى أنموذج مانح - مستقبل وبفرض استمرارية مستويات الطاقة لكلاً من شبه الموصل وجزيئات الصبغة.

تم حساب معدل انتقال فيض الشحنة لأنظمة ZnO/D149، InAs/D149 ، MgO/N749 و ZnO/N74 ، InAs/N749 ، MgO/D149 إعادة التنظيم  $T_S^L (eV)$  وحد الازدواج  $C_{S/L}(\epsilon)$  وحاجز الجهد لمستويات الطاقة عند سطح النظام  $\Delta U^{LS} (eV)$ . بالإضافة الى دراسة طاقة إعادة التنظيم والتي تساعد الأنظمة الستة على إعادة ترتيب مستويات الطاقة لبدأ الانتقال من الصبغة إلى حزمة التوصيل لشبه الموصل في جميع الأنظمة الستة، ووجدنا أن طاقة إعادة التنظيم تزداد كدالة لنقصان معامل الانكسار للمذيبات وزيادة ثابت العزل الكهربائي في جميع الأنظمة الستة.

حاجز الجهد تم حسابه اعتماداً على الفرق بين طاقة الامتصاص للصبغة الحساسة وطاقة إعادة التنظيم وفقاً لأنموذج الاستمرارية في وسط مستقطب.

لحساب الجهد في جميع واجهات السطوح قمنا باستخدام نتائج نظرية لطاقة إعادة الترتيب توضح عملية الانتقال عبر سطح نظام شبه موصل- صبغة في وسط مستقطب. كذلك فإننا نلاحظ زيادة حاجز الجهد مع الطاقة الممتصة وطاقة إعادة التنظيم. وان معدل فيض الشحنة يصل الى أقصى قيمة له عند استخدام البروبانول كمذيب، لكنه يتناقص تدريجياً عند استخدام المذيبات البيوتانول ، الأوكتانول ، الديكلوروايثان و الأسيتونيتريل. اضافة الى ان نظام MgO/D149 يملك أعلى معدل انتقال مقارنة مع أنظمة ZnO/D149 و InAs/D149 لنفس معامل الازدواج، والحسابات بينت أن معدل فيض الشحنة يتناقص مع زيادة حاجز الجهد ويزداد مع تناقص طاقة إعادة الترتيب .



جمهورية العراق  
وزارة التعليم العالي والبحث العلمي  
جامعة بغداد  
كلية التربية للعلوم الصرفة - ابن الهيثم

# دراسة انتقال الشحنة الالكترونية لنظام سائل/ شبه موصل

رسالة مقدمة

إلى مجلس كلية التربية للعلوم الصرفة - ابن الهيثم - جامعة بغداد  
كجزء من متطلبات نيل درجة ماجستير علوم في الفيزياء

من قبل  
حازم هادي ضايف الحسن

بإشراف  
أ. د. هادي جبار مجيب العكيلي